INSTITUTO DE INVESTIGACIÓN TECNOLÓGICA

FINAL REPORT

STEXEM

Task 1: Uncertainty integration and representation of time horizon for long-term models

S. Wogrin, I. González-Romero, D. Tejada-Arango, J.J. Valentín, T. Gómez, E. Centeno

Prepared by IIT for Ministerio de Economía, Industria y Competitividad

December 2020

Version: 1.0

CONTENTS

1. Executive Summary

This report aims to assess and determine the best ways to represent short-term details in longer-term models such that the computational tractability of these long-term models is maintained while the accuracy of the results is not compromised. First, we analyze different options of representing short-term details (e.g., such as varying Renewable Energy (RE) production) in long-term models while aiming for both computational tractability of models and accuracy of results. Second, we also explore the different ways to incorporate both short-term (e.g., uncertainty due to intermittent renewable production) and long-term uncertainties (e.g., RE policies, fuel prices, demand evolution) in long-term models and evaluate them depending on their suitability for long-term transmission and generation expansion models. The corresponding sections of this report are described below:

- Adequate representation of time horizon in long-term models: The representation of the time horizon in long-term models is an issue: there exist approaches that represent each hour of the time horizon individually; and others that approximate the hourly data by a load duration curve or system states. The first approach is not tractable if the modelling time horizon goes over several years or decades, which is the case in the expansion models proposed in this project. However, representative weeks of the year could be considered to achieve computational tractability. In Section 2 such an approach is compared to standard load duration curve models, in order to determine which representation of time is best suited for long-term investment models.
- Integration of short- and long-term uncertainties in long-term models: In the electricity sector there exist different types of uncertainties: short-term uncertainties that mostly affect operations, such as uncertain output of RE sources; and long-term uncertainties such as the evolution of fuel prices over time, policy uncertainty, or the evolution of electricity demand. Both types of uncertainties can have an impact on optimal investment decisions, both in transmission and generation expansion. Section 3 studies the best way to include these types of uncertainty in the models proposed. Different options are explored in order to guarantee that the proposed models can still be solved from a numerical point of view, but that they also adequately capture the uncertainties at hand.

2. Adequate representation of time horizon in long-term models

The representation of the time horizon in long-term models is an issue: there exist approaches that represent each hour of the time horizon individually; and others that approximate the hourly data by a load duration curve or system states. In this section we show the main results obtained from the comparison between standard load duration curve and representative periods (e.g., days or weeks) approaches, in order to determine which representation of time is best suited for long-term investment models. As part of the STEXEM project, these results have been published in Reichenberg et al. [1] and Tejada-Arango et al. [2] and are summarized in the following sections.

2.1 Policy implications of downscaling the time dimension in power system planning models to represent variability in renewable output

In most industrialized countries, concerns about climate change have prompted policymakers to mandate targets for increasing the share of variable renewable energy sources (VRES) such as solar and wind power [3]. In turn, policy-enabling models are relied upon to delineate the design of and transition into a future power system with less CO2 emissions. For example, ReEDS [4] is a linear programming model for the U.S. that uses a demand-based integral method, i.e., representation of time by averages based only on demand fluctuations, with 17 time periods per year to capture variability. By contrast, the POWER model for the U.S. uses extreme days comprising variability in VRES output as well as demand with hourly resolution to study both flexibility [5] and storage [6]. LIMES-EU uses clustering techniques to select representative days in order to assess a sustainable transition for Europe [7].

Such power system planning models are computationally demanding due to their technological and/or spatial detail. They are, therefore, restricted as to their representation of time, and they, thus, typically reduce the number of time steps to 10-20, e.g., 17 annual time steps in the integral model ReEDS and 4 representative days each in LIMES-EU and POWER. When these models originated, the main variable quantity was the demand, which fluctuates rather regularly depending on the time of day, the day of the week, and the season. Thus, variation may be adequately represented using 10-time steps. Although such a time representation does not capture variability on the generation side, viz., for solar and wind power, as long as the solar and wind contribution is marginal, the lack of linkage to variations in solar and wind output does not gravely impact model results. However, as the levelized cost of solar and wind generation has decreased rapidly to reach near parity with that of gas-fired plants [8], VRES may potentially constitute a large part of the generation in a least-cost system. Consequently, it is desirable for policy-enabling planning models to represent variability in solar and wind power output. If a time representation based on demand variation were used in a scenario with low costs of variable generation, then the variations on the

generation side will be underestimated, thereby leading to a gross overestimation of the optimal VRES capacity [9]. Even models with more detailed temporal representation, e.g., using 8760 annual time steps, face a tradeoff in terms of less spatial resolution and more computational effort [10]. Meanwhile, models with more engineering details, e.g., EnergyPLAN, calculate resulting power system operations once VRES capacities are known based on samples from statistical distributions. Yet, as indicated in the documentation[1], EnergyPLAN "optimises the operation of a given energy system on the basis of inputs and outputs defined by the user." Unlike EnergyPLAN, the capacities are endogenously determined by the class of power system models that are studied in the current paper.

Recently, several articles have been produced highlighting the importance of a representation of time that is apt for power systems that can be expected to incorporate substantial levels of VRES as summarized by Pfenninger et al. [11]. In such studies, one may differentiate between two main families of methods to represent the variability in production introduced by VRES. One family of methods classifies the time into "typical" hours in terms of wind output and demand and then averages quantities within these classes. This family of time-reduction methods will be referred to as integral following Nahmmacher et al. [7]. This approach was developed for one-node models by Wogrin et al. [12] with Lehtveer et al. [13] implementing an application to a global model. Wogrin et al. [14] further develop the approach to include storage using a transition matrix to relate the time slices to each other. The second type of method is to select so-called representative days, i.e., to choose certain days and assign unequal weights to them in order to replicate variation during the year with fewer time steps. Nahmmacher et al. [7] develop a method to select representative days based on looking at each day's output of variable quantities (wind, solar, demand) as a vector. Frew and Jacobson [6] use a method where extreme days, e.g., the day with the highest demand and the lowest wind production, are included as well as random days. Merrick [15] uses distance measures to determine how many representative days or weeks are sufficient to capture the effects of variability.

In terms of the number of time steps necessary to represent variability adequately, Wogrin et al. [12] and Wogrin et al. [14] evaluate the number of time slices needed to come within a certain range of the capacities obtained using a model with hourly resolution for a full year. They find that around 100 time slices plus the transition matrix to represent storage are needed for their unit-commitment model. Furthermore, they find that the CPU time is reduced to about a third compared to the hourly model of 8760-time steps. Nahmmacher et al. [7] implement their LIMES-EU model with successively more representative days and find that 20-30 representative days (which amounts to 160-240 time steps) are necessary to converge to the correct system capacity mix. Frew and Jacobson [6] find that the system cost in their POWER model

[1] www.EnergyPLAN.eu

differs by less than 10% for 14 representative days as compared to a “full” implementation.

Besides the aforementioned power system planning models, there are others that either account for the interaction with other parts of the energy system or have a more detailed representation of strategic behavior. For example, inadequate representation of variability in power system modelling will have consequences for a holistic approach to smart energy systems [16]. Likewise, the coupling of the power system with district heating in terms of integrating VRES is important for the Nordic region [17]. More generally, electricity and gas networks may also require further joint analysis [18]. Indeed, more adoption of VRES requires countervailing flexibility, which could be provided by heat storage, combined heat and power, and gas-fired power plants. Thus, additional VRES capacity could also affect the leverage of flexible generators in exerting market power, which would require a game-theoretic framework for analysis [19].

Focusing on power system planning models, although the performance of integral and representative days methods has been evaluated individually against benchmark model results with a high time resolution, e.g., Frew and Jacobson [6]; Nahmmacher et al. [7]; Wogrin et al. [12]; Wogrin et al. [14]; and Merrick [15]; the two approaches have not been compared with each other in the same model apart from an assessment with an equal number of time periods in Poncelet et al. [9]. In this paper, the performances of the two families of methods (integral and representative days) are compared in a cost-minimizing power system planning model and evaluated with respect to how well they predict the capacity mix and the system cost.

The research questions addressed in this paper are:

- Which method comes closer to predicting the benchmark model3 VRES capacity (the main performance metric in this paper) for a given number (10-20) of time steps?
- Which method is more accurate if a larger number of time steps (200) is tractable?
- What, if any, is the impact of using a clustering method rather than arbitrarily picked days?

From a policy perspective, answers to these questions are essential in assessing the impact of proposed environmental regulations on the power system. Since a conventional load-slicing approach in large-scale power system models leads to overestimates of VRES installed capacity, it would provide a biased basis on which to establish future energy policy. Hence, by directly comparing two enhanced time-resolution methods, this paper demonstrates how models should represent temporal dependence between VRES and demand in order to provide a credible basis for policymaking.

2.1.1 Methods

The two time-reduction methods (integral and representative days) are tested using data for several European regions: one each in Germany, Denmark, Spain, France, and Ireland. The regions are chosen to represent a variety in terms of VRES and demand conditions. Demand and weather data are the input to a power system planning model. The results of the time-reduction methods are compared with those from a fully time resolved linear optimization model using 2920-time steps (from now on called the benchmark model). The measure of accuracy for the two approaches and the main performance metric used in this paper is their ability to predict the optimal capacity investment for the different technologies, especially VRES, using results from the benchmark model as comparison.

The two methods are described in steps and illustrated with an example. Several preparation methods have been proposed in order to group data into representative periods, e.g., via either hierarchical (as in Nahmmacher et al. [7] and Merrick [15] or k-means clustering (as in Frew and Jacobson [6] and Wogrin et al. [12]. The latter technique partitions n demand and VRES pairs into k clusters via an iterative procedure that minimizes the sum of weighted distances between each pair and cluster centroid. By contrast, hierarchical clustering starts with clusters of size one data point each and sequentially merges nearby clusters.4 Since k-means clustering is used here, which depends on initial points, 200 replicates are performed, and the closest match is picked. The data are normalized so that solar, wind, and demand observations all attain values between 0 and 1.

2.1.1.1Representative days

Representative days are selected as described in Nahmmacher et al. [7] 5 except for the clustering method: in Nahmmacher et al. [7] hierarchical clustering is used, while k-means clustering is used here. The procedure is illustrated in Fig. 1 and is as follows:

- Partition the data into vectors each consisting of the output of each variable quantity (in this case, solar, wind, and demand) for one day.
- Cluster the vectors into the chosen number of clusters using k-means clustering.
- Pick the day(s) that are closest to the centroids as representative. The number of days in a cluster is used as the weight for that representative day.
- Run the model with the time steps pertaining to these days. Since there are n representative days with time resolution of three hours per step, i.e., 8n time steps are selected, this amounts to:

- Partition the data into 365 vectors, each with 24 elements (elements 1:8 are the wind output, elements 9:16 are the solar output, elements 17:24 are the demand).
- Cluster the vectors into n clusters using k-means clustering.
- Pick the n days that are closest to the centroids as representative. The number of days in a cluster is used as the weight for that representative day. An example of a time series resulting from this procedure can be found in Fig. 2.
- Run the model with the 8n time steps pertaining to these days.

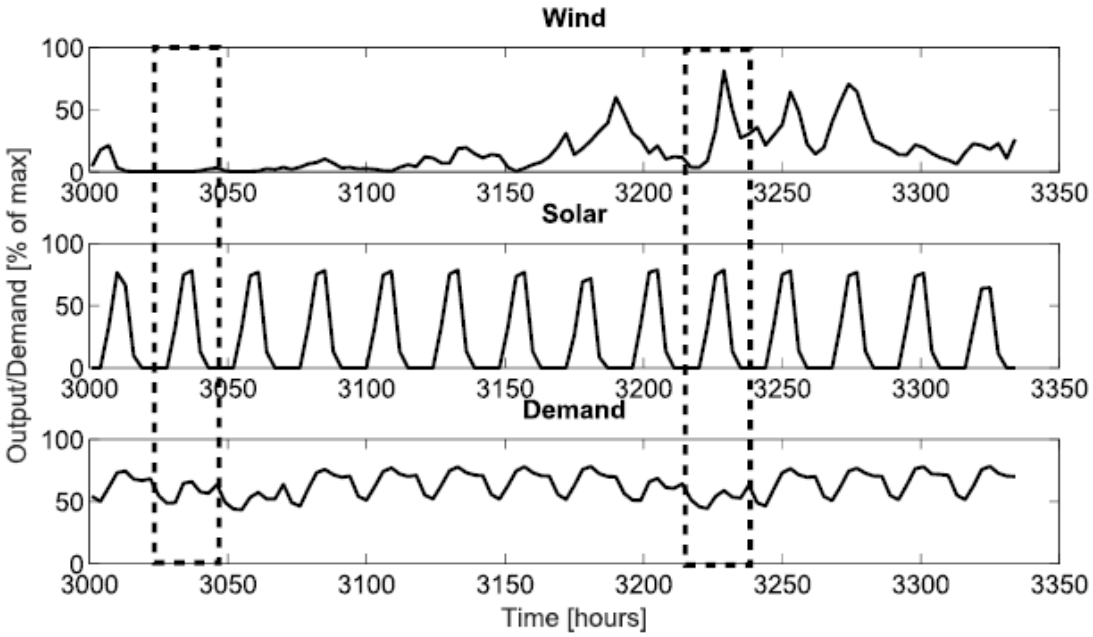

Fig. 1 Representative days to capture the variation during the entire year

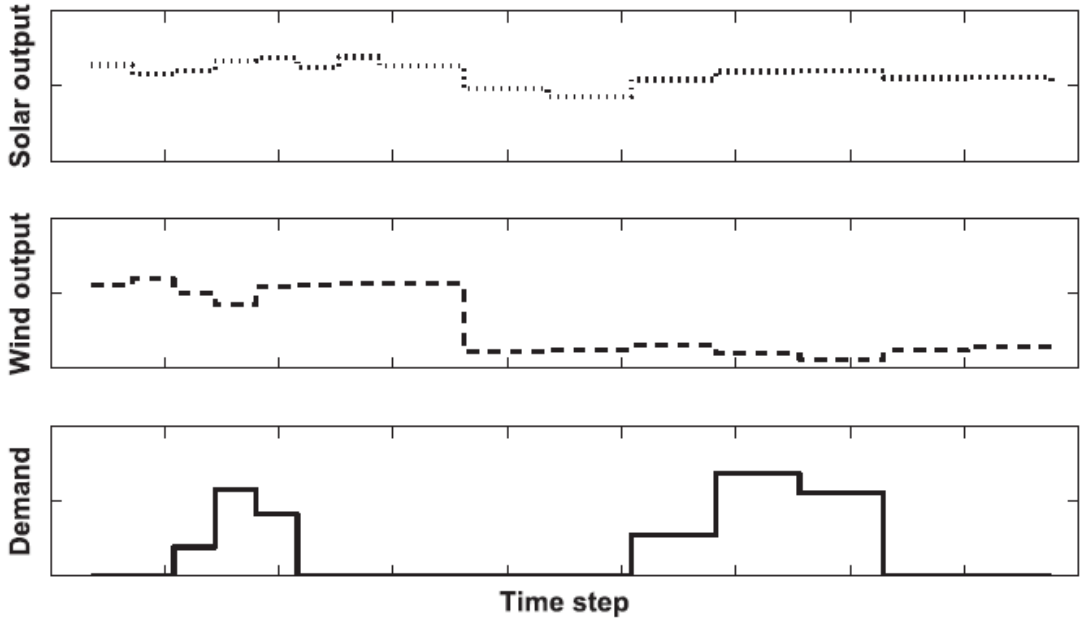

Fig. 2 Representative days - Time series produced with 16-time steps based on k-means clustering

2.1.1.2Integral

The principle behind integral methods is to identify states. States may be described as "typical" situations, e.g., when the wind power output is low, and the demand is high. This is illustrated in Fig. 3, which shows an example where states are based on wind power output and demand only. The method to identify states in this paper follows Wogrin et al. [12]:

- Partition the data into vectors each consisting of the outputs of variable quantities for one-time step. Each such vector is called a state as in Wogrin et al. [12] and Wogrin et al. [14].
- Cluster the vectors into the chosen number of states using k-means clustering.
- Take the centroid of each cluster output for that state. The number of elements in a cluster is used as the weight for that state in the modelling.
- Run the model using the states and weights. In this case, this amounts to:
- Partition the data into vectors with three elements each: solar, wind, and demand for one-time step. There are 2920 such vectors. Each such vector is a state.
- Cluster the vectors into n0 clusters using k-means clustering.

- Take the centroid of each cluster, i.e., a triplet with values for solar, wind, and demand, and use it as the solar output/wind output/demand for that time step. The number of elements in a cluster is used as the weight for that time step. An example of a time series resulting from this procedure can be found in Fig. 4.

- Run the model using the time steps and weights.

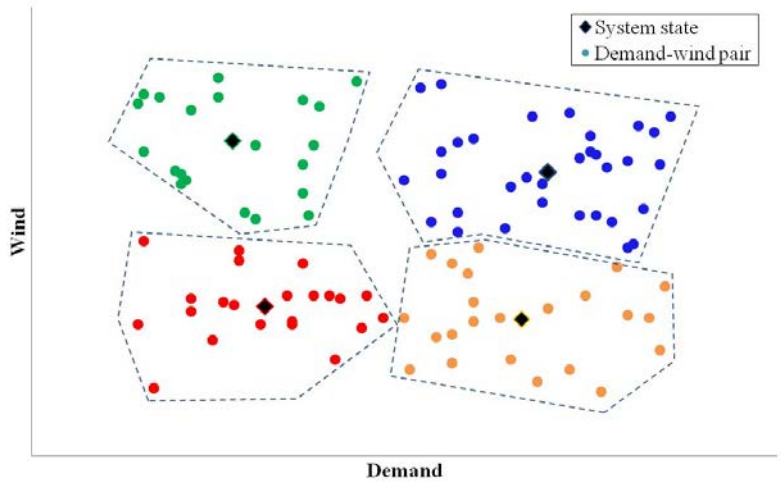

Fig. 3 Integral approach based on partitioning variable quantities by their means (schematic based on only wind power output and demand)

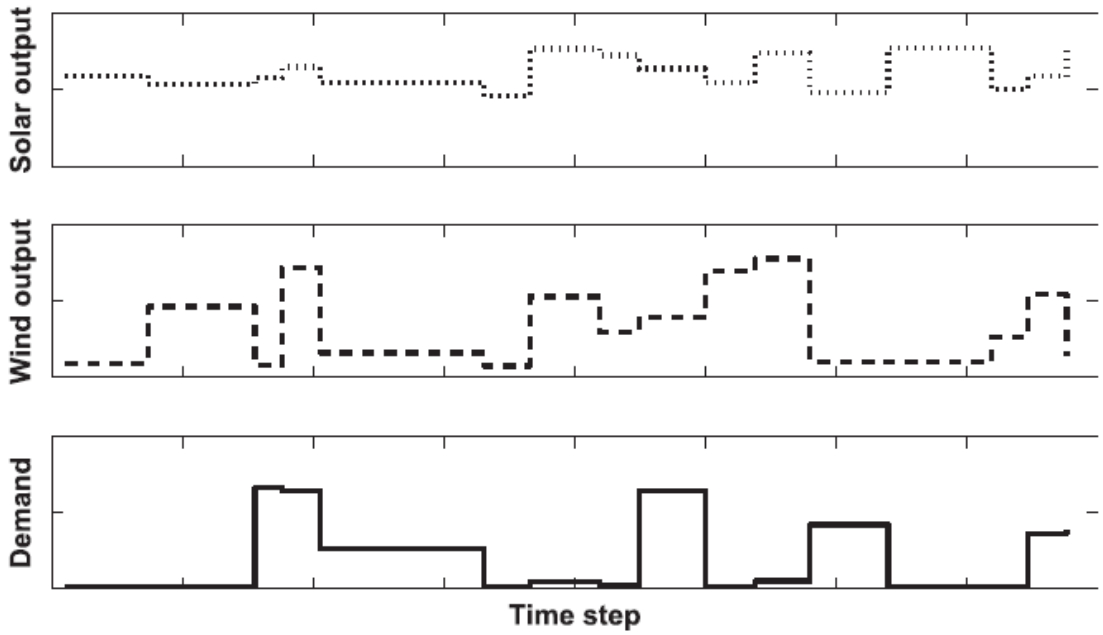

Fig. 4 Integral - Time series produced with 16-time steps based on k-means clustering

The number of states, n0, is between 8 and 200, in steps of 8 (Table 1). As a basis for comparison in terms of predicting the VRES capacity and system cost accurately, a demand-based integral method is adopted, similar to that in Short et al. [20] and

Odenberger et al. [21]; for example. The procedure to find the demand-based states is exactly like the integral method (above), but the states are based only on demand. Consequently, solar and wind conditions do not influence the selection of time steps that define a state in such a conventional representation of time.

Table 1: Attributes of data used in this analysis.

Time resolution	3-hourly
Time steps per year	2920
Time steps per day	8
Varying quantities	3 (demand, wind, solar)
Number of time steps in modelling	8-200 (equivalent of 1-25 days)

2.1.1.3Optimisation model

The basis for comparing the representative days and the integral time-resolution methods is a one-node cost-minimization linear programming model. Demand is assumed to be perfectly price inelastic but varying in time. The model's decision variables are (i) investment capacities in a number of technologies (set I) and (ii) their production over representative time periods in order to minimize annualized investment and operating costs for a target year. The only constraints are that (i) total generation should meet demand at every time step and (ii) output is limited by available capacity. For the VRES technologies, operating costs are zero, but availability depends on weather-based factors. The model is run with different weights on the time steps corresponding to the cluster sizes. For the benchmark model, all 2920-time steps have the same weight.

2.1.2 Numerical examples

2.1.2.1Data

The data consist of time series for demand, solar, and wind for five regions: one each in Denmark, Germany, France, and Spain, as well as the entire island of Ireland. The investment and operating costs for energy technologies are listed in Table 2. The demand data are available on an hourly basis from Eurostat[2]. Since the weather data are available only for every three hours, the demand data points are taken for the same hours, i.e., 2920-time steps for one year. The demand data are used as they are in the

[2] http://ec.europa.eu/eurostat/statistics-explained/index.php/Main_Page

optimization step. However, for the preparation step (integral or representative days method), the demand data are normalized so that the maximum demand event is given a value of 1. The wind and solar data input is based on weather data from the European Centre for Medium-Range Weather Forecasts (ECMWF), processed through a turbine function and a function to mimic the output of solar PV (see Ref. [22] for a more thorough description). Solar and wind output also attain values between 0 and 1, but 1 is equivalent to the nameplate capacity. Sample code and a generic dataset for executing the procedure are available as an electronic companion to this paper.

In addition to the investment options of solar and wind technologies, there are four thermal technology options in the set I, defined by their annualized investment costs and operating costs based on technology data forecasts from Energy Information Administration [8] and Fraunhofer Institute for Solar Energy Systems [23] to allow for sufficient VRES and dispatchable energy capacity to permit an assessment of the time-resolution methods (Table 2). The interest rate is set to 5%/annum, and investment costs are annualized over the technical lifetimes of the plants.

Table 2: Technology attributes.

Technology	Investment Cost [k€/MW]	Annual Fixed Cost [k€/MW]	Lifetime [a]	Operating Cost [€/MWh]
Wind	700	0	25	0
Solar	480	0	25	0
Nuclear	2500	43	60	18
Coal	1700	43	40	45
Gas	1000	40	40	52
Backstop	100	0	40	120

2.1.2.2Results

The approach of Nahmmacher et al. [7] is followed here in using the VRES capacity and the system cost (the value of the objective function) to measure accuracy. The additional measure of the generation per technology is used by Wogrin et al. [12]; Frew and Jacobson [6]; and Merrick [15]. For application to investment models, however, the capacity mix is vital, while the dispatch is not since, given the correct capacities, the dispatch can be determined using a dispatch model in a post-investment analysis. Out of the technologies, the VRES capacity sets the scene for the remaining generation, and, therefore, the exposition of the results is concentrated mainly on these.

Fig. 5 shows the deviation of the integral demand-based, integral, and representative days approaches from the VRES capacity predicted, which is the main performance metric used here, by the benchmark model for all regions. The benchmark results are

those from a model run with an entire year of data 2920-time steps. The vertical axis measures the VRES capacity relative to that predicted by the benchmark model, and each dot represents one of the five regions.

In order to establish the necessity of replacing the use of demand-based states in models with a different method for time representation, Fig. 5 shows the performance of the demand-based slicing in gray. It is clear that, regardless of how many time steps in the modelling (¼states) that are allowed, this method overestimates the optimal amount of VRES capacity by a factor of 2-4. Thus, neglecting VRES variation in time slicing and relying solely on the demand to downscale the time dimension will lead to significant inaccuracies from the perspective of capturing VRES capacity.

If the time representation is to be used in a model that allows for only 16-40 time steps, then the integral method gives a much better prediction of the VRES capacity: the regions with maximum discrepancy are 5-15% off the correct capacity compared to the representative days method, where the maximum discrepancy is 40-50% off the correct capacity (Fig. 5 and Fig. 6). The integral approach is remarkably stable and within a 10% error of the benchmark VRES capacity for all runs with more than 32-time steps. The representative days approach may miscalculate the optimal VRES capacity by 50% for less than 40-time steps. It is rare that the representative days approach miscalculates VRES capacity by more than 20% for a number of time steps of 160 (20 days) or more (Fig. 5). This is in line with the results for the test with the more detailed models in references Nahmmacher et al. [7] and Frew and Jacobsen [6].

The system cost (Fig. 7) shows less discrepancy between the results with fewer time steps and the benchmark model results compared to the VRES capacity (Fig. 5). However, the system cost output from an investment model hides discrepancy in capacity mix that would have a greater impact on cost had they been evaluated in, e.g., a unit-commitment model. The system cost is underestimated for low numbers of time steps, especially for the case of integral demand-based slicing (Fig. 7), while the VRES capacity is overestimated (Fig. 5). When the variability of VRES to a large extent is averaged out (such as is the case for demand-based slicing), the load-covering capacity of VRES is overestimated, and, thus, the optimal capacity of VRES is also overestimated. This leads to an underestimate of system cost. Hence, the demand-based slicing approach also underperforms on the basis of the system cost as a metric.

Both methods (integral and representative days) also predict the thermal capacities fairly well. However, one exception is backstop capacity, the need for which depends heavily on extreme events (high demand, low wind, low solar) (Fig. 9). Although results for only the Danish region are shown, similar trends are observed for other regions, viz., an underestimate of peak capacity by both reduction methods.

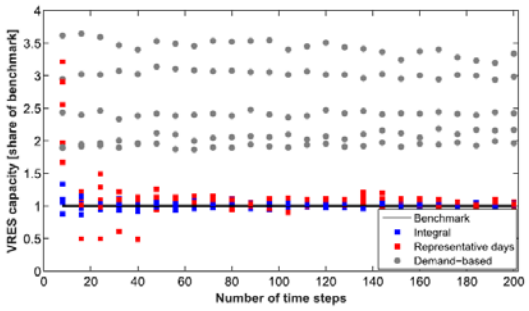

Fig. 5 Performance of time-reduction methods in predicting the VRES capacity.

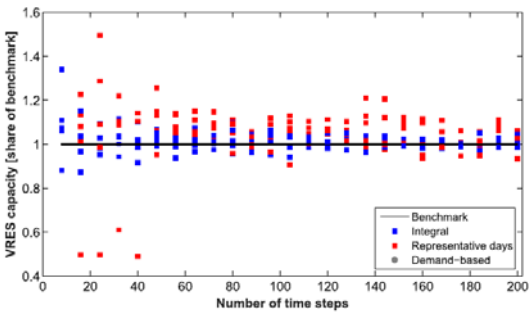

Fig. 6 Performance of time-reduction methods in predicting the VRES capacity (zoom-in of Fig. 5).

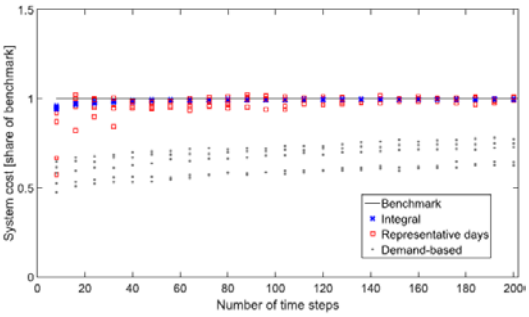

Fig. 7 Performance of time-reduction methods in predicting the system cost.

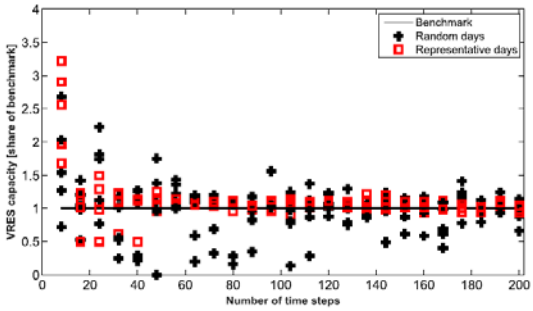

Fig. 8 Performance of randomly selected days in predicting the system cost.

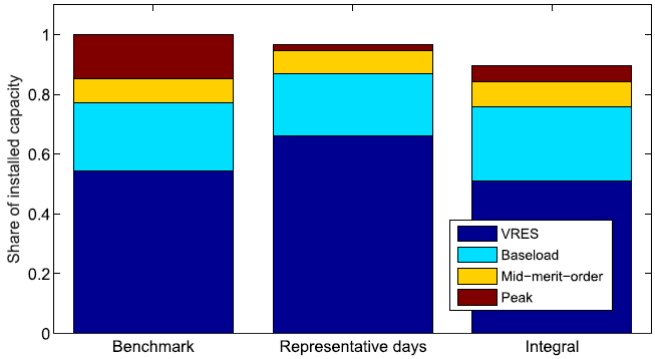

Fig. 9 Installed capacities for the case with 32-time steps (Danish region).

As a corollary to the results on the two methods, results are presented on the importance of the preparation method. Fig. 8 shows the alternative of picking random days instead of performing the preparation step of finding the representative days. As a result, the random-days method may be off by 50% of the VRES capacity predicted by the benchmark model for as many as 168-time steps (21 days).9 Overall, the variance of the VRES capacity is much higher for the random days than for representative days picked using k-means clustering. A similar result is obtained for the integral methods when intervals for finding states are arbitrarily chosen instead of using the clustering method.

2.1.3 Discussion

Two methods (integral and representative days) to downscale the time dimension in power system planning models are compared in order to represent better the cases with a high share of variable generation. The comparison is performed in a simple model, where benchmark results obtained with the full-time resolution may be used as a comparison. The number of time steps to predict VRES capacity within a 10% error margin is approximately 30 for the integral method and approximately 160 for the representative days method. This result may inform developers in choosing an appropriate time representation method for their model and design the model so that it is tractable with the number of time steps needed to come within an acceptable error margin.

Of the two methods tested here, the integral approach has a smaller standard deviation of the resulting VRES capacity for different runs of the heuristic to pick the states/representative days. Even for a low number of time steps, e.g., 32, the integral method with k-means clustering is within 10% accuracy in predicting the VRES capacity. Wogrin et al. [14] use a more complex (unit-commitment) model and find that around 102 time slices are needed. The representative days approach in this work needs 160-200 time steps to reach a 10% accuracy level. The value for the representative days approach in the present study is similar to the results in Nahmmacher et al. [7] and Frew and Jacobson [6]. Frew and Jacobson [6] use another preparation method to find the representative days, which leads to an overestimate of the system cost for around 102 time steps, rather than, as here and in Nahmmacher et al. [7]; an underestimate of the system cost. Merrick [15] uses more stringent measures of accuracy: since he requires several measures (e.g., annual generation) to be within a range of the correct value than just the VRES capacity, his estimate of the number of necessary time steps is instead on the order of 103. Thus, it seems likely that at least 160-time steps are necessary to represent variability with the representative days approach. Due to intractability, many power systems planning models cannot use as many as 160-time steps, and, thus, in order to assure a reliable result, they would need to be redesigned, in effect reducing the technical and/or spatial complexity of the models.

The model that is used for comparing the two time-reduction methods here is a (i) simple (ii) one-node model that (iii) lacks storage options. These three limitations entail that the present experiment can cover only representation of variability and not all variation management strategies. Variation management includes (i) flexibility of the surrounding (mainly thermal) generation system, (ii) flexibility of demand (such as demand-side management, DSM), (iii) curtailment of VRES electricity, (iv) variability smoothing by transmission investment and trade, and (v) storage. These measures become more important as the penetration level of variables increases, and, thus, for many applications, these are, indeed, important to incorporate into models and the method to downscale time. The testing framework is necessarily simplified by using only the technologies that both types of representation methods can incorporate. For

example, the representative days method can handle trade and short-term storage but not overnight storage or hydropower, whereas the integral method has traditionally not been able to handle spatial aspects of a power network. Hence, only by boiling the testing framework down to the current one can one meaningfully compare the two methods' performance in predicting VRES capacity shares directly.

Of the two methods tested here, the representative days method can incorporate trade since it may be employed for network models as is done in Frew et al. [20]; Nahmmacher et al. [7]; and Haller et al. [24]. The representative days method can also represent storage and DSM that takes place within the day-night, which may be a sufficiently good representation for storage that is used mainly for solar power. However, it can neither handle storage over longer periods nor represent the dynamics of hydropower, which may be viewed as a type of storage. The integral method, on the other hand, has traditionally not been employed in a network model with many nodes. Only recently has the integral method been adapted to handle storage operations (but not investment) in a congested network [25]. Thus, it needs further enhancement to tackle investment in the potentially important variation management tool of transmission investment and trade. Both approaches tested here can be expanded to include more variation management strategies. The integral method may be complemented with a transition matrix, as shown in Wogrin et al. [14]; in order to cover cycling and storage. The representative days approach may be expanded to choose representative weeks instead of days, which would a priori be more suited to represent long-term storage, cycling, and hydropower. Both expansions make models larger, thereby increasing computation time, which may render problem instances intractable. A study that extends the test ground for the two families of methods to one that can incorporate all variation management strategies would be beneficial to both the modelling community and policymakers.

The results comparing random days with those selected using one of the two methods show that the preparation step (in this case k-means clustering) is important and impacts the tendency of the model results with the reduced time dimension to underestimate or over-estimate results. In this paper, random picking of days provides little certainty about the accuracy of results: while the k-means clustering method for picking and weighing representative days produces an error margin of 20% or less for greater than 50-time steps, the random picking of days is unstable for all number of time steps tested.

2.1.4 Conclusions and policy implications

Given the importance of VRES capacity investment to most industrialized countries' energy policies, power system modelling that provides a credible basis for devising appropriate regulation is desirable. Thus, large-scale models that rely only on demand-based time slicing are inadequate for assessing power systems with a substantial share of VRES capacity. Indeed, neglecting the dependence between demand and VRES output

could bias a model's predicted VRES capacity share, thereby undermining the basis for policy analysis. In this paper, two time-reduction methods for representing VRES output are compared in order to determine their suitability for inclusion in policy-enabling power system planning models.

It is shown that the integral method for time reduction is well suited to represent variability in a one-node model. To predict VRES capacity well, it is enough to use 30-40 time steps if the time steps are picked using the k-means clustering method described in Nahmmacher et al. [7] and Wogrin et al. [12]. The representative days method needs 160e200 time steps in order to predict VRES capacity with an accuracy of 10%, which is the paper's main performance metric. The conclusions are that:

- For one-node models, at least when the penetration level is below the level where competition between variation management strategies may become important, the integral method seems to be suitable. The model then needs to be designed so that it be convenient to run with 30-time steps. This approach may be adopted in integrated assessment models (IAMs), for example.

- For network models, the representative days approach, with at least 20 such days (160-time steps), is recommended. The requirement of the time dimension exceeds many of the models used for, e.g., policy recommendations, which means that it may be necessary to simplify the models in some other aspect, such as technology description or spatial resolution.

- The preparation step pays off. It is important to apply a stringent method rather than to select periods at random or with some preconceived idea of representativeness.

For future work, the comparison of the two time-slicing methods could be extended to incorporate additional variation management tools, e.g., DSM, storage, and transmission. However, such a study would require enhancing the one-node model by adding constrained transmission lines with the requisite spatial representation. In this case, the representative days approach would have to be based on representative weeks in order to handle storage adequately, while the integral method would require transition matrices to account for both storage and transmission.

2.2 Enhanced Representative Days and System States Modeling for Energy Storage Investment Analysis

Among the different power system planning models, there are short-term models with high time resolution such as unit commitment models, with information pertaining to every hour, half hour, or 10 minutes; and long-term models such as investment models that ignore small time-scale changes so as to make the calculations in a reasonable amount of time.

The introduction of variable renewable energy sources (RES) into the energy system, however, makes it necessary to include more short-term dynamics, such as varying wind or sunlight availability, in long-term models [26]. Models that incorporate information at both time scales include the TIMES modeling framework [27], the Regional Energy Deployment System (ReEDS) framework [4], and the Resource Planning Model (RPM) [28]. These models have multi-year investment decisions as well as 'time slices' within each year that represent a wide variety of possible demand and RES production levels.

The time slices structure allows the models to find solutions on a representative set of situations that the system operator must be able to respond to. However, while they do not include in detail every hour of the time horizon, the calculations are not overly burdensome.

Nowadays, energy storage systems (ESS) have become a promising flexible option to deal with the variability of renewable energy [29]. Realistically modeling ESS requires the preservation of chronological information, because the amount of stored energy available at any given moment depends on the amount of energy stored in all previous time periods [30]. Although some models have endeavored to incorporate ESS investment decisions, they do not preserve chronological information and so do not fully model storage evolution [31], [32]. In this paper We created medium and long-term optimization models for ESS investment with reduced representation of time that nevertheless maintains some chronology for the sake of co-optimizing different types of storage technologies. Moreover, we propose some new models to improve the existing ones in the literature.

2.2.1 Literature review

There are two common ways to reduce temporal information while maintaining some chronology that can be found in the literature: 'representative periods' and 'system states'. The system states are also referred to as load periods, load duration curves, or time slices in more simplified versions. Both methods are based on clustering techniques. In this section, we describe the main characteristics of both methods and review publications that present them.

In the 'representative periods' (RP) method, a certain number of days, groups of days, or in some cases weeks that are representative of the variety of situations that can be found during the course of the time horizon (e.g. year) are chosen. All calculations (e.g. investment decisions and unit dispatch) are done for the selected days or weeks. Each RP 'represents' the periods in the year that are similar to itself, so one can reconstruct the behavior of the system over the whole year by using the values calculated for the RPs in place of the periods they represent. The RPs preserve the internal chronology of their hours, making for a more realistic representation of changing storage level over the course of a day or week. However, the RP method does not preserve the chronology among the RPs. Therefore, any ESS with a cycle longer than the RP (e.g. weekly monthly, or yearly rather than daily) will not be chronologically represented with the highest accuracy. This method has been used for some of the models that try to incorporate both long- and short-term dynamics, such as the RPM model in ref. [33]. There has been much debate about the best way to choose these RPs. Some authors use a heuristic method, choosing one day for each season or one day in each season for the week and for the weekend. Others have proposed methods that involve optimizing both the number and clustering of RPs to minimize the difference between the load duration curve and the approximate one created by the RPs [34], [35]. There has also been debate about the optimal length for RPs. For instance in [36], the authors suggested representative groups of days or representative weeks, whose advantage is that it increases the amount of chronology preserved, and whose disadvantage is, of course, that it increases the calculational burden. The most versatile method for grouping RPs comes from [7], and relies on clustering techniques (e.g. k-means or k-medoids) to group a number of hours with any number of normalized characteristics (solar energy, demand, wind energy, etc). No matter how long the periods or how they are chosen, the drawback of the RP method is that it can only deal with relatively short-term storage cycles, those that charge and discharges in the course of a period (e.g. day), but not, for example, with hydro reservoirs with monthly or yearly cycles.

The other method, 'system states' (SS) was introduced in [12]. It is designed to be an improvement on the entirely non-chronological load duration curve method. The SS method characterizes each time step (e.g. hours) in the time horizon by a set of features such as demand, wind, and solar power availability. Hours with similar values of these features are considered to belong to the same 'system state'. Every hour in the time horizon is then assigned to one of the system states, and calculations are done for each system state in the same way they would be done for each hour of an hourly model. As with the representative periods, each system state gets a weight or duration that depends on the number of real time periods in the time horizon that are represented by it. This is also called time slices in models such as ReEDS [20]. The innovation of SS method in [12] is the transition matrix, which counts up the number of transitions between all system states, allowing the addition of chronological constraints, such as start-up constraints. In ref. [14] the system states method was extended to deal with storage. Although each system state can only calculate the change in energy storage,

the total storage in any given hour can be calculated ex post by adding up all the changes in storage from the beginning of the time horizon to the hour of interest. The total storage is kept within bounds during the modeling process by backtracking to calculate the total storage at certain chosen hours in the time horizon and constraining storage in those hours to be in bounds. This idea was applied and analyzed in [25] for the operation of a network-constrained power system. This paper further extends the use of this SS method to the ESS investment problem.

As we mention at the beginning of this section, this work focuses on the reduction of temporal information. However, there are other types of reduction techniques to deal with the computational burden in long-term planning models, such as transmission network aggregation [37], [38]; exogenous estimation of curtailment reduction, curtailment itself, and capacity value [33], [39]. These methods are compatible with the models proposed in this paper and could be combined to further improve the reduction of the computational burden. Nevertheless, these sorts of combinations are beyond the scope of this work.

The first aim of this paper is to compare the SS method and the RP method for an ESS investment model in order to determine which one is better or what system characteristics the quality of the approximation method depends on. However, we found some difficulties and drawbacks in the basic formulation of both methods, which are explained in Section 2.2.2.5. Therefore, the second aim of this paper is to develop enhanced versions of both methods in order deal with these difficulties. Thus, the main contributions of this paper are:

- The extension of the SS method in [14], [25] to consider ESS investment.
- The formulation of enhanced versions of SS and RP to preserve the chronological information of different kinds of ESS cycles (from hourly to yearly), which outperform existing methods in terms of solution quality and CPU time and allow for the co-optimization of both short- and long-term storage.
- The comparison of SS and RP for ESS investment models using an hourly unit commitment model as a benchmark.

2.2.2 Model Formulation

This section contains the five model formulations compared in this paper.

2.2.2.1Notation

In the following formulation "p/s" refer to the parameters used to identify time divisions: periods (e.g. 1 h) in the detailed model and states in the system states model respectively.

2.2.2.1.1Indices and Sets

$p \in$ P	Periods (hours)
$p_l(p)$	Subset with the last period of the time horizon
$s, s' \in S$	System states
$k \in$ K	Periods in which storage limit constraints are imposed in system states models
$g \in G$	Generation units (thermal or storage)
$t(g)$	Subset of thermal generation units
$h(g)$	Subset of storage units
$h_l(g)$	Subset of long-term storage (e.g., hydro) units
$h_s(g)$	Subset of short-term storage (e.g., batteries) units
$n, n' \in$ N	Electrical nodes o buses
$n_s(n)$	Subset of electrical nodes or buses without slack bus
c	Circuits
$\mathcal{G}_{gn}$	Generators g connected to bus n
$\Theta_{nn'c}$	Circuits c connected between bus n' and n
$rp \in RP$	Set of representative periods (e.g., days, weeks)
Γ_{rpp}	Injective map of each period p to a representative period rp
$H_{pp'}$	Injective map of each period p to a period $p' \in \Gamma_{rpp}$
$p_f(p, rp)$	Subset with the first period p of the representative period rp

2.2.2.1.2Parameters

C_g^{fuel}	Cost of consumed fuel	[k€/MJ]
α_g	Variable term of fuel consumption	[MJ/GWh]
β_g	Fixed term of fuel consumption	[MJ]
γ_g	Fuel consumption during the startup	[MJ]
C_g^{om}	Cost of operation and maintenance	[k€/GWh]
$D_{p/s\,n}$	Electricity demand per node	[GW]
$V_{p/s\,n}^{max}$	Renewable production per node (e.g., wind or solar)	[GW]
Q_g^{max}, Q_g^{min}	Upper and lower bound on production	[GW]
SRR_g	Maximum 10-minute ramp	[GW]
X^{res}	Operating reserve	[p.u.]
$W0_h$	Initial storage level	[GWh]
W_h^{max}, W_h^{min}	Upper and lower bound on energy storage	[GWh]
W_h^{fin}	Minimum final storage level	[GWh]
$I_{p/s\,h}$	Hourly energy inflows	[GWh]
η_h	Efficiency of storage unit	[p.u.]
B_h^{max}	Upper bound on charging/pumping	[GW]
T_s	Duration of state	[h]
$TC_{n\,n'c}^{max}$	Transmission capacity of circuit c	[GW]
$ISF_{n\,n'c\,n_s}$	Injection Shift Factors	[p.u.]
$N_{s\,s'}$	Transition matrix between states	
$F_{s\,s'k}$	Frequency matrix between states and changes	
$RFM_{s\,s'k}$	Reduced Frequency Matrix between states and changes	
WG_{rp}	Weight of representative periods	[h]
$NRP_{rp\,rp'}$	Transition matrix between representative periods	
NP_{rp}	Number of periods at each representative period	[h]
M	Moving window for storage level	[h]

C_h^{inv}	Investment cost for storage units	[k€/GW]
EPR_h^{max}, EPR_h^{min}	Maximum and minimum energy to power ratio	[h]

2.2.2.1.3Variables

$q_{p/s\,g}$	Power production	[GW]
$\hat{q}_{p/s\,g}$	Power production above Q_g^{min}	[GW]
$v_{p/s\,n}$	Renewable production	[GW]
$r_{p/s\,g}$	Spinning reserve	[GW]
$w_{p/s\,h}$	Storage level	[GWh]
$\Delta w_{s\,s'\,h}$	Difference in storage	[GWh]
$b_{p/s\,h}$	Hourly charged/pumped power	[GW]
$sp_{p/s\,h}$	Hourly energy spillage	[GWh]
$pf_{p/s\,nn'c}$	Power flow per circuit	[GW]
$pns_{p/s\,n}$	Power not supply per node	[GW]
$u_{p/s\,g}$	Binary dispatch decision	[0-1]
$y_{p/s\,g}$	Binary startup decision	[0-1]
$y_{s\,s'\,g}$	Binary startup decision for state model	[0-1]
x_h	Storage investment	[GW]

2.2.2.2Hourly Unit Commitment Model (HM)

The following equations describe the hourly unit commitment model used as the benchmark to test the proposed models, which is based on ref. [40].

$$min_{\Omega} \sum_{p,t}\{C_t^{fuel}\cdot[\beta_t u_{pt}+\gamma_t y_{pt}+\alpha_t q_{pt}]+C_t^{om}q_{pt}\}+\sum_h C_h^{inv}x_h \qquad (1a)$$

Subject to:

$\sum_{t\in\mathcal{G}} q_{pt}+\sum_{h\in\mathcal{G}}(q_{ph}-b_{ph})+v_{pn}+\sum_{n'c\in\Theta}(pf_{pn'nc}-pf_{pnn'c})+pns_{pn}=D_{pn}$	$\forall\, p,n$	$(1b)$
$pf_{pnn'c}=\sum_{n_s} ISF_{nn'cn_s}\cdot\left[\sum_{t\in\mathcal{G}_{tn_s}} q_{pt}+\sum_{h\in\mathcal{G}_{hn_s}}(q_{ph}-b_{ph})+v_{pn_s}+pns_{pn_s}-D_{pn_s}\right]$	$\forall\, nn'c\in\Theta,p$	$(1c)$
$q_{pt}=Q_t^{min}u_{pt}+\hat{q}_{pt}$	$\forall\, p,t$	$(1d)$
$0\le\hat{q}_{pt}\le(Q_t^{max}-Q_t^{min})u_{pt}$	$\forall\, p,t$	$(1e)$
$u_{pt}-u_{p-1,t}\le y_{pt}$	$\forall\, p,t$	$(1f)$
$r_{pt}+q_{pt}\le u_{pt}Q_t^{max}$	$\forall\, p,t$	$(1g)$
$0\le r_{pt}\le SRR_t$	$\forall\, p,t$	$(1h)$
$\sum_t r_{pt}\ge X^{res}\cdot\sum_n D_{pn}$	$\forall\, p$	$(1i)$
$u_{pt},y_{pt}\in\{0,1\}$	$\forall\, p,t$	$(1j)$
$w_{ph}=w_{p-1,h}+W0_{p=1,h}+I_{ph}-q_{ph}-sp_{ph}+\eta_h b_{ph}$	$\forall\, p,h$	$(1k)$
$0\le v_{pn}\le V_{pn}^{max}$	$\forall\, p,n$	$(1l)$
$0\le q_{ph}\le Q_h^{max}+x_h$	$\forall\, p,h$	$(1m)$
$0\le b_{ph}\le B_h^{max}+\eta_h x_h$	$\forall\, p,h$	$(1n)$
$0\le sp_{ph}$	$\forall\, p,h$	$(1o)$
$\lvert pf_{pnn'c}\rvert\le TC_{nn'c}^{max}$	$\forall\, nn'c\in\Theta,p$	$(1p)$
$W_h^{min}+EPR_h^{min}x_h\le w_{ph}\le W_h^{max}+EPR_h^{max}x_h$	$\forall\, p,h$	$(1q)$
$w_{p_l,h}\ge W_h^{fin}$	$\forall\, h$	$(1r)$

The objective function $(1a)$ minimizes storage investment costs and the total operating cost of the system (e.g. startup costs, fixed costs, variable costs, operations and maintenance costs, and penalties for spillage and energy not supplied). Constraint $(1b)$ is the demand balance equation. Constraint $(1c)$ represents the power flow equation using Injection Shift Factors (ISF). Constraints $(1d-1e)$ ensure thermal unit production is within minimum and maximum capacity. $(1f)$ is the startup constraint of the unit-commitment. $(1g-1i)$ are reserve constraints. $(1j)$ states that the commitment and connection variables are binary. $(1k)$ is the storage constraint which states that the storage in any hour is the storage in the previous hour plus the net charging and discharging in the current hour. $(1l-1q)$ keep within bounds the renewable production per node, the power output per storage unit, the pumped power per storage unit, the energy spillage, the power flow through a line, and the amount of energy stored in each storage unit. $(1m)$ and $(1n)$ include the power capacity increase due to the storage investment variable. $(1p)$ includes the energy capacity increase considering parameters EPR_h^{max} and EPR_h^{min}. These parameters describe the relationship between the energy that can be stored (maximum and minimum respectively) and the nominal power of the equipment. Finally, constraint $(1r)$ establishes the minimum storage level at the last period of the time horizon.

2.2.2.3System States Model (SS)

This section presents the formulation of the system states model as conceived in [25].

$$min_{\Omega} \sum_{s,t}\left\{C_t^{fuel}\cdot\left[T_s\beta_t u_{st}+\sum_{s'\neq s}N_{s's}\gamma_t y_{s'st}+T_s\alpha_t q_{st}\right]+C_t^{om}T_s q_{st}\right\}+\sum\nolimits_h C_h^{inv}x_h \qquad (2a)$$

Subject to:

$\sum_{t\in\mathcal{G}} q_{st}+\sum_{h\in\mathcal{G}}(q_{sh}-b_{sh})+v_{sn}+\sum_{n'c\in\Theta}(pf_{sn'nc}-pf_{snn'c})+pns_{sn}=D_{sn}$	$\forall\, s,n$	$(2b)$
$pf_{snn'c}=\sum_{n_s} ISF_{nn'cn_s}\cdot\left[\sum_{t\in\mathcal{G}_{tn_s}} q_{st}+\sum_{h\in\mathcal{G}_{hn_s}}(q_{sh}-b_{sh})+v_{sn_s}+pns_{sn_s}-D_{sn_s}\right]$	$\forall\, nn'c\in\Theta, s$	$(2c)$
$q_{st}=Q_t^{min}u_{st}+\hat{q}_{st}$	$\forall\, s,t$	$(2d)$
$0\leq\hat{q}_{st}\leq\left(Q_t^{max}-Q_t^{min}\right)u_{st}$	$\forall\, s,t$	$(2e)$
$u_{st}-u_{s',t}\leq y_{s'st}$	$\forall\, s,t$	$(2f)$
$r_{st}+q_{st}\leq u_{st}Q_t^{max}$	$\forall\, s,t$	$(2g)$
$0\leq r_{st}\leq SRR_t$	$\forall\, s,t$	$(2h)$
$\sum_t r_{st}\geq X^{res}\cdot\sum_n D_{sn}$	$\forall\, s$	$(2i)$
$u_{st}, y_{s'st}\in\{0,1\}$	$\forall\, s,t$	$(2j)$
$0\leq v_{sn}\leq V_{sn}^{max}$	$\forall\, s,n$	$(2k)$
$0\leq q_{sh}\leq Q_h^{max}+x_h$	$\forall\, s,h$	$(2l)$
$0\leq b_{sh}\leq B_h^{max}+\eta_h x_h$	$\forall\, s,h$	$(2m)$
$0\leq sp_{sh}$	$\forall\, s,h$	$(2n)$
$\lvert pf_{snn'c}\rvert\leq TC_{nn'c}^{max}$	$\forall\, nn'c\in\Theta, s$	$(2o)$
$\Delta w_{ss'h}=0.5\cdot(I_{sh}+I_{s'h}+\eta_h b_{sh}+\eta_h b_{s'h}-q_{sh}-q_{s'h}-sp_{sh}-sp_{s'h})$	$\forall\, s,s',h$	$(2p)$

$$\sum_{\substack{s,s' \ s.t. \\ N_{ss'}>0}} N_{ss'} \cdot \Delta w_{ss'h} \geq W_h^{fin} - W0_h + EPR_h^{min} x_h \qquad \forall\, h \qquad (2q)$$

$$\sum_{\substack{s,s' \ s.t. \\ N_{ss'}>0}} N_{ss'} \cdot \Delta w_{ss'h} \leq W_h^{max} - W0_h + EPR_h^{max} x_h \qquad \forall\, h \qquad (2r)$$

$$\sum_{\substack{s,s' \ s.t. \\ F_{ss'k}>0}} F_{ss'k} \cdot \Delta w_{ss'h} \geq W_h^{min} - W0_h + EPR_h^{min} x_h \qquad \forall\, h,k \qquad (2s)$$

$$\sum_{\substack{s,s' \ s.t. \\ F_{ss'k}>0}} F_{ss'k} \cdot \Delta w_{ss'h} \leq W_h^{max} - W0_h + EPR_h^{max} x_h \qquad \forall\, h,k \qquad (2t)$$

The objective function $(2a)$ incorporates storage investment and operational costs just as in the hourly model. The costs of each state are weighted by the number of hours in the time horizon that belong to that state, and the startup costs are multiplied by the transition matrix which gives the number of transitions between each set of states. Constraints $(2b)$ to $(2o)$ are formulated exactly as in the hourly model, except that they are defined for each system state 's' rather than each hour 'p'. $(2p-2t)$ are the system states formulation of the storage constraints. $(2p)$ defines the variable Δw which is the central difference of the net energy storage gained in two states between which there is a transition. $(2q)$ and $(2r)$ ensure that storage in the first and last hours of the time horizon are within upper and lower bounds including the storage investment. The amount of storage in the last hour of the time horizon is determined by multiplying each Δw by the corresponding value in the transition matrix and adding them all up. $(2s)$ and $(2t)$ try to keep the energy storage within bounds throughout the time horizon including the storage investment. At each of the hours, k, a subset of all hours in the time horizon, $(2s)$ and $(2t)$ add up all Δw from the beginning of the time horizon with the aid of the frequency matrices and make certain they are between maximum and minimum storage values.

2.2.2.4Representative Periods (Days/Weeks) Model (RP)

This section describes the RP model which is a commonly used method of reducing temporal information. Although the model is general enough to work with RPs of any length, we will speak of representative days for the sake of simplicity. The formulation is roughly the same as that of the hourly model, except the constraints only apply to the hours within the representative days.

$$min_{\Omega} \sum_{p,rp \epsilon \Gamma_{rpp}} \left\{ WG_{rp} \cdot \sum_t \{ C_t^{fuel} \cdot [\beta_t u_{pt} + \gamma_t y_{pt} + \alpha_t q_{pt}] + C_t^{om} q_{pt} \} \right\} + \sum_h C_h^{inv} x_h \qquad (3a)$$

Subject to:

Equations $(1b) - (1r)$ $\forall\, p \epsilon \Gamma_{rpp}$

$$w_{p=p_f(p,rp)+NP_{rp}-1,h} \geq w_{p=p_f(p,rp),h} \qquad \forall\, (p,rp) \epsilon \Gamma_{rpp}, h \qquad (3b)$$

The objective function $(3a)$ minimizes the storage investment cost and operational cost just as in the hourly model, except that the operational costs associated with each day are multiplied by the number of days in the time horizon that are represented by it to yield the cost for the entire time horizon. The RP model is constrained to equations $(1b)$

to $(1r)$ from the HM benchmark model. Nevertheless, in the RP model, equations $(1b)$ to $(1r)$ only apply to hours belonging to the selected representative days.

Equation $(3b)$ is a special constraint introduced into the RP model that guarantees that the amount of energy stored in each unit at the end of each representative day is greater than or equal to the amount of energy in storage at the beginning of the day. Since each day is calculated separately, this prevents a unit from finishing a day with less energy than the starting level of the next day, and thus creating energy from nothing. This is a very simple way to deal with the maximum energy storage per year. Other approaches ensure that the change accumulated over each representative period does not exceed the storage limits and ensure balance over the whole year. However, for the sake of simplicity, these types of approaches are not analyzed in this paper.

Despite the incorporation of (3b), each representative day is independent of the others and the RP model does not guarantee chronological continuity among the representative days for the ESS.

2.2.2.5Comments about System States and Representative Periods models

The SS and RP models have some drawbacks, which are detailed in a case study in Section 2.2.3. In this section, we summarize these drawbacks:

- The SS model results and CPU time are highly dependent on equations (2s) and (2t). These equations guarantee that storage levels are between the maximum and minimum for each storage unit throughout the time horizon and help to keep some chronological information in the optimization process. Equations (2s) and (2t) do, however, have two disadvantages. First, short-term storage devices such as batteries require several bounds in a day to ensure that storage levels are within bounds, but the greater the number of bounds, the longer the CPU time. Second, in order to determine the number of bounds (i.e. set k size) we need an iterative process detailed in [25] which adds even more CPU time to the SS model.

- The RP model solves each representative period (e.g. day) independently and with the same constraints as the HM model. CPU time thus depends on the number of representative periods instead of on the number of bounds for storage units, as it does in the SS Model. The main drawback is that chronology among the representative periods is lost and storage levels of storage units with a cycle longer than the representative period (e.g. hydro units) are not determined adequately. This is especially important in hydrothermal power systems or power systems with pumped hydro storage potential.

In the following sections, we propose enhanced versions of the SS and RP models to tackle these drawbacks.

2.2.2.6System States Model with Reduced Frequency Matrix (SS-RFM)

This section shows the formulation of the System States Reduced Frequency Matrix Model, hereafter SS-RFM. This is a new variation on the system states model created to reduce the computational time and avoid the iterative process for determining storage bounds constraints.

$Objective\ function$: Equation $(2a)$

Subject to:

Equations $(2b)$ – $(2r)$

$$\sum_{\substack{s,s' \text{ s.t.} \\ F_{ss'k}>0}} F_{ss'k} \cdot \Delta w_{ss'h_l} \geq W_{h_l}^{min} - W0_{h_l} + EPR_h^{min} x_h \qquad \forall\, h_l, k \qquad (4a)$$

$$\sum_{\substack{s,s' \text{ s.t.} \\ F_{ss'k}>0}} F_{ss'k} \cdot \Delta w_{ss'h_l} \leq W_{h_l}^{max} - W0_{h_l} + EPR_h^{max} x_h \qquad \forall\, h_l, k \qquad (4b)$$

$$\sum_{\substack{s,s' \text{ s.t.} \\ RFM_{ss'k}>0}} RFM_{ss'k} \cdot \Delta w_{ss'h_s} \geq W_{h_s}^{min} - W0_{h_s} + EPR_h^{min} x_h \qquad \forall\, h_s, k \qquad (4c)$$

$$\sum_{\substack{s,s' \text{ s.t.} \\ RFM_{ss'k}>0}} RFM_{ss'k} \cdot \Delta w_{ss'h_s} \leq W_{h_s}^{max} - W0_{h_s} + EPR_h^{max} x_h \qquad \forall\, h_s, k \qquad (4d)$$

The objective function $(2a)$ and constraints $(2b - 2r)$ are exactly the same as in the SS model. The difference between the two models lies in the handling of storage which has been separated into long- and short-term storage, each with its own set of constraints. $(4a)$ and $(4b)$ take the same form as $(2s)$ and $(2t)$, but are only applied to long-term storage, which is likely to go through only one or two cycles per year. Set k is a subset of hours in the time horizon in which the upper and lower bound are checked. At each hour k, $(2s)$ and $(2t)$ use the frequency matrices to add up all changes in storage from the beginning of the time horizon to hour k and check that the total is within bounds. $(4c)$ and $(4d)$, represent the storage constraints for short-term storage. At each hour k, they add up all the net changes in storage since the last hour k and constrain that sum to be within bounds. This is done with the aid of the Reduced Frequency Matrix (RFM), an innovation of this model which is just the difference between the frequency matrix ($F_{ss'k}$) corresponding to the current hour k and that corresponding to the previous element in set k, that is, $k-1$. In other words, the difference between these two elements or hours in the set k could be understood as a moving window. It is important to mention that despite the use of the RFM, the storage level could be out of bounds because the hours in set k are predefined in the model and we do not know in advance the storage level value at each hour in set k. The best practice for reducing the number of hours in which the storage levels can be out of bounds is to predefine the moving window considering the smallest storage cycle in the power system.

2.2.2.7Representative Periods Model with Transition Matrix and Cluster Indices (RP-TM&CI)

This section shows the Representative Period with Transition Matrix and Cluster Indices (RP-TM&CI) model which is the second original contribution of this paper. Although the model is sufficiently general to be able to work with representative periods of any length, we will once again speak of representative days for the sake of simplicity.

$Objective\ function$: $(3a)$

Subject to:

Equations $(1b) - (1r)\ \forall\ p \epsilon \Gamma_{rpp}$

$$u_{p'=p_f(p',rp')+NP_{rp}-1,t} = u_{p=p_f(p,rp),t} \qquad \forall\ t,(p,rp)\epsilon\Gamma_{rpp},rp' \ /\ NRP_{rp\,rp'} > 0 \qquad (5a)$$

$$w_{ph} = w_{p-M,h} + W0_{p=1,h} + \sum_{p'=p-M+1}^{p} \sum_{p'' \in H_{p'p''}} \left(I_{p''h} - q_{p''h} - sp_{p''h} + \eta_h b_{p''h}\right) \qquad \forall\ p,h \qquad (5b)$$

The objective function has the same formulation as the regular representative day model, i.e. $(3a)$. The RP-TM&CI model is constrained with equations $(1b)$ to $(1r)$ for all the hours belonging to the selected representative days. $(5a)$ is an innovation of this model. It creates continuity between the representative days and prevents unnecessary startups by using a transition matrix to require that for any pair of representative days that transition from one to the other, the thermal units that are on in the last hour of the first are also on in the first hour of the second. As written here, if there is even one transition between the two days, this constraint is applied. However, the constraint could be set to take effect only if there is a considerable number of transitions between the two days, 5 or 10% of the transitions in the time horizon, for example. $(5b)$ is the second innovation of this model; it creates the continuity in storage across the entire time horizon that allows for the modeling of long-term storage. It does this by checking at regular intervals (1 week) that all the energy charged and discharged since the previous week plus the total energy at the last check point are within bounds. This is possible because, as a result of the clustering procedure to determine the representative days, we know the Cluster Indices (CI), which is a numeric column vector where each row indicates the cluster assignment (i.e. representative day) of the corresponding day of the year. This information is included in the model using the subset $H_{pp'}$.

2.2.3 Case Studies and Results

As a case study, we chose the Spanish power system in target year 2030. The Spanish case is interesting because it has hydro reservoirs (i.e. ESS with monthly or yearly cycle) and, according to ENTSO-E [41], the next ten years will likely bring investment in Battery Energy Storage System (BESS) and Pumped Hydroelectric Energy Storage (PHES), i.e. ESS with daily or weekly cycle. We ran four different scenarios or visions for 2030 on the

hourly model and the four approximate models. The wind and solar profiles for these visions were taken from [42], [43] while hourly demand data and annual production per technology were taken from the ENTSO-E 'Ten Year Network Development Plan 2016' [41]. Vision 1 and 3 were based on national predictions, whereas visions 2 and 4 were designed with the whole of Europe and climate protection goals in mind. The scenarios include a significant development of renewable electricity sources, supplying 35% to 60% of the total annual demand, depending on the Vision. Moreover, the hourly demand curve of each Vision reflects the potential for demand response, which rises from 5% in Vision 1 to 20% in Vision 4. A summary of the main assumptions of each vision can be found in the Appendix.

For each of the four visions, the SS and RP models were run with four different numbers of clusters for increasing time resolution. The RP and RP-TM&CI models used 4, 9, 18, and 37 representative days which corresponds respectively to 1%, 2%, 5% and 10% of the time horizon. Time resolution within each representative day is hourly. The SS and SS-RFM models used 26, 48, 96, and 216 system states. These numbers of states were chosen because they provided a 'fair' comparison with the clusters used with the RP models by having roughly the same number of binary variables.

The representative days were chosen by normalizing time series for the hourly demand, wind availability, solar availability, and hydro inflows, and combining 24 hours of those time series (96 dimensions in all) into a single point to be clustered with the rest of days of the year using k-medoids. The system states were chosen in an analogous manner. The four-time series were normalized, but this time each point to be clustered represented only one hour (4 dimensions) and the clustering method was k- means so that the resulting system state was the centroid of the cluster (a composite hour) rather than a true hour.

We performed two analyses. In the first one, we ran the models without ESS investment in order to determine the accuracy of the models from the operational point of view. In the second, we analyzed the ESS investment to compare the results of investment decisions made by the four approximate models to those of the benchmark, HM model.

2.2.3.1Operation Only Results

For this case study, we considered a total BESS installed capacity of 10 GWh with a maximum output of 1 GW and a 0.9 efficiency coefficient.

Fig. 10 shows a box & whisker plot for CPU Time and objective function error considering the results for each vision. All models were solved until optimality, i.e. until the integrality gap equaled zero. Fig. 10 shows the time necessary for the solution of each model as a fraction of the time taken by the hourly model as the number of clusters (i.e. system states or representative days) increases. As expected, the amount of time necessary for model solution increases with the temporal resolution, but up to the 3rd

time resolution (18rp, 96ss) all four approximate models took less than 5% of the time that the hourly models took. Also, as expected, increasing the number of system states or representative days reduced the error in the objective function, see Fig. 11. Fig. 11 also shows the improvement obtained with the SS-RFM and RP-TM&CI models proposed in this paper. The SS-RFM model took between 4 and 20 times less CPU time than the SS model without hampering the performance of the approximation in the objective function error. Moreover, the RP-TM&CI model reduced the objective function error of RP model as the number of representative days increase without a significant rise in the CPU time. These results show some of the advantages of the model proposed in this paper. For the sake of simplicity, the rest of this section shows only the results for the 3rd time resolution (18rp, 96ss) because it has a good trade-off between CPU time and objective function error.

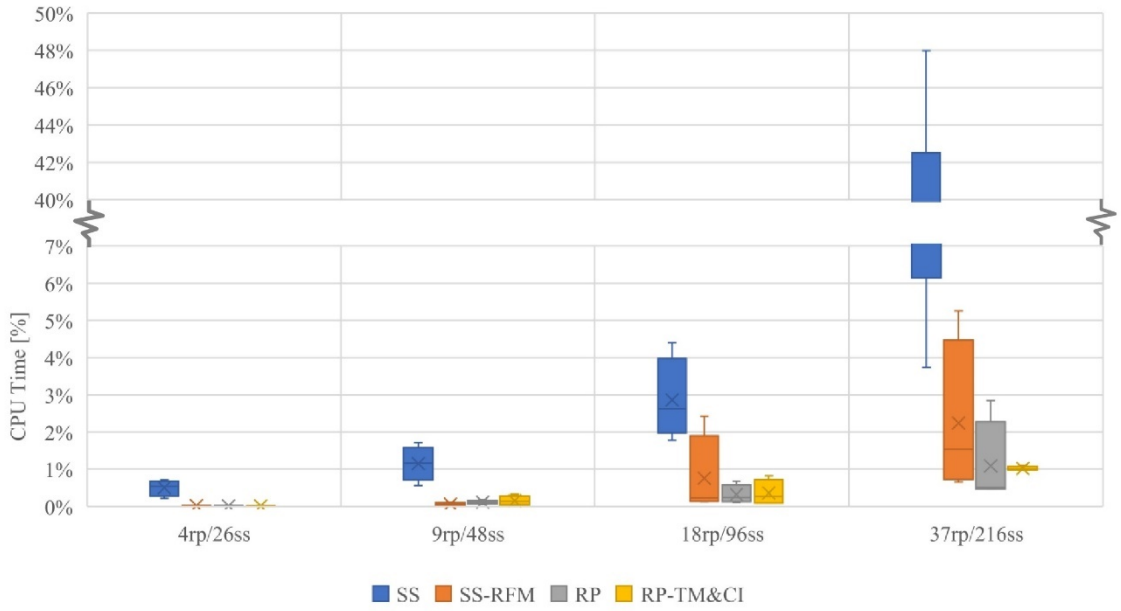

Fig. 10 CPU time.

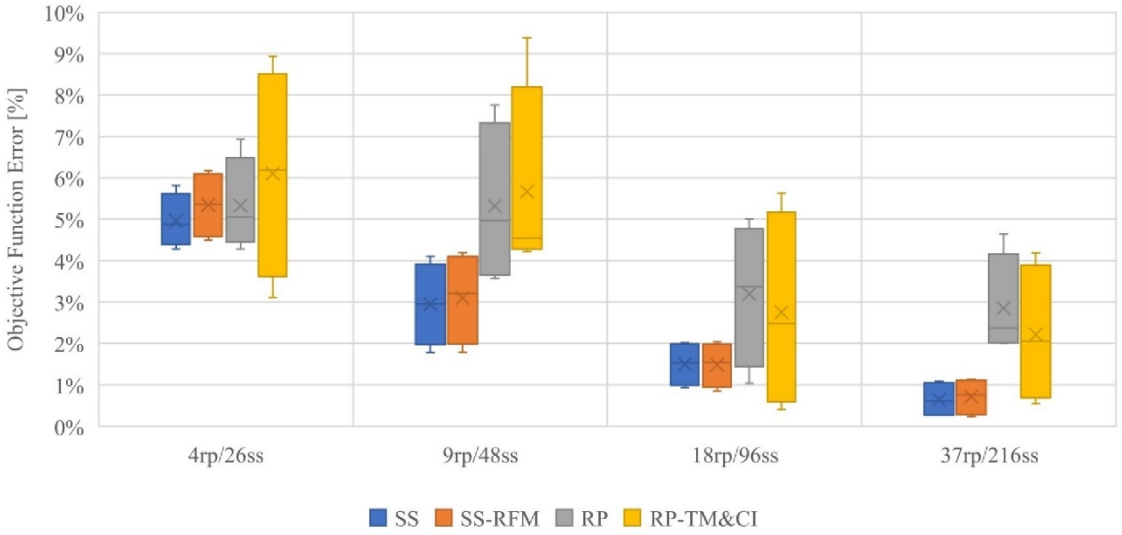

Fig. 11 Objective function error.

So far, we have used objective function error to judge the accuracy of the approximate models, nevertheless, results such as annual production per technology, total number of startups, and energy prices allow for a more detailed comparison. Table 3 shows the average error for these results when comparing each approximate model to the hourly model. Negative values in Table 3 show overestimation in the approximate model while positive values are underestimation. For thermal production SS, SS-RFM, and RP-TM&CI models have errors lower than 3% while the RP model has error between 5% and 11% because it solves each representative day individually. The SS and SS-RFM models give the estimation of total hydro production closest to that of the hourly model while the RP model gives a very poor estimate. This is because the RP model constrains the storage at the end of each day to be higher than at the beginning so hydro storage cannot evolve according to its natural yearly cycle. The RP-TM&CI model, however, does succeed in estimating the annual hydro production, which is what it was designed to do. The SS and SS-RFM models do not approximate the annual battery production very well, as the models cannot keep the energy fully within bounds throughout the time horizon. The RP-TM&CI model gives a value of the total annual battery production that is closest to the HM model. RES production is estimated with good accuracy (i.e. errors less than 0.5%) for all models, while the RES curtailment has more error and is underestimated in all models. However, representative periods-type models have slightly better accuracy than system states-type models. The RP model overestimates the number of necessary startups during the year of peaking units (CCGT), which is only to be expected since it treats each day as separate from the others. Because they maintain some chronology between periods using the transition matrix, SS and SS-RFM do a better job of estimating startups than the RP. However, the RP-TM&CI model has the number of startups closest to that of the HM model, as it uses its transition matrix to keep continuity between the thermal units at the end of one day and the beginning of the next. These results also demonstrate the effectiveness of the RP-TM&CI model over the RP model. In the case of the energy prices, the RP model makes the worst estimate due to the previous results.

The average prices in SS, SS-RFM, and RP-TM&CI are all quite accurate, but the maximum price is better estimated in the enhanced models, SS-RFM and RP-TM&CI. This is important because the storage investment results are partially driven by the differences between the maximum and minimum prices.

Table 3: Average errors.

Result		SS	SS-RFM	RP	RP-TM&CI
Production	Nuclear	-0.3%	-0.2%	5.4%	-0.2%
	Coal	1.9%	1.2%	10.5%	-2.0%
	CCGT	2.3%	2.8%	-10.6%	1.3%
	Hydro	-0.2%	-0.2%	-10.4%	0.8%
	Battery	7.3%	11.3%	-17.0%	-4.8%
	Renewable	-0.5%	-0.5%	-0.4%	-0.5%
RES curtailment		24.7%	24.9%	18.4%	18.6%
Start-up	Coal	-53.9%	-54.3%	-52.4%	-9.3%
	CCGT	-73.6%	-75.2%	-91.3%	-21.0%
Price	Average	-0.5%	0.03%	8.0%	0.7%
	Max	-25.4%	-8.5%	-22.7%	2.1%
	Min	0.0%	0.0%	0.0%	0.0%

Fig. 12 shows the storage level evolution for hydro unit and BESS for vision 1. Not only is the total yearly hydro production estimated by SS, SS-RFM, and RP-TM&CI very close to that of the HM as shown in Fig. 12, but the overall storage evolution closely follows that of the HM, Fig. 12. The RP model cannot correctly estimate the evolution of storage levels considering the production, consumption, inflows, and spillages for each representative day because the representative days are not related among themselves. The RP-TM&CI model fixes this by considering chronology among the representative days using the transition matrix and cluster indices. In fact, the RP-TM&CI model yields the prediction of hydro storage levels that is most similar to that of the HM model. The BESS storage level is shown in Fig. 13 for a week of the year. RP and RP-TM&CI models perform best when the BESS charge and discharge in a single day. If, however, the true BESS charges and discharges over the course of more than one day then the RP and RP-TM&CI have trouble approximating that, as they are limited to the representative days. Despite this, the RP-TM&CI model performs better than the RP model due to the chronological information shared among the representative days. The SS and SS-RFM models have better performance than the representative days models because they are not limited to the period length, i.e. 24 hours, and this allows them to capture charging and discharging periods longer than a day. However, as mentioned in Section 2.2.2.6, the SSs model cannot guarantee that BESS storage levels stay within bounds. In Fig. 13 both SS and SS-RFM predict that BESS storage levels will exceed the upper bound, which is unrealistic in a power system operation. To correct that behavior, the number of constraints should be increased, but this vastly increases CPU time in the SS model and increases the error in the SS-RFM model. If the extra constrained hours are chosen using the iterative method, this increases the CPU time still further.

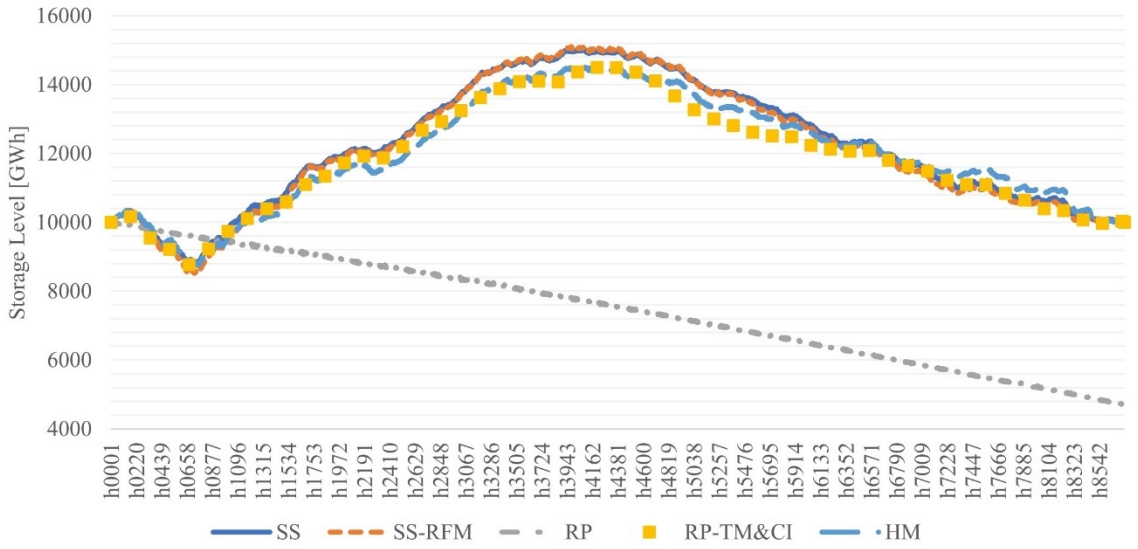

Fig. 12 Hydro storage level.

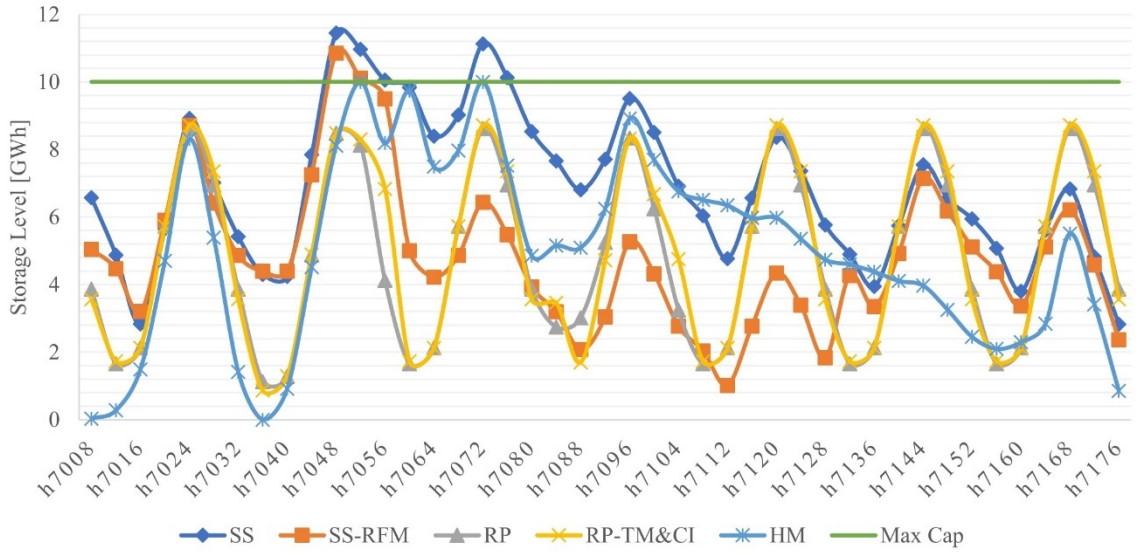

Fig. 13 BESS storage level.

2.2.3.2ESS Investment Results

For this case study only, the investment results are shown because the trend is similar to that of the operational results (e.g. production, number of start-ups, prices. We consider the possibility of investment in BESS technology. Unlike the previous case study, BESS initial capacity is not predefined. We consider an investment cost of 20 [€/kW] for BESS according to the report "Technology development roadmap towards 2030" [44] and a maximum energy to power ratio (EPR_h^{max}) of 4 hours. Table 4 shows objective function error and investment error for each vision using the HM model results as a reference. All four models underestimate the objective function, especially when there is a high share of variable RES (vision 4). However, the range of the error values

remains similar to those shown in Fig. 11. As for the investment error, the RP-TM&CI model offers the best approximation. This is because it is the model that most accurately estimates energy prices and energy production of each technology. Both the SS-RFM and RP-TM&CI models, the original contributions of this paper, represent significant improvements on their former versions SS and RP.

Table 4: Investment result error per vision.

Result	Vision	SS	SS-RFM	RP	RP-TM&CI
Objective Function Error [%]	V1	0.5%	0.1%	0.8%	0.1%
	V2	1.2%	1.0%	4.4%	0.7%
	V3	0.5%	0.4%	4.8%	5.4%
	V4	6.4%	6.5%	1.8%	5.6%
Battery Investment Error [%]	V1	72.4%	52.0%	38.3%	-10.3%
	V2	35.4%	32.9%	22.2%	-8.3%
	V3	57.1%	49.8%	32.3%	-2.5%
	V4	34.4%	28.8%	31.7%	3.9%

Fig. 14 shows BESS investment obtained with all the models for each vision, and the share of variable RES (i.e. wind and solar productions). As expected, BESS investment increases when the variable RES share increases in the power system. The SS model and the SS-RFM model underestimate the investment by the greatest amount due to their main drawback, which is that they do not fully guarantee that the energy stored in the batteries is lower than the capacity of the batteries. This means that they permit energy to be stored beyond what investment has paid for, and therefore require less investment to achieve the same results as the RP model and the RP-TM&CI model.

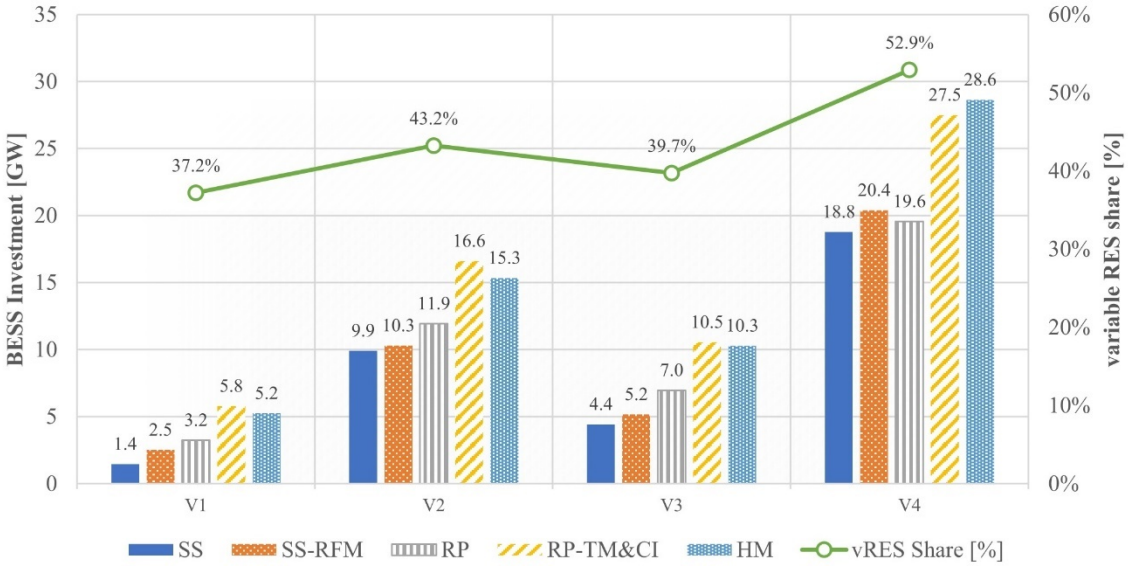

Fig. 14 BESS investment and variable RES share for each vision.

2.2.4 Discussion

In this section we want to highlight two main aspects of the results: the relationship between RES curtailment and storage investment, and the link between short- and long-term storage.

First, Fig. 15 shows the variable RES curtailment as a percentage of the total available RES for each vision. The amount of curtailment determined by all models underestimates the reference values from the hourly model. While a portion of the under-investment in storage shown in Section 2.2.3.2 is due to the inaccuracies in the way storage is represented in each model, some of the underinvestment may also come from the models' underestimation of variable RES curtailments. This is based on the tight connection between RES curtailment and storage needs, as shown in ref. [39]. Models such as ReEDS and RPM use exogenous estimations to relate these two aspects in systems with high share of RES. However, the models proposed in this paper determine this relationship endogenously. Improvements in the clustering process could be performed to improve this relationship; however, further research is needed to verify this hypothesis.

Second, in this paper we focus on modeling energy storage investment with operational detail, considering long-term (i.e. seasonal) hydro storage generation as well as short-term (i.e. hours) storage systems such as batteries. These are very different resources in the power system. Therefore, the following question arises: Why try to model both with the same methodology? Hydro storage already exists in most real power systems and more could be built in the future, and short-term storage (e.g. BESS) is getting cheaper and could be a good technical solution to reduce RES curtailments even with relatively low energy to power ratios (e.g. 1-4 h). Moreover, if both types of storage are not considered at the same time, then an assumption must be included regarding storage operation. For example, it is possible to consider maximum available hydro energy without tracking the storage level, or to assume a peak shaving for short-term ESS. In either case one decision is fixed while the other is optimized. Therefore, possible synergies between both storage systems are neglected. This is the case of more traditional hydrothermal dispatch models.

The RP-TM&CI model co-optimizes both types of storage. Hence, the operational decisions of short- and long-term storage are now linked and depend on each other. The benefits of this co-optimization are shown in the results of Section 2.2.3. In fact, the best results are obtained with the RP-TM&CI model, which represents the relationship between both types of storage better than the other approximate models. It should also be noted that the RP-TM&CI model could be used to improve traditional hydrothermal models in which the water value serves as a consistent way of coupling long-term reservoir management with short-term operations of storage units. Using the RP-TM&CI model it might be possible to obtain the water value of long-term reservoirs internalizing the information of short-term storage, which is not possible in traditional hydrothermal models.

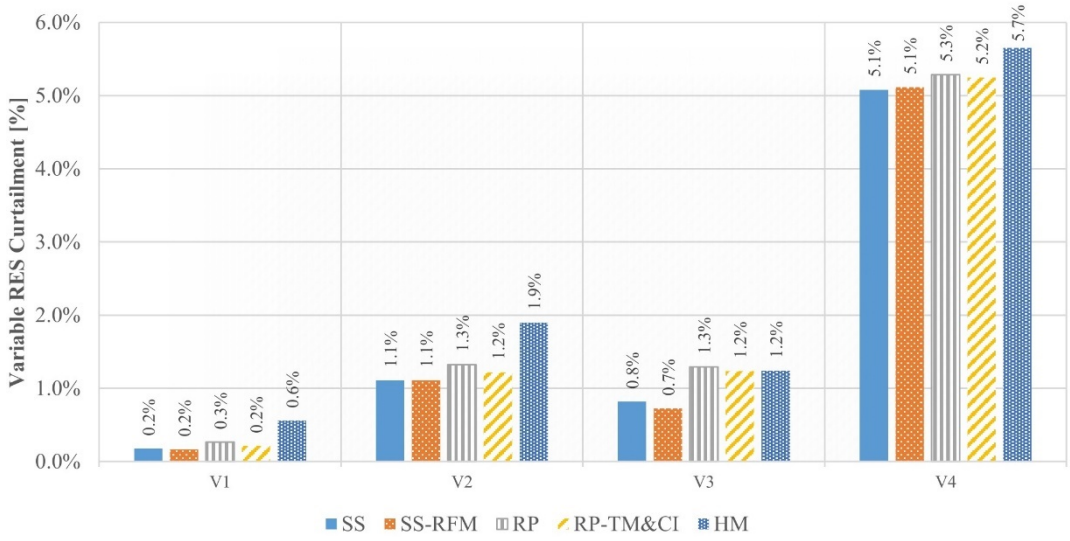

Fig. 15 variable RES curtailment.

2.2.5 Conclusion

This paper compares four different methods of approximating time representations in an hourly unit-commitment model with ESS investment. These methods include the SS model and the RP method as well as enhanced versions of the SS and RP models (the SS-RFM model and the RP-TM&CI models) which are the new contributions of this paper and perform better than the original versions.

The SS model was originally developed to include chronology and high time resolution details in mid- and long-term models. While it can deal with long-term storage, it cannot accurately estimate short-term storage, and quickly becomes calculation intensive because of the storage constraints. The SS-RFM model takes much less time to run than the regular SS model, because it reformulates the storage constraints, but it does not improve the accuracy of the short-term storage modeling. Moreover, SS models could lead to infeasible results (i.e. more energy stored than the maximum storage capacity), which is their major drawback, and means that they require additional adjustments for most practical applications.

Unlike the SS models, the RP model cannot handle long-term storage, but it deals well with short-term storage as it preserves within-day chronology. The RP-TM&CI model combines aspects of the SS and RP models to account for both short and long-term storage. According to the case study results, it is the most accurate of the four approximate models and does not require a significant increase of CPU time. These results support the idea that including chronological information among representative periods may be an efficient way to include small time scale variations in longer-term planning models that involve storage. Doing so is a critical need in the adequate

representation of power systems that include a significant and increasing quota of variable renewable sources and energy storage systems.

Looking forward, the RP-TM&CI model could be used to analyze the co-optimization of the water value in hydro storage with the storage value of short-term storage such as batteries. This kind of analysis could improve traditional hydrothermal dispatch models in which short-term storage is rarely considered. Moreover, the RP-TM&CI model could be extended to a stochastic model to consider uncertainty in renewable energy production or hydro inflows for long-term storage. Therefore, the main challenge in this topic is the representation at the same time of long- and short-term uncertainties, such as in [45].

2.3 Opportunity Cost Including Short-Term Energy Storage in Hydrothermal Dispatch Models Using a Linked Representative Periods Approach

Due to climate policy and the increasing reduction of renewable investment costs, power systems are transitioning to accommodate wind and solar generation, which will require system flexibility for balancing requirements to maintain system performance [46]. Most ways to determine the value of flexibility of a power system, are based in running Unit-Commitment (UC) models [47]. In this work, UC constraints are considered in order to represent the value of this flexibility as the short-term opportunity cost in hydrothermal dispatch models. Since the current technologies have limited technical capabilities to provide this flexibility, new alternatives are required. In this context, short-term storage systems, e.g., Battery-based Energy Storage Systems (BESS) or Pumped-hydro energy storage (PHS), are one of the most promising options that can deliver technical and economic benefits in the electric power sector such as providing the required flexibility and reducing system operational costs [29]. For instance, authors in [48] have shown that PHS reduces the operational cost by 2.5–11% in a wind power integration context for the Great Canary island in Spain. Therefore, there are significant short-term opportunity costs that should be considered in the medium- and long-term planning (e.g., hydrothermal dispatch is the focus in this paper). However, these opportunity costs are not properly considered or simplified in the classical hydrothermal models. In this context, both flexibility requirements and short-term storage systems operation require chronological information in order to be properly addressed in medium- and long-term planning models. Some authors have made an effort to make this analysis by using representative periods in their models. For instance, authors in [49] use a representative day to study the allocation and investment of ESS while authors in [35] focus on how to select the representative periods considering renewable energy sources. This is a common and valid assumption for power systems with a low share of hydro generation. However, hydrothermal power systems are highly dependent on seasonal hydro storage. Therefore, the interaction between short-term storage (intra-day or intra-week) and seasonal storage is relevant to co-optimize the use of hydro

generators with short-term storage units that can provide similar services, such as energy arbitrage and operating reserves procurement for flexibility requirements [50].

This research focuses on the representation of short-term operational decisions in hydrothermal dispatch models, how these decisions change the operational decisions, and opportunity costs of seasonal storage. These results are useful for planning and policy analysis, as well as for bidding strategies of ESS owners in day-ahead markets and not taking them into account may lead to infeasible operation or to suboptimal planning. For instance, an underestimation of the opportunity cost in hydro generation during the operational planning may lead to use more hydro production, which could represent a risk for the power system during a dry season. The results in Section 2.3.5 show that classic hydrothermal dispatch models systematically underestimate the opportunity cost, while the proposed hydrothermal dispatch model significantly reduces this underestimation problem.

2.3.1 Literature Review

The hydrothermal dispatch problem aims at minimizing the total fuel cost of thermal generation units while properly dispatching the hydro and thermal generation units. There are two main types of models, the ones that are focused on the long-term decision under hydro inflows uncertainty [51] and the ones that are focused on the short-term decisions considering detailed technical generation unit constraints [52].

On the one hand, the long-term hydrothermal dispatch problem aims at obtaining an optimal use of generation resources, most commonly under water inflows uncertainty, for the hydro and thermal generation units over a planning horizon considering multiple years [53]. Several models have been proposed for solving this problem in the literature, e.g., Ref. [51] is one of the classic references in this topic and more recently Ref. [54] gives a comprehensive review of different characteristics and model formulations on this topic. In addition, there are several commercial tools that aim to solve the hydrothermal dispatch problem that have been used in scientific research, such as: SDDP developed by PSR, PLEXOS Integrated Energy Model by Energy Exemplar, ProdRisk by SINTEF, NEWAVE by CEPEL [55], and StarNet Model by IIT [56]. For medium- or long-term studies, these tools use a Load Duration Curve (LDC) approach (also known as load-levels approach) with monthly or weekly stages. This is mainly due to the computational efficiency of LDC for large-scale systems. However, the LDC approach lacks chronological information within stages (e.g., weeks or months) and fails to represent short-term constraints (e.g., ramps, storage balance, etc.) [12].

On the other hand, the short-term hydrothermal dispatch aims at minimizing the fuel cost of thermal units for 1 day or 1 week while meeting various detailed hydraulic and electric system constraints, such as ramps, unit commitment [57], and nonlinear constraints of hydro units [52]. Although these approaches emphasize more the

representation of short-term operation, they are not suitable to determine the opportunity cost of seasonal storage (also known as water value in the hydrothermal dispatch context) since their planning horizon covers only one week or less. However, short-term decisions may affect the operation of hydro reservoirs in the long term. Despite this situation, no relevant work has aimed to improve the representation of short-term operational decisions in long-term hydrothermal dispatch models. However and more recently, the *representative periods* (RP) method has been applied to long-term models in order to consider short-term decisions, such as renewable energy variability in the short-term [7] and UC constraints [58]. Generation dispatch and investment decisions are made for the selected periods (e.g., days or weeks) with a more detailed size of periods (hourly, for example). The RPs preserve the internal chronology of the hours, rendering a more realistic representation of changing storage levels over the course of a day or week. However, the basic definition of the RP does not preserve the chronology among them. Therefore, any Energy Storage System (ESS) with a full charge-discharge cycle longer than the RP (e.g., monthly or yearly) will not be adequately represented. In order to improve this situation, some authors have proposed methods to aggregate time series by modeling both intra-day and seasonal storage. For instance, the authors in [59] superpose inter-period and intra-period storage inventories to model short- and long-term ESS, while the authors in [60] proposed a hierarchical clustering method to maintain the chronology of the input time series throughout the whole planning horizon to achieve the same goal. Moreover, the authors have proposed a linked RP model that also overcomes this shortcoming in [61]. Based on this last reference, a Linked Representative Periods (LRP) is proposed in this paper. By linking several RPs, it is possible to preserve some chronology among the RPs by superposing intra-period and inter-period storage balance equations. In addition, the selection of RPs is an important aspect of the RP approach. Some authors have proposed methods that optimize both the number and clustering of RPs to minimize the difference between the LDC and the approximate one created by the RPs [34]. The most versatile method for grouping RPs comes from [7] and relies on clustering techniques (e.g., k-means or k-medoids) to group a number of hours with any number of normalized characteristics (solar energy, demand, wind energy, etc.). Furthermore, several authors have debated about the optimal length for RPs [1]. For instance, in [36], the authors suggested representative groups of days or representative weeks, which gives the advantage of increasing the amount of chronology preserved. However, the effectiveness of linking shorter RPs versus longer RPs has not been analyzed in the LRP approach. The impact of the proposed model and the conclusions are analyzed in Section 8.

These recent developments in the representative periods can be applied to the hydrothermal dispatch problem framework in order to overcome the lack of detailed short-term decisions in long-term hydrothermal dispatch models. Despite these developments in short-term and seasonal storage interaction, in the literature opportunity costs in stochastic hydrothermal planning models have not been analyzed taking into account the possible interaction of short-term dynamics in the long term. This research article focuses on this gap. Moreover, the interpretation of opportunity

costs for energy storage systems is not as intuitive as in the LDC models due to the superposition of both balance equations, i.e., intra-period and inter-period. Therefore, the opportunity cost for energy storage, considering short- (intra-period) and long-term (inter-period) operation is defined and analyzed in the proposed LRP model. This definition of the opportunity cost using both balance equations has not been determined before in the literature, which computes separately the short- and long-term opportunity costs for energy storage. These results can be used to improve the operational planning of hydrothermal power systems in the context of a high share of renewables energy sources and flexibility resources such as the BESS.

The challenge that have been tackled in this paper is to obtain the hourly opportunity cost for storage technologies that usually operate on very different time scales. For example, BESS might have a full charge/discharge cycle within a couple of hours or days, whereas a seasonal hydro storage facility – depending on the size of the reservoir – could have cycles of weeks, months or even years. Other important aspects of hydrothermal dispatch models such as uncertainty modeling [62] are out of its scope. A general formulation is proposed based on stochastic programming, which is compatible with different techniques to solve the dimensionality problem such as scenario reduction [63] and stochastic dual dynamic programming [64].

In this state-of-the-art context, the main contribution of this paper is the derivation and analysis of the hourly opportunity cost of storage technologies using the proposed LRP model, that improves the operational decisions in hydrothermal dispatch models. In other words, the LRP model can obtain an approximation of the ESS hourly opportunity cost within the studied time horizon without solving an hourly model. Moreover, the LRP model has the advantage that it obtains hourly detailed opportunity cost for different types of ESS technologies which operate on different time scales (hydro versus battery). This is a novel contribution since, so far, this has not been possible because classic LDC-type models lack chronological information among individual hours belonging to different load levels. Moreover, due to the reduction of temporal information in the proposed hydrothermal LRP model, this model is suitable for application on real-life case studies. This is relevant because it means that the proposed model can include short-term details that impacts the long-term operational and economic decisions without solving an hourly detailed model and in an efficient computational time.

An hourly model (HM) is used as a benchmark to compare our proposal to the classic LDC model and then to quantify the improvements in a stylized Spanish hydrothermal system. The HM can be solved for small case studies, however, in practice, for large-scale case studies it may not be possible to be solved.

The remainder of the paper is organized as follows: Sections 2.3.2 and 2.3.3 describe the main concepts in hydrothermal dispatch models and explain the main differences among the three models in this paper: the hourly model (HM) (the benchmark model),

load duration curve model (LDC) (the classic model), and linked representative periods (LRP) (the novel model proposed in this paper). Section 2.3.4 defines the short-term storage value and water value definition for the LRP model. The definition of the hourly opportunity cost of different storage technologies represents one of the main contributions of this paper as it represents the storage opportunity cost extracted from hydrothermal dispatch models that accounts for both short- and long-term dynamics of the power system. Section 2.3.5 analyzes the results in a stylized Spanish case study based on European data for the year 2030. Section 2.3.6 discusses the coordination between short- and medium-term models in the LDC model and its equivalent in the proposed LRP model.

2.3.2 Hydrothermal Topology and Scenario Tree

In the context of hydrothermal dispatch, it is important to establish the hydro topology in order to determine the relationship among the water basins because of its impact on the dispatch and on the opportunity cost (also known as water value) in hydro generators. Fig. 16 shows an example hydro topology where three reservoirs (r1, r2, r3), including their hydro units (h1, h2, h3), are related among them. For instance, reservoir r3 receives its hydro inflows, turbined water and spilled water from reservoirs r1 and r2, and the pumped water from its own hydro unit h3.

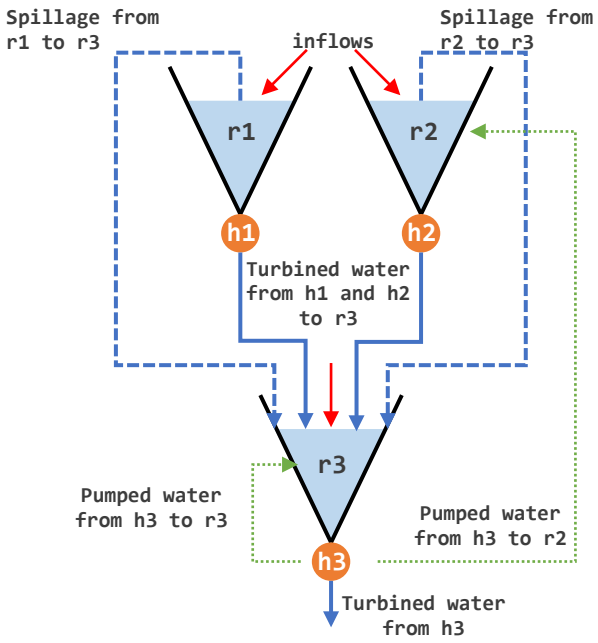

Fig. 16. Example of hydro topology or water basin

The main source of uncertainty in hydrothermal power systems is the water inflow [51]. This uncertainty is normally represented as a scenario tree [62], in which each node in the tree represents a hydro inflow level with a certain probability. In addition, the nodes are related among them, creating different scenarios to sample different realizations of the hydro inflows. Fig. 17 shows an example of a simple scenario tree with three scenarios: wet season, average inflows, dry season. In this example, the first stage decisions are taken in the first month represented in the tree (i.e., October) and the second stage decisions are taken for the following months. In addition, for each month in the second stage there are three different values of hydro inflows from each scenario.

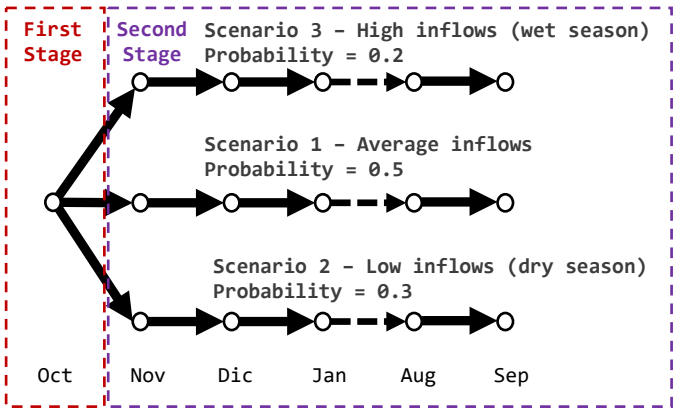

Fig. 17. Scenario tree example

Both hydro topology and scenario tree shown in this section are used as a reference in the remainder of this paper.

2.3.3 Model Formulation

2.3.3.1 Nomenclature

Indices

$p \in \mathcal{P}$	Periods (e.g., hours)
$m \in \mathcal{M}$	Months
$MP_{m,p}$	Set that relates hours and months
$w \in \mathcal{W}$	Type of day in the week (e.g., weekdays or weekend)
$l \in \mathcal{L}$	Load levels or load blocks
$rp \in \mathcal{RP}$	Representative periods (e.g., days)
$TM_{rp',rp}$	Set that relates transitions among rp
$k \in \mathcal{K}$	Hours inside a representative period
$CI_{p,rp,k}$	Set that relates hours with representative periods (i.e., cluster index)
$r \in \mathcal{R}$	Reservoirs
$g \in \mathcal{G}$	Generators
$t \subset g$	Subindex of Thermal units
$s \subset g$	Subindex of Storage units
$b \subset s$	Subindex of Short-term storage units (e.g., batteries)
$h \subset s$	Subindex of Hydro units

$HUR_{h,r}$	Set with hydro plants that are upstream of a reservoir
$HPR_{h,r}$	Set with pumped hydro plants that are upstream of a reservoir
$RUH_{r,h}$	Set with reservoirs that are upstream of a hydro plant
$RPH_{r,h}$	Set with reservoirs that are upstream of a pumped hydro plant
$RUR_{r,r}$	Set with reservoirs that are upstream of another reservoir
$\omega \in \Omega$	Scenarios
$a(\omega)$	Scenario tree relations

Parameters

d_*, o_*	Demand, operating reserve [MW]
wg_*	Load level duration or rp weight [h]
$\bar{p}_g, \underline{p}_g$	Maximum, minimum output [MW]
f_t, v_t	No load cost [$/h], variable cost [$/MWh]
su_t, sd_t	Startup, shutdown cost [$]
c_h, η_s	Production function and efficiency [p.u.]
$\bar{r}_r, \underline{r}_r$	Maximum and minimum storage level of the reservoir [hm3]
r'_r	Initial and final storage level of the reservoir [hm3]
$\overline{soc}_b, \underline{soc}_b$	Maximum, minimum state of charge [p.u.]
$i^{\omega}_{*,r}$	Stochastic hydro inflows [m3/s]
p^{ω}_{*}	Scenario probability [p.u.]
v'	Energy not served cost [$/MWh]
v''	Operating reserve not served cost [$/MWh]

Variables

$UC^{\omega}_{*,t}, SU^{\omega}_{*,t}, SD^{\omega}_{*,t}$	Commitment, startup, and shutdown {0,1}
$P^{\omega}_{*,g}$	Production of generation units [MW]
$P'^{\omega}_{*,t}$	Production above minimum output [MW]
$C^{\omega}_{*,h}, C^{\omega}_{*,s}$	Consumption of a hydro/storage unit [MW]
$O^{\omega}_{*,g}$	Operating reserve of generation unit
$R^{intra,\omega}_{*,r}, R^{inter,\omega}_{*,r}$	Intra and inter reservoir level [hm3]
$S^{\omega}_{*,r}$	Reservoir spillage [hm3]
$ENS^{\omega}_{*}, RNS^{\omega}_{*}$	Energy and operating reserve not served [MW]
$SoC^{intra,\omega}_{*,b}$, $SoC^{inter,\omega}_{*,b}$	State-of-charge of a battery [p.u.]

In the previous nomenclature, "$*$" refers to the parameters used to identify time divisions: p for hours in the detailed model, (m, w, l) in the load-levels model, and (rp, k) in the linked representative periods model respectively.

2.3.3.2 Model Description

Three optimization models are presented and solved in this paper using a stochastic formulation: An Hourly Model (HM), which is used as a benchmark, the classic Load Duration Curve (LDC) model, and the proposed Linked Representative Periods (LRP). The objective function and constraints of each model are detailed in the Appendix.

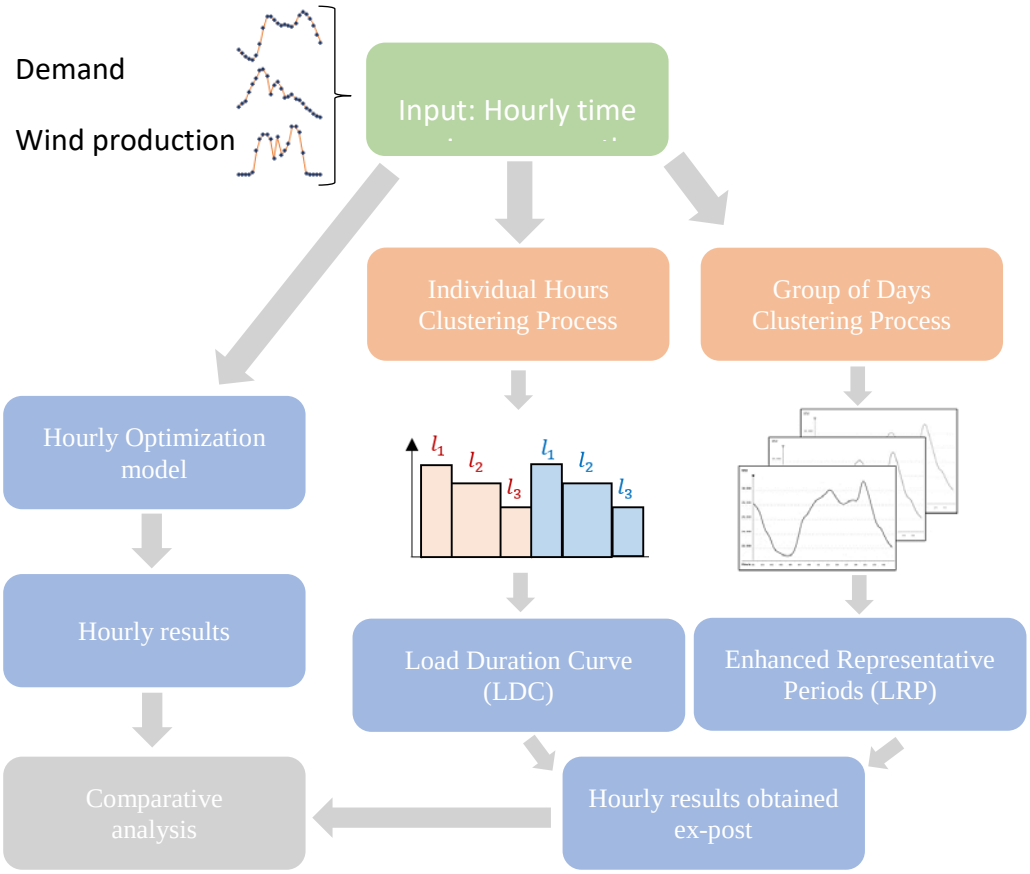

Fig. 18. Analysis overview: comparison of LDC and LRP models

Fig. 18 shows an overview of the analysis carried out in this paper. Hourly demand, wind, and solar time series are used as input data. Therefore, the HM model can be solved to obtain the benchmark results. In addition, two different clustering procedures are applied per each node of hydro inflow uncertainty, (i.e., per month) in order to obtain the input data necessary for the LDC and the LRP model respectively. First, individual hours are clustered in order to obtain the load levels for the LDC model per month. Second, the time series are grouped by periods (e.g., for the case study, representative

days are considered) and then they are clustered in order to obtain the representative periods for the LRP model per month. Finally, the hourly results of each model are compared to determine the quality of the approximations in terms of objective function, productions, energy stored, and dual variables (e.g., prices, storage value, and water value).

It is important to highlight that both load levels and representative periods are selected per month because the uncertainty in the hydro inflows is per month, see Fig. 17. Scenario tree example

Therefore, the load levels and representative periods are different among months. This is guaranteed through a time division structure in both models. Fig. 19 shows an example of the structure of the LDC model, where two months (m_1, m_2) have a subdivision in weekdays (w_1) and weekend (w_2), each one with three different load levels (l_1, l_2, l_3).

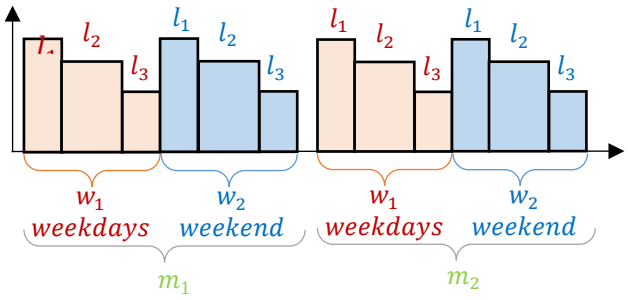

Fig. 19. Structure of LDC time division

Fig. 20 shows an example of the structure for the LRP model, where the two months have their own representative periods (i.e., rp_1 and rp_2 for m_1, and rp_3 and rp_4 for m_2), each one with a set of chronological hours (k_1 to k_{24} in a 24-hour representative period example).

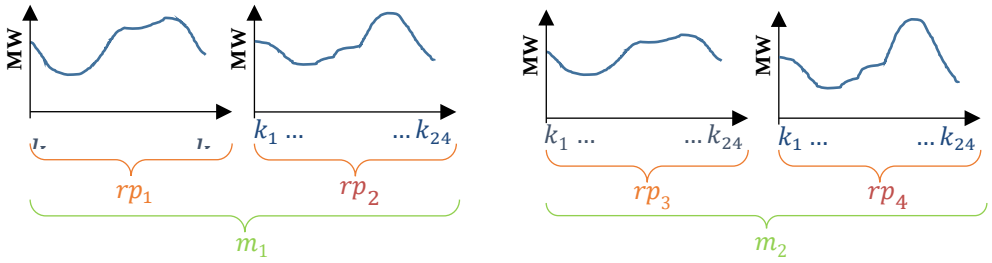

Fig. 20. Structure of LRP time division

These time divisions facilitate the formulation of storage balance constraints in both models considering the scenario-tree structure. Sections 4.1 to 4.8 show the storage

balance constraints in the three optimization models. Although the detailed optimization models are shown in appendices A to C, the storage balance equations are shown here to help understand the analysis in the following sections.

2.3.3.3 Long-term Energy Storage Balance Constraint in the Hourly Model

$$R_{p-1r}^{intra,\omega'} - R_{pr}^{intra,\omega} + i_{pr}^{\omega} - S_{pr}^{\omega} + \underbrace{\sum_{r' \in RUR_{r',r}} S_{pr'}^{\omega}}_{Water\ spillage\ from\ upstream\ reservoirs} + \tag{1}$$

$$\underbrace{\sum_{h \in HUR_{h,r}} {P_{ph}^{\omega}}/{c_h}}_{Turbined\ water\ from\ upstream\ hydro\ plants} -$$

$$\underbrace{\sum_{h \in RUH_{r,h}} {P_{ph}^{\omega}}/{c_h}}_{Turbined\ \ water\ from\ hydro\ plants\ in\ reservoir\ r} +$$

$$\underbrace{\sum_{h \in HPR_{h,r}} {C_{ph}^{\omega}}/{c_h}}_{Pumped\ water\ from\ hydro\ plants\ to\ reservoir\ r} - \underbrace{\sum_{h \in RPH_{r,h}} {C_{ph}^{\omega}}/{c_h}}_{Pumped\ water\ to\ other\ reservoirs} =$$

$$0 \quad \forall \omega pr \ \ \omega' \epsilon\, a(\omega)$$

2.3.3.4 Short-term Energy Storage Balance Constraint in the Hourly Model

$$SoC_{p-1b}^{intra,\omega'} - SoC_{pb}^{intra,\omega} - P_{pb}^{\omega} + C_{pb}^{\omega} = 0 \quad \forall \omega pb \quad \omega' \epsilon\, a(\omega) \tag{2}$$

2.3.3.5 Long-term Energy Storage Balance Constraint in the Load Duration Curve

$$R_{m-1r}^{inter,\omega'} - R_{mr}^{inter,\omega} + i_{mr}^{\omega} - S_{mr}^{\omega} + \underbrace{\sum_{r' \in RUR_{r',r}} S_{mr'}^{\omega}}_{Water\ spillage\ from\ upstream\ reservoirs} + \tag{3}$$

$$\underbrace{\sum_{wl} \sum_{h \in HUR_{h,r}} {wg_{mwl} \cdot P_{mwlh}^{\omega}}/{c_h}}_{Turbined\ water\ from\ upstream\ hydro\ plants} -$$

$$\underbrace{\sum_{wl} \sum_{h \in RUH_{r,h}} {wg_{mwl} \cdot P_{mwlh}^{\omega}}/{c_h}}_{Turbined\ \ water\ from\ hydro\ plants\ in\ reservoir\ r} +$$

$$\underbrace{\sum_{wl}\sum_{h\,\in\,HPR_{h,r}} wg_{mwl}\cdot C^{\omega}_{mwlh}/_{c_h}}_{Pumped\ water\ from\ hydro\ plants\ to\ reservoir\ r} -$$

$$\underbrace{\sum_{wl}\sum_{h\,\in\,RPH_{r,h}} wg_{mwl}\cdot C^{\omega}_{mwlh}/_{c_h}}_{Pumped\ water\ to\ other\ reservoirs} = 0 \quad \forall \omega mr \quad \omega' \epsilon\, a(\omega)$$

2.3.3.6 Short-term Energy Storage Balance Constraint in the Load Duration Curve

$$SoC^{inter,\omega'}_{m-1b} - SoC^{inter,\omega}_{mb} - \sum_{wl} wg_{mwl}\cdot P^{\omega}_{mwlb} + \sum_{wl} wg_{mwl}\cdot C^{\omega}_{mwlb} = \tag{4}$$

$$0 \quad \forall \omega mb \quad \omega' \epsilon\, a(\omega)$$

2.3.3.7 Intra-period Balance Constraint for Long-term Energy Storage in the Linked Representative Periods

$$R^{intra,\omega'}_{rp,k-1,r} - R^{intra,\omega}_{rp,k,r} + i^{\omega}_{rp,k,r} - S^{\omega}_{rp,k,r} + \underbrace{\sum_{r'\,\in\,RUR_{r',r}} S^{\omega}_{rp,k,r'}}_{Water\ spillage\ from\ upstream\ reservoirs} + \tag{5}$$

$$\underbrace{\sum_{h\,\in\,HUR_{h,r}} P^{\omega}_{rp,k,h}/_{c_h}}_{Turbined\ water\ from\ upstream\ hydro\ plants} -$$

$$\underbrace{\sum_{h\,\in\,RUH_{r,h}} P^{\omega}_{rp,k,h}/_{c_h}}_{Turbined\ \ water\ from\ hydro\ plants\ in\ reservoir\ r} +$$

$$\underbrace{\sum_{h\,\in\,HPR_{h,r}} C^{\omega}_{rp,k,h}/_{c_h}}_{Pumped\ water\ from\ hydro\ plants\ to\ reservoir\ r} - \underbrace{\sum_{h\,\in\,RPH_{r,h}} C^{\omega}_{rp,k,h}/_{c_h}}_{Pumped\ water\ to\ other\ reservoirs} =$$

$$0 \quad \forall \omega, rp, k, r \quad \omega' \epsilon\, a(\omega)$$

2.3.3.8 Inter-period Balance Constraint for Long-term Energy Storage in the Linked Representative Periods

$$R_{m-1,r}^{inter,\omega'} - R_{mr}^{inter,\omega} + \sum_{(rp,k)\in\{CI_{p,rp,k}\cap MP_{m,p}\}}\left[R_{rp,k,r}^{intra,\omega} - R_{rp,k-1,r}^{intra,\omega'}\right] = \quad (6)$$

$$0 \quad \forall \omega mr \quad \omega' \epsilon\, a(\omega)$$

2.3.3.9 Intra-period Balance Constraint for Short-term Energy Storage in the Linked Representative Periods

$$SoC_{rp,k-1,b}^{intra,\omega'} - SoC_{rp,k,b}^{intra,\omega} - P_{rp,k,b}^{\omega} + C_{rp,k,b}^{\omega} = 0 \quad \forall \omega, rp, k, b \quad \omega' \epsilon\, a(\omega) \quad (7)$$

2.3.3.10 Inter-period Balance Constraint for Short-term Energy Storage in the Linked Representative Periods

$$SoC_{m-1,b}^{inter,\omega'} - SoC_{mb}^{inter,\omega} + \sum_{(rp,k)\in\{CI_{p,rp,k}\cap MP_{m,p}\}}\left[SoC_{rp,k,r}^{intra,\omega} - SoC_{rp,k-1,r}^{intra,\omega'}\right] = \quad (8)$$

$$0 \quad \forall \omega mb \quad \omega' \epsilon\, a(\omega)$$

2.3.3.11 Comparison of Storage Balance Constraints Among the Models

Here the previous constraints are analyzed for each model. First, in the *HM* model, the storage balance constraints are imposed for each period p, equations (1) and (2). Therefore, reservoir level and SoC are determined for each hour in the time horizon. These results are used as a benchmark to test the LDC and LRP model, see Fig. 18. Constraints for LTESS and STESS are stated for $\omega' \epsilon\, a(\omega)$, which allows to relate the different scenarios through the scenario tree. For instance, Fig. 17 shows a scenario tree with three scenarios: wet season, average inflows, dry season. In this example, the ancestor $a(\omega)$ of scenario 3 in November is scenario 1 in October. Therefore, the set $a(\omega)$ is relating a scenario with the corresponding predecessor scenario in the tree.

Second, in the *LDC* model, both storage balance equations (3) and (4) (i.e., LTESS and STESS) include the load-level duration (wg_{mwl}) to consider the number of hours that are represented for each load level. In other words, the multiplication by wg_{mwl} guarantees that all the charged/discharged energy is considered within the month m. These equations are for the inter-period variables. Intra-period variables are not available in this model due to the lack of chronology within the month m.

Third, in the *LRP* model, the storage balance constraints are defined for inter- and intra-periods, equations (5)-(8). These equations create the continuity in storage across the entire time horizon that allows for the modeling of short-term and long-term storage simultaneously. Intra-period constraints (7)-(8) ensure the storage balance within the RP, while inter-period constraints guarantee the storage balance between representative periods by checking at regular intervals (e.g., aggregation of hours such as months m) that all the energy charged and discharged since the previous month plus the total energy at the last checkpoint are within bounds. This is possible because the cluster index, $CI_{p,rp,k}$, and the relationship between periods and months, $MP_{m,p}$, are known as a result of the clustering procedure to determine the RPs. The intersection of both sets $\{CI_{p,rp,k} \cap MP_{m,p}\}$ indicates which RPs belong to the month and, therefore, must be considered in the inter-period balance.

Finally, notice that constraints for LTESS and STESS are equivalent if, for example, a hydro reservoir has a pump unit which is not in a hydro basin and it has no hydro inflows. However, both constraints are kept in order to facilitate the distinction between both types of storage technologies. In real hydro power plants, there is a nonlinear dependence between the reservoir head and the reservoir volume [56]. Nevertheless, and for the sake of simplicity in storage balance constraints for LTESS, a linear function of the turbine outflow is assumed. Although nonlinear dependence could be considered at the expense of more complex optimization models such as in [56].

2.3.4 Analysis of Energy Storage Opportunity Cost

The energy storage opportunity cost is the substitution cost of the stored energy that can be calculated as the decrease on total system cost when an extra energy storage unit is available, also known as dual approach [65]. In hydrothermal dispatch context, this value is determined by the thermal generation unit that is replaced by the energy storage unit, i.e., hydro generation.

In Section 2.3.3, three models have been formulated for the hydrothermal dispatch as Mixed Integer Programming (MIP) problems. This is a frequent approach in short-term hydrothermal scheduling in order to consider practical limitations of the generation units such as ramps and UC constraints [66]. However, as it is mentioned in [65], the value of dual variables in a MIP is not well-defined. Hence, it is a common practice to approximate the dual variables of interest by fixing the integer variables (e.g., commitment decisions) obtained in the MIP solution and then solving the model again as a Linear Programming (LP) problem [56]. Under this assumption, the opportunity cost of ESS can be obtained from the dual variable of the storage balance equations of each model, while the opportunity cost of hydro reservoirs is normally called water value [65]. However, the name *water value* cannot be applied to BESS since there are no hydro inflows for this type of technology. Instead, the *storage value* is used to describe the opportunity cost of short-term storage (i.e., BESS).

- *Hourly Model (HM)*: The opportunity cost for each type of storage is obtained from the dual variables of equations (1) and (2). Therefore, water value $\left(\mu_{pr}^{intra,\omega}\right)$ is obtained from (1) and storage value $\left(\mu_{pb}^{intra,\omega}\right)$ from (2). These opportunity costs are for each hour in the time horizon.
- *Load Duration Curve Model (LDC)*: Water value $\left(\mu_{mr}^{inter,\omega}\right)$ is obtained from (3) and storage value $\left(\mu_{mb}^{inter,\omega}\right)$ from (4). Since there is no chronology between load levels, the opportunity cost for each type of storage is obtained only for an aggregation of hours (e.g., months).
- *Linked Representative Periods Model (LRP)*: This model has two balance equations for each storage technology. One for the storage balance inside the representative period (intra-period) and another for the storage balance through the aggregation of hours in the time horizon (inter-period). Each balance equation has its dual variable; however, the combination of both dual variables is necessary to determine the hourly dual variable that is comparable to the one obtained from the HM model. Equation (9) defines the hourly storage/water value for short- and long-term storage using the LRP model. $\mu_{rp,k,s}^{intra,\omega}$ is obtained from the dual variables of (5) and (7) for hydro reservoirs and BESS, respectively. In the same way, $\mu_{m,s}^{inter,\omega}$ is obtained from the dual variables of (6) and (8). Equation (9) shows the opportunity cost of energy storage as a linear combination of short- (intra-period balance) and long-term decisions (inter-period balance). Therefore, the LRP model distinguishes the impact of short-term decisions within the total opportunity cost, which is not possible in the HM model. Section 2.3.6 shows the relevance of (9) in the opportunity cost of storage since it allows to differentiate the share of short- and long-term economic information in this opportunity cost.

$$\mu_{ps}^{intra,\omega} = \sum_{(rp,k)\in CI_{p,rp,k}} \sum_{m\in MP_{m,p}} \frac{1}{p_m^{\omega}} \cdot \left(\frac{\mu_{rp,k,s}^{intra,\omega}}{wg_{rp}} + \mu_{m,s}^{inter,\omega} \right) \quad \forall \omega ps \tag{9}$$

2.3.5 Case study and Results

As a case study, a stylized Spanish power system in target year 2030 is chosen. The Spanish case is relevant because it has hydro reservoirs (i.e., seasonal storage) and, according to ENTSO-E [41], the next ten years will likely bring investment in Battery Energy Storage System (BESS), i.e., short-term energy storage. The wind and solar profiles were taken from [42] and [43] respectively, while hourly demand data and annual production per technology were taken from the vision 1 in the ENTSO-E *Ten Year Network Development Plan 2016* [41]. For the sake of simplicity, the case study is represented as a single node example. The transmission network may change the results in the case study, especially if there is any congestion; however, since transmission network constraints have already been successfully included in the classic hydrothermal LDC model [67] as well as in the former version of the LRP model [61], they are omitted here. In addition, Ref. [25] shows that network congestion improves the accuracy of the

clustering techniques to reduce temporal information, such as the ones used in this paper for the proposed hydrothermal LRP model.

The water basin is represented by three reservoirs. Reservoirs 1 and 2 are upstream of reservoir 3, and, therefore, reservoir 3 receives, besides its hydro inflows, the hydro production and water spillage from reservoirs 1 and 2, such as in Fig. 16. The scenario tree is a simplified structure of three scenarios in order to consider monthly hydro inflows in dry, average, and wet seasons, see Fig. 17. The probabilities for each scenario are 30%, 50%, and 20%, respectively. The first-stage decision is taken for October[3] and second-stage decisions are taken from November to September. For the sake of simplicity, the stability of the solution for different scenario trees is not verified. This will be addressed in future research to determine the impact of different scenario trees in the results.

Load levels and representative periods are obtained via the k-means clustering procedure for each month. The clusters were chosen by normalizing time series for the hourly demand, wind availability, and solar availability, see Fig. 18. For the LL model, 12 load levels (6 for weekdays and 6 for the weekend) per month have been defined. For the LRP model, some sensitivities for the selection of the representative periods have been defined: 1 representative period with 24h per month (1RPx24h), 1 rp with 48h per month (1RPx48h), 1 rp with 96h per month (1RPx96h), 2 rp with 24h per month (2RPx24h), and 4 rp with 24h per month (4RPx24h). These sensitivities are performed in order to identify if it is better to have only one rp per month sharing information or to have more rp per month sharing information among them and between months. Based on previous results in [61], more rp per month sharing information may be better than one rp per month.

Finally, a BESS with a power rating of 200MW, energy capacity of 4 hours, and round-trip efficiency of 90% is considered. The BESS is installed to deal with hourly variation of variable renewable energy sources.

2.3.5.1 Objective Function and Time to Solve

Table 5 shows the results using as a reference the results obtained for the HM. The objective function error is calculated using the value of the objective function of the hourly model as the theoretical value, while the CPU time is shown as a fraction of the time taken by the hourly model to solve the problem. All models were solved until optimality, i.e., until either their optimal point or the integrality gap equaled zero.

The analysis of the results shows two main situations. First, the LRP 4RPx24h as the best performance in terms of the objective function. The objective function error is lower

[3] October is the beginning of the hydrological year in Spain.

than 1% compared to the HM model, and it only takes one tenth of the time to solve. In addition, all the LRP results for the different sensitivities have objective function errors lower than 4%. Second, although the LDC is one of the fastest models to solve the problem, its objective function error exceeds 10%.[4] Therefore, the LRP improves the results of the hydrothermal dispatch problem without hampering the computational efficiency.

The results obtained for the sensitivities of the LRP model confirm that more rps per month sharing information is better than one longer rp per month. For instance, the 1RPx48h and 2RPx24h take the same number of hours per month and produce similar CPU time performance. However, the objective function error in 2RPx24h is half of that obtained with 1RPx48h. Therefore, and for the sake of simplicity, only the LRP 4RPx24h model results are shown in the following sections.

Table 5. Objective Function Error and CPU Time

	LRP 4RPx24h	LRP 2RPx24h	LRP 1RPx96h	LRP 1RPx48h	LRP 1RPx24h	LDC
OF Error [%]	0.1	1.7	3.4	3.6	3.6	11.7
CPU Time [p.u.]	0.10	0.02	0.05	0.02	0.01	0.01

2.3.5.2 First- and Second-Stage Production Results

Table 6 shows the errors in production per technology for both LDC and LRP model. Negative values indicate an underestimation in comparison to the HM result, while positive values indicate an overestimation. The black color is used to highlight absolute values lower or equal to 5%, light orange color for absolute values greater than 5% and lower or equal to 10%, and the dark red color for absolute values higher than 10%. Technologies such as coal and fuel oil are not shown because their total production is negligible. Additionally, technologies such as wind, solar, and run-of-river are also not shown, in this case because the total production error is lower than 1% in both models.

The results are classified into two groups: first and second stage. The LRP model has better results than LDC model in both groups. In fact, BESS production error in the LRP model is almost ten times lower than the result with the LDC model for the first stage,

[4] Considering twice the number of LL, the LDC objective function error reduces to an error of 6%, but the CPU time increases six-fold.

and almost twenty times smaller for the second stage. The Open Cycle Gas Turbine (OCGT) is more difficult to estimate in both models because it is the peak technology, and yet the LRP improves the approximation made by the LDC.

The LDC model underestimates Combined Cycle Gas Turbine (CCGT) production (marginal technology most of the time) due to the loss of chronology among the load levels that overestimates BESS production, see Table 6. This leads to an underestimation of BESS storage values, see Table 6. On the other hand, the CCGT production error in the LRP model is lower than 5% as well as the BESS storage value in Table thanks to the more accurate representation of chronological constraints. These results show the interdependence between the marginal technologies and the BESS storage value.

Table 6. Total Production Error per Technology [%]

Tech	First Stage		Second Stage	
	LDC	LRP	LDC	LRP
Nuclear	4.6	1.7	Sc1 2.9	Sc1 -0.3
			Sc2 2.8	Sc2 -0.4
			Sc3 3.3	Sc3 -0.7
CCGT	-35.8	-0.5	Sc1 -8.6	Sc1 -3.5
			Sc2 -5.7	Sc2 -4.4
			Sc3 -6.8	Sc3 -2.6
OCGT	-30.7	-22.7	Sc1 -68.4	Sc1 -49.0
			Sc2 -44.3	Sc2 -0.5
			Sc3 -68.8	Sc3 -16.9
Hydro	-5.5	-4.3	Sc1 -0.4	Sc1 -0.3
			Sc2 0.6	Sc2 -0.5
			Sc3 -0.3	Sc3 -0.3
BESS	110.9	9.1	Sc1 133.9	Sc1 -5.4
			Sc2 115.1	Sc2 -5.1
			Sc3 123.7	Sc3 4.6

2.3.5.3 Hydro Reservoir and State-of-Charge Results

In this section, the storage level is analyzed for both technologies, i.e., hydro (seasonal storage) and BESS (short-term storage). First, storage level for hydro reservoir is

approximated with more accuracy in the LRP model compared to the LDC model. For instance, Fig. 21 (top) shows the storage level for reservoir 2 in scenario 1 for both models in comparison to the HM model. The storage-level-average error over all the scenarios and reservoirs is 4.5% for the LRP model and 9.0% for the LDC model. Therefore, the LRP model is twice as accurate as the LDC model for the reservoir levels.

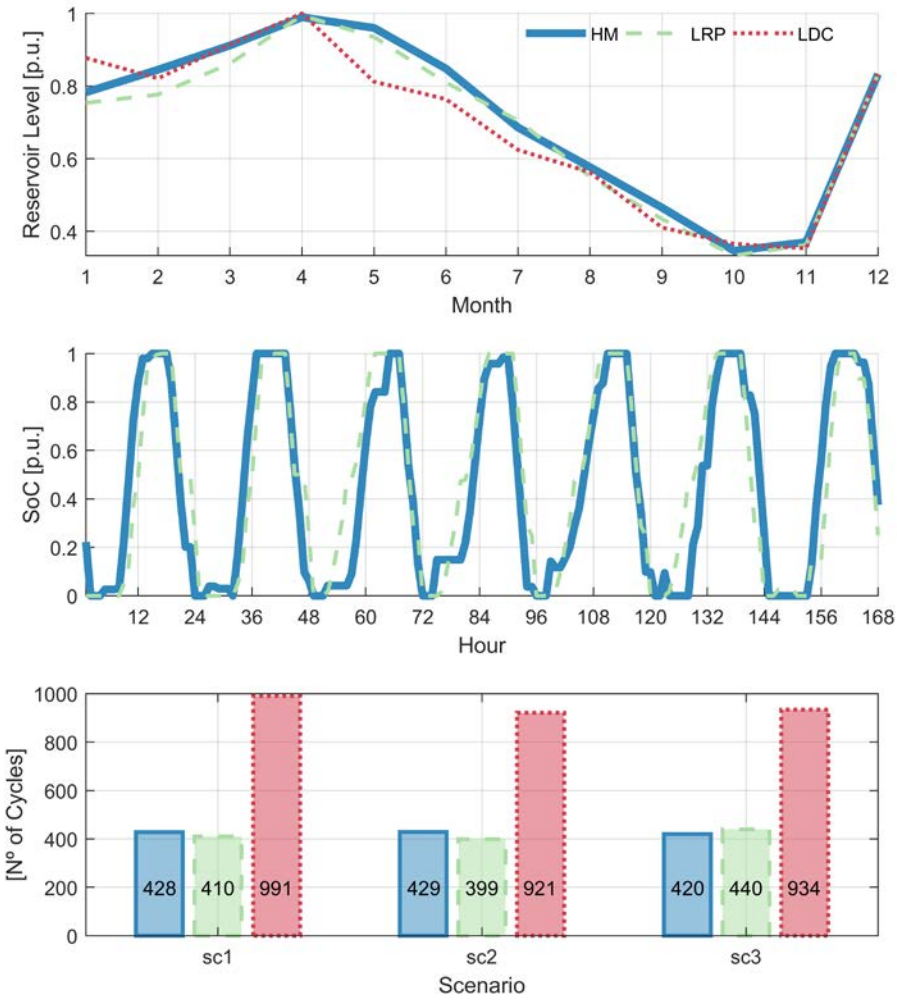

Fig. 21. Reservoir Level [p.u.] (top). BESS SoC [p.u.] over a week (middle). Total number of cycles for the BESS (bottom)

Second, the hourly BESS SoC can be obtained for the LRP model, which is not possible with the LDC model. Fig. 21 (middle) shows the hourly evolution of the SoC in a particular week for the HM and the LRP model. It is possible to observe the daily cycles of the BESS

and how the LRP model results mimic the HM solution. The total number of cycles[5] obtained from each model in the target year are compared in Fig. 21 (bottom). This figure shows the total number of cycles per scenario for each model. The total number of cycles determined from the LDC results doubles the number obtained with the HM model, which was expected due to the overestimation in the BESS production shown in Table 6. By contrast, the average error in the number of cycles for the LRP model is 5%. This result is important because the number of cycles is key to determine replacement or maintenance in BESS.

2.3.5.4 Marginal and Opportunity Costs

Table 7 shows the errors with Stochastic Marginal Cost (SMC) and Opportunity Cost (OP). The HM results have been chosen as a reference for the error calculation. The SMC is calculated as the weighted dual variable from the balance equation in each model. The OP is calculated as the weighted dual variable from the inter-period storage balance equation in each model, equations (3), (4), (6), and (8). The same color notation as in Table 6 is used. On the one hand, the LRP model mostly leads to errors lower than 5% and is the most accurate model in almost all results. On the other hand, the LDC model yields in most of the cases errors higher than 10% and, as expected from the results in previous sections, exhibits the worst performance in the opportunity cost of the BESS throughout the time horizon, overestimating most of the months the economic signal of energy storage.

The errors in reservoir 3 are higher than those in reservoir 1 and 2. This is a reasonable result, considering that reservoir 3 is downstream of reservoir 1 and 2. Therefore, errors in reservoirs 1 and 2 propagate to reservoir 3 and complicate the estimation.

In Section 2.3.4, the equation (9) has been presented, which allows us to determine the intra-period or hourly opportunity cost in the LRP model. This represents the main advantage over the LDC. Fig. 22 shows the opportunity cost (or storage value) of BESS in the HM, LRP, and LDC models for a particular week. The opportunity cost obtained from the LRP model mimics the trend followed by the results in the HM model. In fact, almost 75% of the time, the difference between the results of both models is lower than 10%. Fig. 22 shows one value for the LDC model throughout the week because it only determines one opportunity cost value per month, see equations (3) and (4).

Table 7. Stochastic Marginal Cost and Opportunity Cost Results – Error [%]

[5] The cycles are estimated for all models using the total charge/discharge energy over the year and dividing it by the BESS' maximum energy capacity.

Month	SMC		OP Res 1		OP Res 2		OP Res 3		OP BESS	
	LDC	LRP	LDC	LRP	LDC	LRP	LDC	LRP	LDC	LRP
Oct	-13.7	1.3	-16.3	-0.6	-6.6	-0.6	-23.9	2.8	-6.7	-2.0
Nov	-4.7	-2.0	-16.3	-0.6	-6.6	-0.6	-23.9	2.8	-4.7	-0.4
Dec	-28.5	0.3	-16.3	-0.6	-6.6	-0.6	-23.9	2.8	-16.3	-3.6
Jan	-10.8	-1.3	-17.7	-2.4	-8.2	-2.4	-22.6	-1.2	-32.2	-0.9
Feb	-8.7	0.7	-12.5	-0.4	-8.2	-0.4	-22.6	-1.0	-32.4	-3.1
Mar	-13.5	6.6	-12.5	-0.4	-8.2	-0.4	-21.4	-1.0	-27.4	5.6
Apr	-9.5	0.6	-12.5	-0.4	-8.2	-0.4	-21.4	-1.0	-29.0	-3.2
May	-14.0	0.2	-12.5	-0.4	-8.2	-0.4	-21.4	-1.0	-26.7	0.0
Jun	-9.4	1.4	-12.5	-0.4	-8.2	-0.4	-21.4	-1.0	-26.3	4.3
Jul	-23.1	2.0	-12.5	-0.4	-8.2	-0.4	-21.4	-1.0	-37.9	4.3
Aug	-13.8	4.7	-11.9	1.2	-6.9	-0.6	-22.3	-1.4	-30.2	1.9
Sep	-15.0	1.5	15.4	0.4	-6.9	-0.6	6.0	0.3	-28.8	-0.9
Mean Absolute Error	13.7	1.9	14.1	0.7	7.6	0.7	21.0	1.4	24.9	2.5

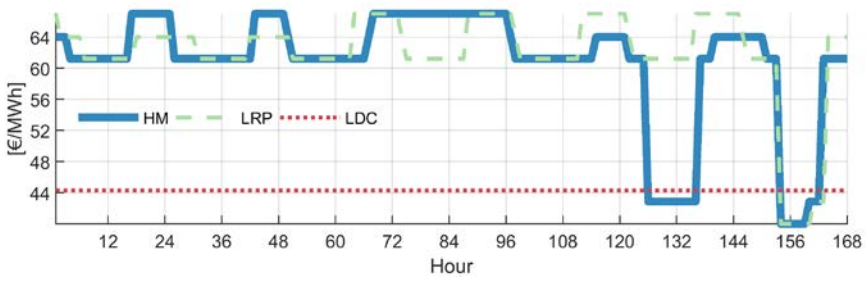

Fig. 22. Opportunity Cost or Storage Value of BESS [€/MWh]

2.3.6 Discussion

The main drawback of the previous result is that the medium-term model, i.e., LDC model, does not consider short-term chronological information. In fact, as shown in Section 2.3.5, the LDC model has the worst performance. All the time resolutions tested

for the LRP model have shown a better performance than the LDC model. This means that LRP succeeds in the internalization of short-term chronological information in the medium-term hydrothermal problem, which enables inclusion of the operation of BESS without solving the HM model for the entire medium-term horizon. In other words, the LRP model co-optimizes both medium- (or long-) and short-term decisions. Moreover, equation (9) in the LRP has the advantage that it allows to differentiate between both components: intra-period and inter-period opportunity cost and therefore, know the share of each component in the total opportunity cost.

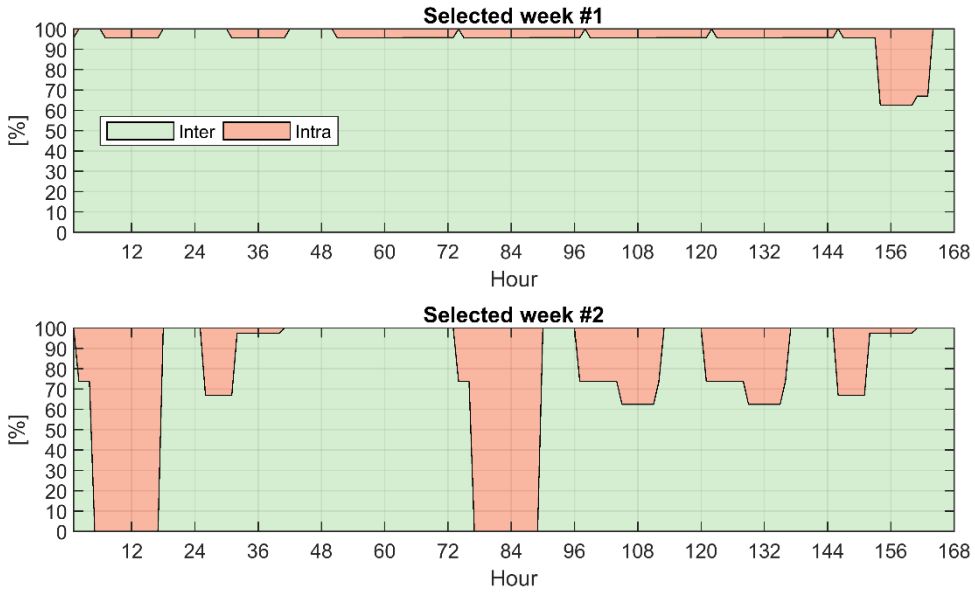

Fig. 23. ***Share of Inter/Intra Values in total Opportunity Cost of BESS***

Fig. 23 (top) shows the share of these components in the E-RP model for the same week in Fig. 22. Most of the time, the inter-period value represents more than 90% of the total value through the week, while the intra-period value gets more relevance, near 40%, at the end of the week (around hour 156), when the opportunity cost has the biggest change in Fig. 22. However, this share in the composition cannot be taken as a general behavior. For instance, Fig. 23 (bottom) shows results for another week in the same case study. Here, it can be observed that there are hours where the intra-period represents the 100% of the total value of the opportunity cost in the BESS. Therefore, the share changes depending on the characteristics of the case study as well as the location within the time scope. These types of results and analysis cannot be developed in the classic LDC model and represent a novel contribution in this research. This contribution opens the door to new analysis and studies. For instance, these results give insights to market participants of when short-term storage opportunities are more relevant than long-term storage opportunities and then considering this situation in their market bids.

Another important aspect to discuss is that the coordination of short- and medium-term hydrothermal models has been traditionally performed by using two separate models and sharing information between them as in [68] and more recently in [69]. One medium-term model is run first using a reduced chronology, such as the LDC model described in Appendix B, in order to obtain the end volume or the water value from each reservoir. Under the assumption that a Stochastic Dual Dynamic Programming (SDDP) [70] approach has been used to solve the medium-term model, a piecewise-linear Future Cost Function (FCF) can be utilized to meet end-point conditions from the medium-term model in the short-term model as it was formerly proposed in [71] and more lately in [72]. This information is used as input data in a short-term model to find the daily levels and hourly opportunity costs.

Finally, the LRP model is also compatible with decomposition techniques, such as Benders' decomposition or SDDP, in order to consider a large number of scenarios in the scenario tree. Therefore, it could be obtained the FCF internalizing the hourly dynamics of short-term storage, which is not possible with the current LDC model approach.

2.3.7 Conclusion

This paper introduces a novel formulation for stochastic hydrothermal models in which short-term opportunity costs are included in the medium- and long-optimization process. It has been validated the initial hypothesis, that short-term energy storage (e.g., BESS) decisions on energy production impact the opportunity cost (or water value) of seasonal storage. In the presented case study, in a comparison with a detailed hourly model used as benchmark, the classic LDC approach systematically underestimates the water value between 6% and 24% for seasonal hydro reservoirs, while the proposed LRP model error varies between 0% and 6.6%, sometimes underestimating and others overestimating. In addition, operational results (e.g., productions, number of cycles for short-term storage, and storage levels) have a better estimation in the LRP model than in the LDC model. Another advantage of the proposed model is the possibility to obtain hourly detailed opportunity costs of ESS without solving an hourly hydrothermal dispatch model. Moreover, the proposed model formulation allows to differentiate between the short- and long-term opportunity costs. For instance, the results show that depending on the hour, the intra-period storage value (short-term opportunity cost) constitutes up to 100% of the total opportunity cost, demonstrating that inter-period opportunity cost may be also relevant for the long-term storage value. The derivation of an hourly opportunity cost of ESS that accounts for both short- and long-term dynamics represents a novel contribution, as it is not possible to obtain its value from a classic LDC model. In addition, the temporal reduction using the linked representative periods in the proposed LRP model makes it also suitable to solve real-size case studies. Furthermore, long-term opportunity costs due to hydro seasonality in power system internalize the hourly opportunity costs. In other words, the water value in seasonal storage includes the impact of short-term operational decisions.

This result is important to help market participants or planning authorities in their decision-making processes (bids or investment decisions in storage assets) by determining correct opportunity costs (i.e., short-term prices and long-term expected values) with the co-optimization approach in the LRP model and therefore avoiding sub-optimal solutions from iterative processes (e.g., fixing the hydro reservoirs levels obtained from a medium-term model in a short-term operational model).

Looking forward, the LRP model could be applied to analyze energy and operating reserve markets in hydrothermal power systems in a more natural way than using the LDC approach.

2.4 Power-Based Generation Expansion Planning for Flexibility Requirements

Generation Expansion Planning (GEP) is a classic long-term problem in power systems that aims at determining the optimal generation technology mix [73]. Environmental policies, such as renewable targets [74] or CO2 emission reduction [75] influence in GEP decisions, leading to the integration of vast amounts of variable Renewable Energy Sources (vRES), i.e., wind and solar, in GEP. Nevertheless, vRES integration has consequences in GEP modeling. For instance, previous studies [9], [76], [77] have shown the importance of including short-term dynamics on GEP decisions in order to consider the increased need of operational flexibility due to vRES integration. Therefore, correctly modeling flexibility in GEP models is crucial to reach the right conclusions in the energy transition process.

In order to consider operational flexibility in GEP, Unit Commitment (UC) modeling is needed to determine system operation [77], [78]. For example, it is known that units are being cycled more frequently due to higher vRES flexibility requirements [79]. Studies have shown that ignoring startup and shutdown processes highly overestimates the flexibility and costs of the system [80]. Another example is ramping constraints. If we focus on flexibility and want to know a good (optimal) future generation-mix and interconnection capacities for a given scenario, the GEP problem must include at least detailed ramping constraints. Moreover, operating reserve decisions have also become more relevant in GEP with the integration of vRES because they may ensure that generation technologies have an extra income to recover their investment costs through these types of ancillary services.

Despite the recent developments to consider flexibility requirements in GEP, classic GEP models use energy-based formulations, such as TIMES modeling framework [27], the Regional Energy Deployment System (ReEDS) framework [4], Resource Planning Model (RPM) [28], and COMPETES [81]. Recent studies [80], [82], [83] have shown that energy-based UC models cannot capture variability on demand and vRES, and even

assuming that they capture it, they cannot deliver the flexibility that they promise, that is, they intrinsically and hiddenly overestimate the flexibility of the system. In addition, energy-based formulations inherently lead unfeasible ramping constraints as widely discussed in the literature [84], [85]. This is mainly because average energy levels (e.g., average level in one hour) do not provide detailed information about the instantaneous output of a generator, and constraints such as ramping-limits and demand-balance are dependent on instantaneous outputs rather than average levels. This means that more flexibility than planned by energy-based models is used in real-time operation (through operating reserves and allowing deviations on schedules) to deal with all the problems introduced by these traditional energy-based models. These problems are hidden in the formulations, and to assess really their performance, real-time simulations are required (e.g., 5-min dispatch), as it is widely discussed in [80].

More recently, power-based models have been proposed [82], [86] to overcome these problems by better exploiting the system flexibility [80], by allowing the correct modeling of ramping constraints and operating reserves [82], [83] in order to deliver the expected and actual flexibility from the generation resources. This is possible because a power-based model has a clear distinction between power and energy in its core formulation. Demand and generation are modeled as hourly piecewise-linear functions representing their instantaneous power trajectories. The schedule of a generating unit output is no longer an energy stepwise function, but a smoother piece-wise power function.

Another important aspect to determine the flexibility requirements in power systems is time resolution. In order to model correctly the real operation of power systems a high resolution is needed (e.g., minutes). Current GEP models are based on hourly resolution where the underlying assumption is that it is enough to capture the variability and flexibility requirements of power systems. However, it has already been shown in [80] that real-time simulations (e.g., 5-min time step) help to determine the performance of different schedules (operational decisions) to meet the real-time flexibility requirements in the power system. This type of real-time validation is not common to be carried out because it is considered unnecessary. Nevertheless, to validate correctly flexibility capabilities and requirements of the system, this real-time evaluation is paramount [80]. Therefore, we carry out a real-time validation stage (e.g., 5-min simulation) in order to evaluate the quality of investment and operational decisions obtained with the models that have been analyzed in this paper.

In this paper, we propose a novel power-based model for GEP presenting advantages over the traditional energy-based models. The proposed model optimizes investment decisions on vRES, Energy Storage Systems (ESS), and thermal technologies. ESS are included because they represent one of the most promising options to provide flexibility in power systems in the future [29]. In addition, the investment and operational decisions are tested in a real-time validation stage to better reflect the actual flexibility that these decisions can provide. The main contributions of this paper are as follows:

I. This paper proposes an investment decision model for generation and energy storage technologies using a power-based UC formulation as an extension of the classic energy-based UC formulations. The proposed power-based GEP-UC model improves the classic energy-based long- term capacity expansion models by representing the flexibility requirements of power systems more accurately (i.e., reserve decisions and ramping constraints) in a long-term horizon considering investment decisions. Moreover, we also propose a novel power-based formulation for ESS (e.g., batteries), so it can be included in the proposed power-based model for operation and investment decisions. It is important to highlight that both the power-based GEP-UC and the power-based ESS modeling for investment and operation represent original contributions as they have not been proposed in the literature before.

II. In order to improve how this extended problem can be addressed, we also propose a semi-relaxed version of the power-based GEP-UC model, which aims at reducing the computational burden without losing accuracy in the results. In fact, the real-time validation stage shows that this semi-relaxed version performs better than the classic energy-based (integer) model, i.e., makes investment and operation decisions that lead to lower costs and emissions than those obtained by short-term models, while also solving considerably faster. To the authors' knowledge, this type of insight has not been obtained before in the literature.

The paper is organized as follows: Section 2.4.1 shows model formulations used for the GEP problem, considering both energy- and power-based equations. Section 2.4.2 explains the procedure to evaluate the power system flexibility. Section 2.4.3 summarizes the data of each case study. Section 2.4.4 discusses the main results, including a sensitivity analysis to the ramp capacity of the generation units. Finally, Section 2.4.5concludes this paper.

2.4.1 Generation Expansion Model Formulations

This section presents the objective function and set of constraints for the energy- and the power-based GEP-UC formulations. These constraints include investment decisions for different generation technologies: thermal generation, ESS, and VRES.

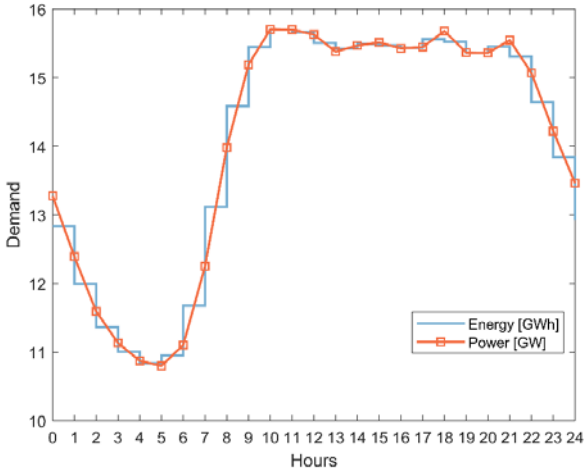

Fig. 24. Power demand trajectory and hourly energy demand.

Before presenting and discussing the energy- and power-based model formulations, let us briefly comment on input data of the respective models. As indicated by the model name, in the power-based model most of the constraints are represented in terms of power, whereas their equivalent in the energy-based model is formulated in terms of energy. As a consequence, a power-based model requires power data (e.g., in MW units), and energy-based models require energy data (e.g., in MWh units). While the actual input data might be different in type and units, it stems from the same original data, which makes the model comparison fair. For example, consider the demand curve given in Fig. 24. The energy-based model uses data corresponding to energy blocks (as given by the blue step function), whereas the power-based model uses data representing a power trajectory (as given by the orange piecewise linear curve). It is important to highlight that the total energy in both models is the same. However, decision variables and constraints change depending on whether we optimize the energy- or the power-based model, as we show in the following sections. Please note that similar transformations occur for vRES time series.

Finally, operational decisions are considered using a clustered UC formulation (i.e., aggregating similar generating units into one group or cluster), which is commonly applied in long-term planning models [78], [87], [88].

2.4.1.1Energy-Based Formulation

The GEP seeks to minimize the investment costs plus the expected value of operating costs: production cost, up/down reserve cost, CO2 emission cost, no-load cost, shutdown cost, startup cost. Notice that $\Psi = \{x, e, \hat{e}, \hat{c}, r^{+}, r^{-}, u, y, z, \delta, \phi\}$ corresponds to the set of decision variables considered in this model.

$$\min_{\Psi} \sum_{j\in\mathcal{J}} C_j^I x_j + \sum_{\omega\in\Omega} \pi_\omega \sum_{t\in\mathcal{T}} \left\{ \sum_{j\in\mathcal{J}} \left[C_j^{LV} \hat{e}_{\omega jt} + C_j^{R+} r_{\omega jt}^{+} + C_j^{R-} r_{\omega jt}^{-} \right] + \sum_{g\in\mathcal{G}} \left[C_g^{EM} \hat{e}_{\omega gt} + C_g^{NL} u_{\omega gt} + C_g^{SD} z_{\omega gt} + \sum_{k\in\mathcal{K}_g} C_{gk}^{SU} \delta_{\omega gkt} \right] \right\} \quad (1)$$

The system-wide constraints are guaranteed by energy demand balance (2), transmission limits (3), and reserve requirements (24)-(25):

$$\sum_{j\in\mathcal{J}} \hat{e}_{\omega jt} - \sum_{s\in\mathcal{S}} \hat{c}_{\omega st} = \sum_{b\in\mathcal{B}^D} D_{\omega bt}^{E} \quad \forall \omega, t \quad (2)$$

$$-\overline{F}_l \le \sum_{j\in\mathcal{J}} \Gamma_{lj}^{J} \hat{e}_{\omega jt} - \sum_{s\in\mathcal{S}} \Gamma_{ls}^{S} c_{\omega st} - \sum_{b\in\mathcal{B}^D} \Gamma_{lb} D_{\omega bt}^{E} \le \overline{F}_l \; \forall l, \omega, t \quad (3)$$

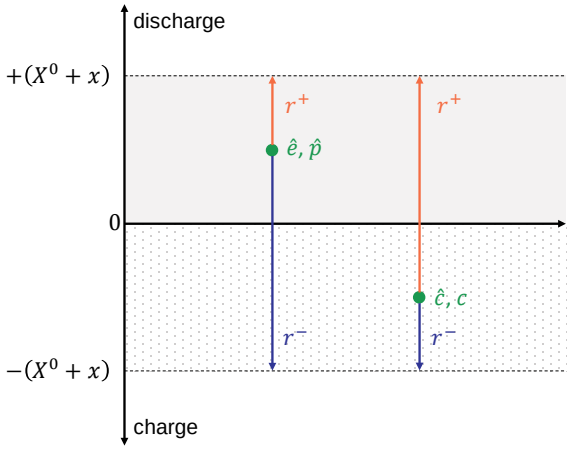

Fig. 25. ESS providing reserves from different operation points.

The relationship between operational and investment decisions for each technology type is guaranteed with (4) for thermal technologies, (5)-(6) for ESS, and (7) for vRES. Notice that (5)-(6) model the reserve variables that ESS can provide whether the ESS is charging or discharging, see Fig. 25. These constraints define the flexibility reserves that ESS can provide.

$$u_{\omega gt} \le X_g^0 + x_g \quad \forall \omega, g, t \quad (4)$$

$$\hat{e}_{\omega st} - \hat{c}_{\omega st} + r_{\omega gt}^{+} \le X_s^0 + x_s \quad \forall \omega, s, t \quad (5)$$

$$\hat{e}_{\omega st} - \hat{c}_{\omega st} - r_{\omega gt}^{-} \ge -(X_s^0 + x_s) \quad \forall \omega, s, t \quad (6)$$

$$\hat{e}_{\omega vt} \le V_{\omega vt}^{E}(X_v^0 + x_v) \quad \forall \omega, v, t \quad (7)$$

Thermal generation constraints include: commitment/ startup/ shutdown logic (8), minimum up/down times (9)-(10), startup type selection (11)-(12) (e.g., hot, warm, and cold startup), energy production limits including reserve decisions (13)-(16) (where $\mathcal{G}^1$ is defined as the thermal technologies in $\mathcal{G}$ with $TU_g = 1$), and total energy production (17). The UC formulation presented here is based on the tight and compact formulation

proposed in [40]. Furthermore, Gentile et al. [89] have proven that the set of constraints (8)-(10) together with (13)-(17) is the tightest representation (i.e., convex hull) for the energy-based model.

$$u_{\omega gt} - u_{\omega g,t-1} = y_{\omega gt} - z_{\omega gt} \quad \forall \omega, g, t \tag{8}$$

$$\sum_{i=t-TU_g+1}^{t} y_{\omega gi} \leq u_{\omega gt} \quad \forall \omega, g, t \in [TU_g, T] \tag{9}$$

$$\sum_{i=t-TD_g+1}^{t} z_{\omega gi} \leq (X_g^0 + x_g) - u_{\omega gt} \; \forall \omega, g, t \in [TD_g, T] \tag{10}$$

$$\delta_{\omega gkt} \leq \sum_{i=T_{gk}^{SU}}^{T_{g,k+1}^{SU}-1} z_{\omega g,t-i} \quad \forall \omega, g, k \in [1, K_g), t \tag{11}$$

$$\sum_{k \in \mathcal{K}_g} \delta_{\omega gkt} = y_{\omega gt} \quad \forall \omega, g, t \tag{12}$$

$$e_{\omega gt} + r_{\omega gt}^{+} \leq (\overline{P}_g - \underline{P}_g) u_{\omega gt} - (\overline{P}_g - SD_g) z_{\omega g,t+1} - \max(SD_g - SU_g, 0) y_{\omega gt} \quad \forall \omega, g \in \mathcal{G}^1 \tag{13}$$

$$e_{\omega gt} + r_{\omega gt}^{+} \leq (\overline{P}_g - \underline{P}_g) u_{\omega gt} - (\overline{P}_g - SU_g) y_{\omega g,t} - \max(SU_g - SD_g, 0) z_{\omega g,t+1} \quad \forall \omega, g \in \mathcal{G}^1 \tag{14}$$

$$e_{\omega gt} + r_{\omega gt}^{+} \leq (\overline{P}_g - \underline{P}_g) u_{\omega gt} - (\overline{P}_g - SU_g) y_{\omega g,t} - (\overline{P}_g - SD_g) z_{\omega g,t+1} \quad \forall \omega, g \notin \mathcal{G}^1, t \tag{15}$$

$$e_{\omega gt} - r_{\omega gt}^{-} \geq 0 \quad \forall \omega, g, t \tag{16}$$

$$\hat{e}_{\omega gt} = \underline{P}_g u_{\omega gt} + e_{\omega gt} \quad \forall \omega, g, t \tag{17}$$

Traditional energy-based UC formulations ignore the inherent startup (SU) and shutdown (SD) trajectories of thermal generation, assuming they start/end their production at their minimum output. Authors in [80], [82] have shown the relevance of the SU and SD processes when they are included in the scheduling optimization. Therefore, we also analyze the energy-based formulation including the SU/SD trajectories proposed in [90]. Thus, if SU/SD trajectories are considered then (17) is replaced by (18).

$$\hat{e}_{\omega gt} = \underbrace{\sum_{k=1}^{K_g} \sum_{i=1}^{SU_{gk}^{D}} E_{gki}^{SU} \delta_{\omega gk,(t-i+SU_{gk}^{D}+1)}}_{Startup\ trajectory} + \underbrace{\sum_{i=1}^{SD_g^{D}} E_{gi}^{SD} z_{\omega g,(t-i+1)}}_{Shutdown\ trajectory} + \underbrace{\underline{P}_g u_{\omega gt} + e_{\omega gt}}_{Output\ when\ being\ up} \quad \forall \omega, g, t \tag{18}$$

ESS constraints include: logic to avoid charging and discharging at the same time (19)-(20), the definition of the storage inventory level (21), storage limits including reserve (22)-(23). Since ESS can provide reserves (Fig. 25), the binary variable $\gamma_{\omega st}$ in (19)-(20) guarantees that the ESS is only charging or discharging at time period t. Without (19)-(20), the optimization model could find a non-realistic solution where the ESS is charging and discharging simultaneously in order to provide more reserves from the ESS.

$$\hat{c}_{\omega st} \leq (1 - \gamma_{\omega st}) \cdot (X_s^0 + \overline{X}_s) \quad \forall \omega, s, t \tag{19}$$

$$\hat{e}_{\omega st} \leq \gamma_{\omega st} \cdot (X_s^0 + \overline{X}_s) \quad \forall \omega, s, t \tag{20}$$

$$\phi_{\omega st} = \phi_{\omega s,t-1} + \eta_s \hat{c}_{\omega st} - \hat{e}_{\omega st} \quad \forall \omega, s, t \tag{21}$$

$$\phi_{\omega st} \leq EPR_s(X_s^0 + x_s) - \sum_{i=t-1}^{t} r_{\omega gi}^- \quad \forall \omega, s, t \tag{22}$$

$$\phi_{\omega st} \geq \sum_{i=t-1}^{t} r_{\omega gi}^+ \quad \forall \omega, s, t \tag{23}$$

$$\sum_{j \in \mathcal{J}} r_{\omega jt}^+ \geq R_{\omega t}^+ \quad \forall \omega, t \tag{24}$$

$$\sum_{j \in \mathcal{J}} r_{\omega jt}^- \geq R_{\omega t}^- \quad \forall \omega, t \tag{25}$$

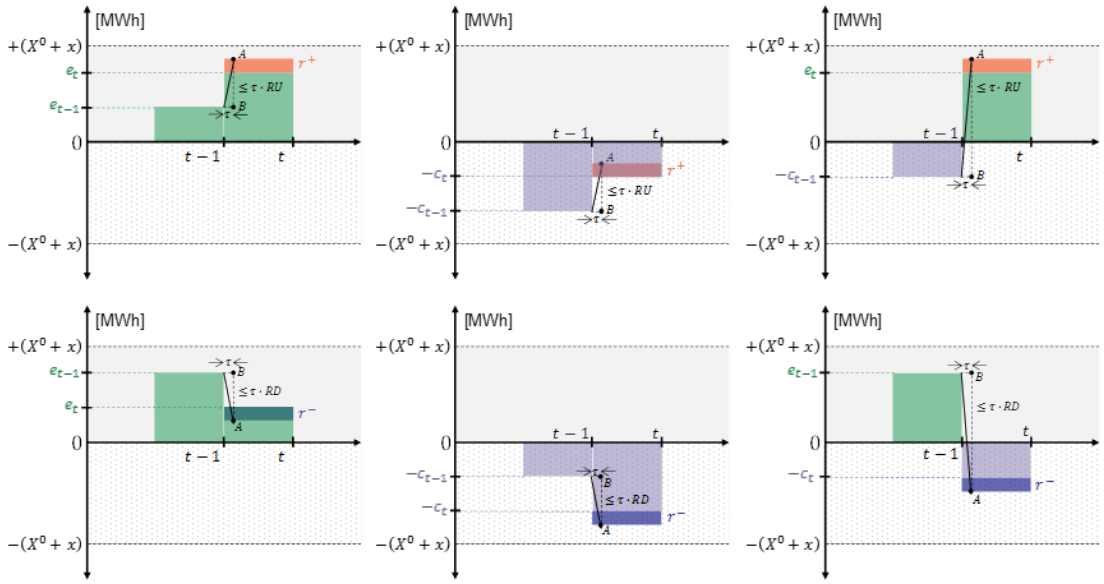

Fig. 26. Ramping constraints for ESS in the energy-based model.

Flexibility requirements in the power system are represented by ramping constraints including reserve decisions. In order to guarantee that scheduled reserves are feasible to provide at τ-min (e.g., τ=5) using the energy-based formulation, it is necessary to consider the ramping capability at τ-min. For instance, ramp capability limits imposed with (26)-(27) consider the reserve that thermal technologies can provide at τ-min. ESS ramp capability limits (28)-(29) consider the charged energy in addition to the energy output (i.e., discharged energy), as in [91]. Fig. 26 shows the ramping constraints for ESS in the energy-based model for all possible operational conditions of the ESS going from time period $t-1$ to t. Notice that (28)-(29) allow ESS to switch from charging to discharging within the ramp limit, i.e., segment AB in Fig. 26.

$$\left(e_{\omega gt} - e_{\omega g,t-1}\right) + r_{\omega gt}^+ \leq \tau RU_g u_{\omega gt} \quad \forall \omega, g, t \tag{26}$$

$$-\left(e_{\omega gt} - e_{\omega g,t-1}\right) + r_{\omega gt}^- \leq \tau RD_g u_{\omega g,t-1} \quad \forall \omega, g, t \tag{27}$$

$$\left(\hat{e}_{\omega st} - \hat{e}_{\omega s,t-1}\right) - \left(\hat{c}_{\omega st} - \hat{c}_{\omega s,t-1}\right) + r_{\omega st}^+ \leq \tau RU_s(X_s^0 + x_s) \; \forall \omega, s, t \tag{28}$$

$$\left(\hat{c}_{\omega st} - \hat{c}_{\omega s,t-1}\right) - \left(\hat{e}_{\omega st} - \hat{e}_{\omega s,t-1}\right) + r_{\omega st}^- \leq \tau RD_s(X_s^0 + x_s) \; \forall \omega, s, t \tag{29}$$

2.4.1.2Power-Based Formulation

This section shows the GEP-UC equations in terms of power. However, some of the terms in these equations are naturally linked to energy. For instance, the objective function (30) includes the so-called calculated energy $\hat{e}_{\omega jt}$ to obtain the variable cost and CO2 emission cost. Equation (31) determines the energy output from the power output variables $\hat{p}_{\omega jt}$. Since the variable and CO2 costs are intrinsically based on energy, energy variables are then used in the objective function for both power- and energy-based models. In addition, for ESS the charged energy $\hat{c}_{\omega st}$ is also determined using the charged power in (32). Notice that $\Lambda = \{x, p, \hat{p}, \hat{e}, c, \hat{c}, r^+, r^-, u, y, z, \delta, \phi\}$ corresponds to the set of decision variables in this model.

$$\min_{\Lambda} \sum_{j\in\mathcal{J}} C_j^I x_j + \sum_{\omega\in\Omega} \pi_\omega \sum_{t\in\mathcal{T}} \left\{ \sum_{j\in\mathcal{J}} \left[C_j^{LV} \hat{e}_{\omega jt} + C_j^{R+} r_{\omega jt}^+ + C_j^{R-} r_{\omega jt}^- \right] + \sum_{g\in\mathcal{G}} \left[C_g^{EM} \hat{e}_{\omega gt} + C_g^{NL} u_{\omega gt} + C_g^{SD} z_{\omega gt} + \sum_{k\in\mathcal{K}_g} C_{gk}^{SU} \delta_{\omega gkt} \right] \right\} \quad \textbf{(30)}$$

$$\hat{e}_{\omega jt} = \frac{\hat{p}_{\omega jt} + \hat{p}_{\omega j,t-1}}{2} \quad \forall \omega, j, t \quad (31)$$

$$\hat{c}_{\omega st} = \frac{c_{\omega st} + c_{\omega s,t-1}}{2} \quad \forall \omega, s, t \quad (32)$$

Demand balance constraint (33) and power-flow transmission limits (34) also use the power output instead of energy output. The power trajectories, e.g., $D_{\omega bt}^P$ for demand, can be obtained and forecasted using the system operator real-time data. Then, the hourly energy can be calculated from the power trajectory using the area under the curve. Ref. [92] shows the relation between energy and power schedules. Reserve requirements (24)-(25) remain the same because they are already expressed in terms of power.

$$\sum_{j\in\mathcal{J}} \hat{p}_{\omega jt} - \sum_{s\in\mathcal{S}} c_{\omega st} = \sum_{b\in\mathcal{B}^D} D_{\omega bt}^P \quad \forall \omega, t \quad (33)$$

$$-\overline{F}_l \le \sum_{j\in\mathcal{J}} \Gamma_{lj}^J \hat{p}_{\omega jt} - \sum_{s\in\mathcal{S}} \Gamma_{ls}^S c_{\omega st} - \sum_{b\in\mathcal{B}^D} \Gamma_{lb} D_{\omega bt}^P \le \overline{F}_l \quad \forall l, \omega, t \quad (34)$$

In terms of the relationship between operational and investment decisions, thermal unit constraint (4) remains the same. However, constraints for ESS and vRES technologies change to (35)-(36) and (37), respectively. As in the energy-based model, (35)-(36) consider reserve variables, see Fig. 25.

$$\hat{p}_{\omega st} - c_{\omega st} + r_{\omega gt}^+ \le X_s^0 + x_s \quad \forall \omega, s, t \quad (35)$$

$$\hat{p}_{\omega st} - c_{\omega st} - r_{\omega gt}^- \ge -(X_s^0 + x_s) \quad \forall \omega, s, t \quad (36)$$

$$\hat{p}_{\omega vt} \le V_{\omega vt}^P (X_v^0 + x_v) \quad \forall \omega, v, t \quad (37)$$

Unit commitment constraints (8)-(12) do not change in the power-based formulation. Equations (38)-(39) limit the power output of thermal technologies. The total power output constraint is different depending whether it is a quick- or slow-start unit. Quick-

start technologies $\mathcal{G}^F$ are thermal generators that can startup/shutdown within one hour (i.e., $SU_{gk}^D = SD_g^D \leq 1$), while slow-start technologies $\mathcal{G}^S$ are those with a SU/SD duration greater than one hour as well as a SU/SD capacity equal to the minimum power output (i.e., $SU_g = SD_g = \underline{P}_g$). Therefore, the total power output of slow-start technologies considers SU/SD trajectories (41), whereas (40) for quick-start technologies does not. For a better understanding of the modeling of quick- and slow-start technologies, the reader is referred to [86], [89]. The formulation presented here is based on the tight and compact formulation proposed in [82]. Furthermore, Morales-España et al. [86] has proven that the set of constraints (8)-(10) together with (38)-(41) is the tightest possible representation (i.e., convex hull) for the power-based model.

$$p_{\omega gt} + r^{+}_{\omega gt} \leq \left(\overline{P}_g - \underline{P}_g\right)u_{\omega gt} - \left(\overline{P}_g - SD_g\right)z_{\omega g,t+1} + \left(SU_g - \underline{P}_g\right)y_{\omega g,t+1} \;\forall \omega, g, t \tag{38}$$

$$p_{\omega gt} - r^{-}_{\omega gt} \geq 0 \quad \forall \omega, g, t \tag{39}$$

$$\hat{p}_{\omega gt} = \underline{P}_g\left(u_{\omega gt} + y_{\omega g,t+1}\right) + p_{\omega gt} \quad \forall \omega, g \in \mathcal{G}^F, t \tag{40}$$

$$\hat{p}_{\omega gt} = \underbrace{\sum_{k=1}^{K_g}\sum_{i=1}^{SU_{gk}^D} P_{gki}^{SU}\delta_{\omega gk,\left(t-i+SU_{gk}^D+2\right)}}_{Startup\ trajectory} + \underbrace{\sum_{i=2}^{SD_g^D+1} P_{gi}^{SD} z_{\omega g,(t-i+2)}}_{Shutdown\ trajectory} + \underbrace{\underline{P}_g\left(u_{\omega gt} + y_{\omega g,t+1}\right) + p_{\omega gt}}_{Output\ when\ being\ up} \forall \omega, g \in \mathcal{G}^S, t \tag{41}$$

ESS constraints for storage level (21) and storage level limits including reserve (22)-(23) continue the same. Nevertheless, the logic to avoid charging and discharging at the same time (42)-(43) is updated to consider the power output and charged power.

$$c_{\omega st} \leq (1 - \gamma_{\omega st}) \cdot \left(X_s^0 + \overline{X}_s\right) \quad \forall \omega, s, t \tag{42}$$

$$\hat{p}_{\omega st} \leq \gamma_{\omega st} \cdot \left(X_s^0 + \overline{X}_s\right) \quad \forall \omega, s, t \tag{43}$$

One of the main advantages of power-based formulation is that it allows to describe a more detailed set of constraints to represent the flexibility requirements, which are described in terms of power instead of energy. The proposed power-based equations in [82] ensure that reserves can be provided at any time within the hour by guaranteeing that the reserve does not exceed the ramp-capability at τ-min (e.g., τ=5 min) and power-capacity limits at the end of the hour (i.e., 60 min). Therefore, (44)-(45) guarantee that τ-min ramp capability is ensured for thermal technologies, while (46)-(47) guarantee the power- capacity limit for both τ-min and at the end of the hour. These constraints have been defined for thermal generation units in [82]. However, ramping constraints in power-based models have not been defined for ESS in the literature before. This paper then proposes a set of constraints for flexibility requirements in power-based models. Fig. 27 shows different operating points and reserves for ESS at τ-min within hour t. Here, segments EA and AF must be below the ramp-capability limits τRU_s and τRD_s, as well as points E and F must be within the maximum and minimum power-capacity limit. Therefore, constraints (48)-(51) guarantee these conditions for all operating points of

ESS in Fig. 27. Notice, that here it is important to highlight that (42)-(43) avoid simultaneous charging and discharging.

$$\frac{\tau(p_{\omega gt}-p_{\omega g,t-1})}{60}+r^{+}_{\omega gt}\le \tau RU_g u_{\omega gt} \quad \forall\omega,g,t \tag{44}$$

$$-\frac{\tau(p_{\omega gt}-p_{\omega g,t-1})}{60}+r^{-}_{\omega gt}\le \tau RD_g u_{\omega g,t-1} \quad \forall\omega,g,t \tag{45}$$

$$\frac{\tau p_{\omega gt}+(60-\tau)p_{\omega g,t-1}}{60}+r^{+}_{\omega gt}\le (\overline{P}_g-\underline{P}_g)u_{\omega gt}\ \forall\omega,g,t \tag{46}$$

$$\frac{\tau p_{\omega gt}+(60-\tau)p_{\omega g,t-1}}{60}-r^{-}_{\omega gt}\ge 0 \quad \forall\omega,g,t \tag{47}$$

$$\frac{\tau(\hat{p}_{\omega st}-\hat{p}_{\omega s,t-1})}{60}-\frac{\tau(c_{\omega st}-c_{\omega s,t-1})}{60}+r^{+}_{\omega st}\le \tau RU_s(X^0_s+x_s) \qquad \forall\omega,s,t \tag{48}$$

$$\frac{\tau(\hat{p}_{\omega st}-c_{\omega st})+(60-\tau)(\hat{p}_{\omega s,t-1}-c_{\omega s,t-1})}{60}+r^{+}_{\omega st}\le X^0_s+x_s \qquad \forall\omega,s,t \tag{49}$$

$$\frac{\tau(c_{\omega st}-c_{\omega s,t-1})}{60}-\frac{\tau(\hat{p}_{\omega st}-\hat{p}_{\omega s,t-1})}{60}+r^{-}_{\omega st}\le \tau RD_s(X^0_s+x_s) \qquad \forall\omega,s,t \tag{50}$$

$$\frac{\tau(\hat{p}_{\omega st}-c_{\omega st})+(60-\tau)(\hat{p}_{\omega s,t-1}-c_{\omega s,t-1})}{60}-r^{-}_{\omega st}\ge -(X^0_s+x_s) \qquad \forall\omega,s,t \tag{51}$$

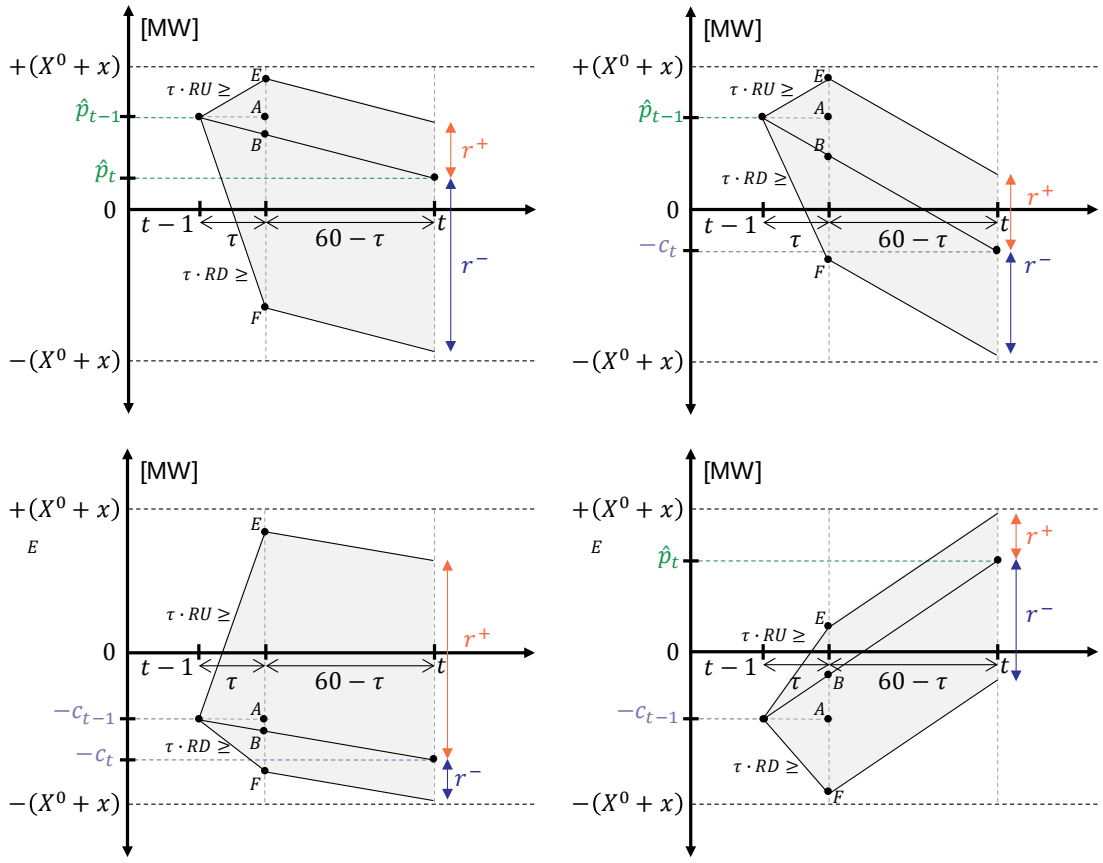

Fig. 27. Ramping constraints for ESS in the power-based model.

2.4.2 System Flexibility Evaluation

As mentioned in the previous section, two main formulations are analyzed for GEP: the traditional energy-based (EB), and the power-based formulation (PB). We also analyze the traditional energy-based using SU/SD trajectories (EBs). **¡Error! No se encuentra el origen de la referencia.** shows a summary with all the equations that define these models. All models include an hourly UC (either energy- or power-based) in order to consider operating constraints, involving those related to the power system flexibility (i.e., ramping and reserve constraints). In order to measure the quality of the obtained solution under real-time flexibility requirements, we carry out an evaluation of investment and operational decisions through a simulation using the same scenarios as in the GEP-UC hourly optimization (in-sample simulation). This evaluation allows us to establish the problems associated to each formulation rather than those associated to the uncertainty representation by itself.

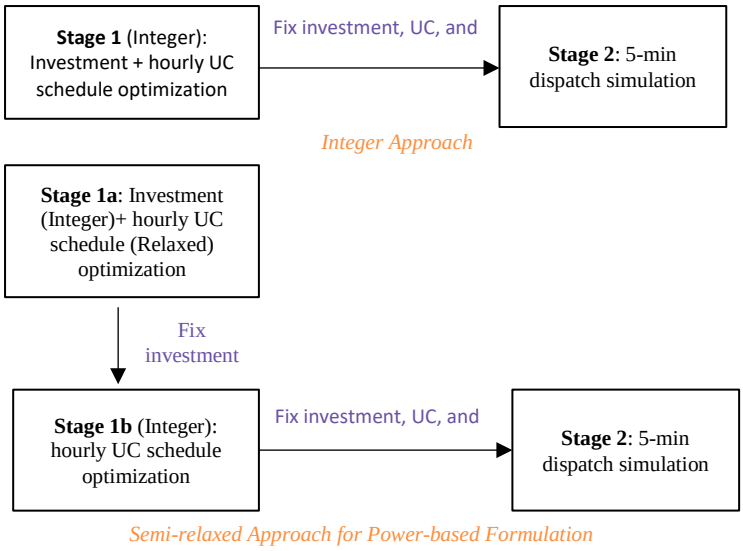

Fig. 28. Stage sequence for integer (top) and semi-relaxed (bottom) approaches.

The complete procedure to calculate investment decisions and ex-post real-time evaluation is shown in Fig. 28 (top). During stage 1, the investment and hourly UC schedule are optimized solving the formulations shown in Section 2.4.1Then, investment, commitment, and reserve decisions are fixed. Stage 2 tests the results through a real-time simulation model, using a 5-min optimal dispatch (emulating real-time markets as in [80]) in order to evaluate the GEP-UC solution. Dispatch decisions (e.g., production, charge/discharge) obtained in stage 2 are called redispatches, allowing us to evaluate the deviations with respect to the stage 1. This is called the *integer approach*. In addition, we proposed a *semi-relaxed approach* for the power-based

formulation, which is shown in Fig. 28 (bottom). Here we split stage 1 in two. First, the stage 1a solves the power-based formulation considering integer investment decisions and continuous UC decisions ($u_{\omega gt}$, $y_{\omega gt}$, $z_{\omega gt}$). This approximation allows to solve the GEP problem much faster. Then investment decisions are fixed in stage 1b, where the power-based formulation is solved considering integer UC decisions. Once again, investment, unit commitment, and reserve decisions are fixed to simulate a 5-min optimal dispatch.

2.4.3 Case Studies

To evaluate the performance of the different approaches, we use two case studies: a modified IEEE 118-bus test system and a stylized Dutch power system in target year 2040. Input data for both case studies is available online at [93], including the 5-min demand and renewable production profiles. Both case studies are solved considering a green-field investment approach (i.e., no initial capacity) for thermal generation and ESS investment, while the vRES capacity is predefined.

The modified IEEE 118-bus test system is described in Morales-España [94] for a time span of 24 h. This system was originally conceived for UC problems and it has 118 buses, 186 transmission lines, 91 loads, 54 slow-start thermal technologies, 10 quick-start technologies, and three buses with wind production. Nevertheless, we adapt this case study for GEP problems. Thermal unit investments are allowed in buses where there was a unit connected in the initial UC problem. In addition, ESS investment decisions are available in three types of technologies (PSH, CAES, and Li-ION) for buses with renewable production. The total (5-min) load average is 3578.6MW, it has a peak of 5117.5MW and a minimum of 1435.4MW.

The stylized Dutch system case study for year 2040 is mainly based on the information available in the *Ten Year Network Development Plan 2018* [95] (e.g., hourly demand profile, renewable capacity, technical characteristics and available technologies). However, the wind and solar profiles were taken from [42], [43] since this information is not available in [95]. Instead of solving 8760 h for the whole year, we have selected four representative weeks using the proposed method in [61] and k-medoids clustering technique [96]. Other authors [60], [97] have proposed different approaches to select the representative periods (e.g., weeks or days) that are compatible with the proposed GEP-UC models in this paper. Each representative week is considered as one scenario in the optimization problem, and the scenario probability is obtained from the clustering process. For investment decisions, four different thermal generation technologies are considered, Combined Heat and Power (CHP), combined cycle gas turbine (CCGT), open cycle gas turbine (OCGT), and Light Oil (Oil). Moreover, three ESS (PSH, CAES, Li-ION) technologies are considered for investment decisions.

For each case study, four different models are implemented: traditional energy-based (EB), energy-based including SU/SD power trajectories (EBs), the proposed power-based

formulation (PB), and the semi-relaxed power-based formulation (SR-PB). Table VIII shows the summary with all the implemented models. All models consider $\tau = 5$min for constraints associated to flexibility constraints. All optimizations were carried out using Gurobi 8.1 on an Intel®-Core™ i7-4770 (64-bit) 3.4-GHz personal computer with 16GB of RAM memory. The problems are solved until they reach an optimality tolerance of 0.1%.

Table VIII: GEP-UC Models

Equations	EB	EBs	PB	SR-PB
Objective function	(1)		(30)	
System constraints	(2)-(25)		(24)-(25), (31)-(34)	
Investment constraints	(4),(5)-(6),(7)		(4), (35)-(36),(37)	
UC constraints	(8)-(12)			
Thermal unit constraints	(13)-(16)		(38)-(39)	
Total output thermal technologies	(17)	(18)	(40)-(41)	
constraints	(19)-(23)		(21)-(23),(43)-(42)	
Constraints for flexibility requirements ($\tau = 5$min)	(26)-(29)		(44)-(51)	
Integer variables	$u_{\omega gt}, y_{\omega gt}, z_{\omega gt}, \gamma_{\omega st}, \delta_{\omega gkt}, x_j$			Stage 1a: x_j Stage 1b: $u_{\omega gt}$, $y_{\omega gt}, z_{\omega gt}, \gamma_{\omega st}, \delta_{\omega gkt}$

2.4.4 Results

2.4.4.1Modified IEEE 118-bus System

Table IX shows the main results for each model. The total investment cost (ESS + Thermal) is higher in the classic EB model than the one obtained with the PB model. Generally, increasing the investments lowers operating cost. Nevertheless, here we obtain a counterintuitive result. Even though the classic EB model invests more (6%), the operating cost is worse than the one in the PB model (15%). Moreover, the CO2 emissions and curtailment are also higher in the classic EB model, despite its higher capacity in clean ESS and lower capacity in thermal technologies.

This is also a counterintuitive result, because at a first glance, less thermal generation should pollute less, and more storage should allocate more renewables. However, this result is related to how the technology mix is selected in each model. Therefore, it is not only a matter of how much the model invests, it is also a matter of how the technology mix is selected, see Table X.

For instance, although the total coal capacity is higher in the proposed PB model, the actual total coal production is lower (7%) than the one in the classic EB model, see Table XI. This is compensated by a higher use of wind, gas (that have less CO2 emission factor) and oil, which overall results in less CO2 emissions. As mentioned in Section 2.4.1.2 the PB model equations allow to schedule the thermal technologies in a way that correctly represents the requirements and actual availability of system's flexibility, such as the load ramps. The results show the benefits of accurately considering the flexibility requirements and of correctly modelling the flexibility capabilities of the system by modelling in terms of power instead of energy.

TABLE IX
IEEE 118-bus System: Performance for each formulation

	Result	EB	EBs	PB	SR-PB
Stage 1	Total Cost [M$]	10.15	9.29	8.94	8.96†
	ESS Invest Cost [M$]	0.43	0.35	0.19	0.17
	Therm. Invest Cost [M$]	1.01	1.42	1.17	1.24
	Operating Cost [M$]	8.71	7.52	7.58	7.55†
	CO2 emissions [ton]	63.11	53.06	53.98	53.74
	Curtailment [%]	5.76	4.18	0.73	0.70
	CPU Time [s]	10717	6767	4478	500
Stage 2	Operating Cost [M$]	8.22	7.53	7.58	7.55
	Total Cost [M$]	9.66	9.30	8.94	8.96
	CO2 emissions [ton]	59.31	52.48	53.95	53.71
	Curtailment [%]	0.00	0.00	0.60	0.62

† Values from Stage 1b

TABLE X
Technology investment decisions [MW]

Technology	EB	EBs	PB	SR-PB
PSH	1250	1000	500	441
CAES	0	0	0	0
Li-ION	150	150	150	150
GAS	360	600	420	480
COAL	4380	6080	5030	5330
OIL	50	100	100	100

TABLE XI
Technology production decisions [MWh]

Technology	EB	EBs	PB	SR-PB
PSH	7352	5944	2449	2019

CAES	0	0	0	0
Li-ION	1053	1003	1035	1033
GAS	494	2719	2482	2680
COAL	67540	63939	62913	62570
OIL	52	900	950	900
WIND	18880	19196	19887	20018

The EBs model improves the classic EB model by including the SU/SD power-based ramps. In stage 1, the total cost in the EBs model is 8.5% lower than the classic EB model. However, it is still 4% higher than the PB model and with more curtailment (5.7 times). The EBs technology mix is also different, as it invests more in PHS and coal (Table X). And yet, the PB model allocates more wind with less ESS, see Table XI. Therefore, the PB model invests more efficiently due to the more accurate representation of flexibility requirements and capabilities of the power system.

Regarding the CPU time, the PB model is faster than its energy counterparts (2.4 and 1.5 times respectively). Nevertheless, for large-scale investment decision problems, the integer nature of the UC variables especially could make the problem intractable to solve. Therefore, the proposed SR-PB models aims at overcoming this situation. For instance, it solves the problem 9 times faster than the PB model and with only a 0.2% difference in the objective function. Moreover, the difference in the CO2 emissions is only 0.4%. The main difference appears in the curtailment (90%) due to the increase in the investment made by the SR-PB that allows to reduce the operating cost by increasing wind production. When the SR-PB and the EB are compared, it may be concluded that the even the semi-relaxed version of the power-based model (i.e., SR-PB) shows better performance than the discrete version of the energy-based models (i.e., EB and EBs). In other words, the SR-PB model has a lower total cost than the EB model, investing and operating with lower cost, while simultaneously solving 21+ times faster.

The results in Table IX for the stage 2 are also showing interesting information: comparing the operating cost between stage 1 and 2, the classic EB shows a decrease of 6%, while in the other models remain almost the same. Moreover, the curtailment is also reduced from stage 1 to stage 2 in both energy-based models, while it remains almost the same in the power-based models. These results suggest that the obtained schedule in stage 1 with energy-based models leads to more redispatches in the technologies in stage 2. Fig. 29 illustrates this situation with the deviation with respect to the hourly thermal production obtained in stage 2 for each model.

In both energy-based models, downward deviations are higher than upward deviations, which explains why the operating cost is reduced from stage 1 to stage 2 in the classic EB model as well as the reduction on the curtailment for both energy-based models. The power-based models show deviations in both directions lower than 3%, which means that the hourly schedule (stage 1) is better fitted for the 5-min real-time

operation (stage 2). This high deviation of the energy-based models is due to its intrinsic incapability to accurately represent the flexibility needs and capabilities. These conclusions are aligned with those in [9] where different case studies where carried out disregarding investment decisions.

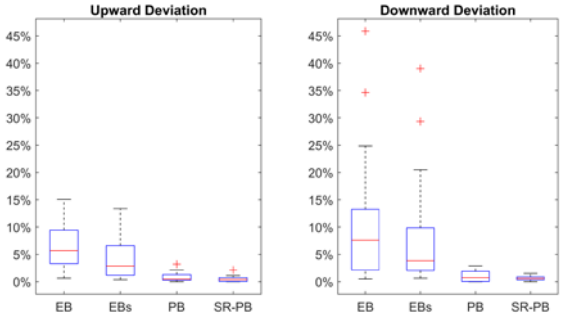

Fig. 29. Stage 2 deviation in scheduled thermal output.

TABLE XII
IEEE 118-bus System: Stage 2 – sensitivity results

	Result	EB	EBs	PB	SR-PB
Stage 2	Operating Cost [M$]	8.35	7.66	7.60	7.55
	Total Cost [M$]	9.79	9.43	8.96	8.96
	CO2 emissions [ton]	59.89	52.71	54.04	53.73
	Curtailment [%]	1.99	0.98	0.62	0.13

Notice that ESS plays an important role in the reschedules made in stage 2. Therefore, we run a sensitivity case in which the State-of-Charge (SoC) at the end of each hour is a lower bound for the ESS in the stage 2. This limits the reschedules made in this stage, increasing the operating cost.

Table XII shows that situation, where with this additional constraint the operating cost, CO2 emissions and curtailment are higher than in the base case. It is important to highlight that in this sensitivity case energy-type models cannot reduce the curtailment to zero as it was in the base case. Therefore, the flexibility provided by the ESS was partly responsible for the reduction of the curtailment between stage 1 and 2 in this type of models. Fig. 30 shows the SoC in the batteries during stage 2 for the base case and the sensitivity case.

The difference between both results in each model shows how the energy-type models were taking advantage of the ESS to reduce the operating cost in stage 2 at the

cost of more rescheduling in the thermal technologies.

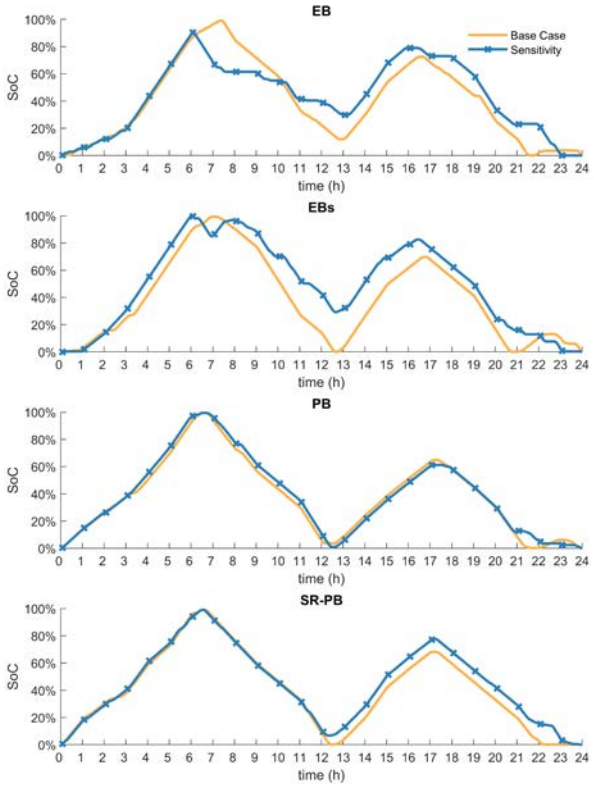

Fig. 30. Battery SoC in Stage 2 obtained for each model.

2.4.4.2 Stylized Dutch System

Table XIII shows the results for a stylized Dutch power system. The main conclusions drawn from the previous case study remain valid. That is, the classic EB model obtains the most expensive investment, and the operating cost is also the highest, while also resulting in the highest CO2 emissions. The amount of ESS invested in the EB model is also the highest, hence allowing it to obtain less curtailment than PB in the stage 2. Nevertheless, still the PB model results in the lowest total cost in both stages and solves the GEP problem faster than EB. In addition, the SR-PB further reduces the CPU time without losing accuracy in the results. Therefore, modeling flexibility requirements with the PB model leads to a better solution than the classic EB model. In addition to the base case shown in Table XIII, Table XIV shows a sensitivity where ramp capabilities of thermal technologies are twice than before, i.e., thermal technologies are now much more flexible. As the flexibility of the thermal resources increases, the difference between energy-based and power-based models decreases. For instance, the difference between the EB the PB models changes from 7.4% to 4.3%. Therefore, if the power system does not have ramp problems, i.e., flexibility is not a problem in general, the difference between energy-based and power-based models is less significant. However, if flexibility is a limited resource and needs to be correctly managed, then the power-based models

are the right option to obtain the capacity expansion planning for the system.

TABLE XIII
Stylized Dutch System: Performance for each formulation

	Result	EB	EBs	PB	SR-PB
Stage 1	Total Cost [M$]	73.18	70.39	68.14	68.16†
	ESS Invest Cost [M$]	13.47	11.15	10.53	10.88
	Therm. Invest Cost [M$]	13.79	14.12	13.43	13.47
	Operating Cost [M$]	45.92	45.12	44.18	43.81†
	CO2 emissions [kton]	112.10	98.06	89.46	88.77
	Curtailment [%]	44.72	45.47	45.46	45.34
	CPU Time [s]	571	161	131	60
Stage 2	Operating Cost [M$]	45.76	46.61	44.90	44.52
	Total Cost [M$]	73.02	71.88	68.86	68.87
	CO2 emissions [kton]	107.73	100.01	94.29	93.44
	Curtailment [%]	47.88	48.35	48.34	45.39

† Values from Stage 1b

TABLE XIV
Stylized Dutch System: Sensitivity to Ramp Capacity

	Result	EB	EBs	PB	SR-PB
Stage 1	Total Cost [M$]	70.51	67.93	67.60	67.61†
	ESS Invest Cost [M$]	13.35	10.97	10.66	10.74
	Therm. Invest Cost [M$]	13.47	13.47	13.43	13.47
	Operating Cost [M$]	43.69	43.49	43.51	43.40†
	CO2 emissions [kton]	103.10	90.84	88.46	88.17
	Curtailment [%]	44.32	45.22	45.16	45.19
	CPU Time [s]	142	130	100	43
Stage 2	Operating Cost [M$]	44.37	45.92	44.25	44.21
	Total Cost [M$]	71.19	70.36	68.34	68.42
	CO2 emissions [kton]	100.76	94.35	93.07	93.07
	Curtailment [%]	44.62	45.30	45.24	45.28

† Values from Stage 1b

2.4.5 Conclusions

This paper proposes a power-based model to determine the GEP, including energy storage technologies. The proposed power-based model uses the installed investments more efficiently and more effectively as 1) it represents the reality of flexibility requirements of the power system more adequately, and 2) it adequately exploits the

flexibility capabilities of the system. That is, the decisions made with the power-based model simultaneously yield lower investment costs, operating cost, CO2 emissions, and renewable curtailment with respect to the energy-based model. This is mainly because the energy-based model overestimates flexibility capabilities, failing to capture the flexibility requirements such as load and vRES ramps even in a deterministic approach (i.e., without uncertainty on demand, or renewable production). Moreover, the advantages of the power-based approach could become much more significant considering uncertainty [9].

Therefore, correctly modeling the system flexibility changes the optimal expansion capacity decisions. For instance, the power-based model obtains less total investment (6-12%) because it is more accurate in the representation of ramping characteristics for generation resources (e.g., thermal technologies and ESS), which leads to less operating cost (2-8%) in the real-time validation. In addition, the power-based model has computational advantages in terms of CPU time. The results show that the power-based model is 2 to 4 times faster than the energy-based model. We also have demonstrated that the semi-relaxed power-based model is even faster (10 to 21 times) without losing accuracy in the results compared with the non-relaxed power-based model (less than 0.2% objective function error). This is relevant for applications with large-scale long-term capacity expansion planning problems where relaxed models are more often used due to computational power limitations.

The results show an important insight for ISOs because, even without uncertainty, the current energy-based models impose more rescheduling in the real-time operation than the power-based models. For planning authorities this is also important because decisions made with power-based models lead to a generation technology mix that is better adapted to real-time system operation.

Finally, the proposed power-based UC model relies on available data in terms of power trajectories instead of energy trajectories, i.e., demand and renewable profiles. Forecasting power profiles, thus having higher quality on ramping information, is an interesting topic that could be addressed in future research.

2.5 Storage Allocation and Investment Optimization for Transmission Constrained Networks Considering Losses and High Renewable Penetration

As renewable energy penetration increases on a grid-scale, the issues of intermittency and price control continue to grow. One method tackling these issues is relying on large-scale storage technologies to provide grid flexibility [98] . Previous studies have investigated using large-scale storage to perform services like energy arbitrage, power regulation and peak shaving [99]. But planning such solutions goes beyond simply determining the required storage capacity. Designing a storage network on a grid-scale requires examining capacity requirements, resource allocation, and grid-specific properties . A common method used to account for this is the optimal power flow (OPF) framework. Studies [100]–[102] have explored adding charge and discharge dynamics to AC OPF functions in order to explore the effects of energy trading, demand reduction and power regulation. Others e.g. [103], [104] have looked at expanding this type of modelling to include multiperiod storage location optimization. Studies such as [105] have also used AC OPF models to study the economic benefits realized using energy storage for emissions reductions and/or congestion relief.

In general, OPF Problems are nonconvex and NP hard making them difficult to solve. Therefore, DC OPF linear approximations [106] as opposed to the AC OPF models mentioned above, have been used extensively to explore optimal storage siting problems for both customary and renewable energy grids. Much attention has been brought to using DC OPF Functions to fluctuation challenges associated with high renewable penetration [107], [108]. These models have also been used to understanding how storage can be used as a risk mitigating measure with regard to the uncertainty of renewable generation [109], [110].

The choice of model for this study was based on the following: General transportation models only consider Kirchhoff´s First Law of energy/power conservation which is not a viable means of planning technology expansion. Contrarily DC power flow models (DCPF) consider both Kirchhoff's First Law and a linearized version of his second law to account for voltage balance. These models allow users to approximately represent losses but not stability considerations in transmission. This makes them suitable for medium and long-term planning for investment in and allocation of new elements in the power grid (i.e. generators, transmission lines, transformers, etc.) [111]. Because this study is not concerned with exploring voltage and stability problems associated with grid operation, building upon the DC OPF-based model in[98] was sufficient. This allows for increased computational tractability that would be lost had this model been expanded to an AC power flow representation. Authors in [98] expanded on the DC OPF-based storage allocation formulas to include a portfolio of storage technologies operating on different time-scales into the OPF-based siting and dispatch problems. This was used to optimally allocate and invest in storage in both congested and uncongested networks.

Congestion can strongly impact the sizing and siting of storage facilities by preventing proper power distribution, leading to outages or increased system stress. Losses in power flow throughout a network can similarly affect grid reliability by preventing the right amount of power from reaching demand centres. Studies such as [112], [113] have explored how energy storage technologies can improve overall grid efficiencies by relieving congestion, stabilizing power and minimizing transmission and battery round-trip losses. While this is crucial in effectively integrating distributed storage solutions, it neglects to give a system planner an optimal network-level strategy for designing new storage projects. Ignoring line losses may initially reduce costs but can lead to expensive investment adjustments down the road [114]. This work expands on [98] to account for both network congestion and transmission losses. A linearized approximation of ohmic losses was adapted to do this [115]. By investigating physical constraints in a transmission network, the impact that storage expansion will have on grids operating with non-dispatchable power can be better analysed.

The remainder of this paper is organized as follows. Section 2.5.1 provides the mathematical formulation used for optimizing storage capacity and siting across a transmission-constrained network considering ohmic losses. Section 2.5.2 includes several case studies that utilize the modelling framework for an IEEE benchmark test system to analyse how losses, congestion and varying degrees of wind generation drive allocation and investment decisions, as well as how they influence each other. Conclusions and considerations for future research are presented in Section 2.5.3.

2.5.1 **Problem Formulation**

In this section the mathematical formulation for the optimal storage allocation problem over a transmission constrained network is explained. Generally, the model is an extension of the OPF storage problem. It includes multiple options for storage technologies, creating a larger problem size. To increase the tractability of the problem a linearized DC OPF approximation was adopted. Section 2.5.1.1 fixes the total storage capacity available for the mix of technologies and optimizes the allocation of these resources throughout the network while considering linearized ohmic losses. Section 2.5.1.2 breaks down how the linearized approximation and subsequently its related terms and constraints are formulated. Section 2.5.1.3 further extends the model to include investment costs for installing storage capacity. Lastly, Section 2.5.1.4 outlines three additional storage metrics that were created using parameters from Sections 2.5.1.1 to Section 2.5.1.3 to better analyse the model results.

2.5.1.1 Storage Allocation with Losses Model

Consider a network with a set of buses $N := \{1, \dots, N\}$ and define n as the index referring to this set. The set of different storage technologies available in the network can be denoted by $J := \{1, \dots, J\}$ and is indexed with j throughout the model. The set of time intervals is defined as $T := \{1, \dots, T\}$ and indexed with t. In addition, consider the set $K := \{1, \dots, K\}$ of linear approximation segments used in Section 2.5.1.2 to form a piecewise linear approximation of transmission losses. The decision variables used throughout the DC OPF storage optimization model comprise the set $\Omega := \{ p_n^g(t), r_{jn}^c(t), r_{jn}^d(t), s_{jn}(t), k_{jn}, \delta_n(t), \Delta_{nm}(t), \Delta'_{nm}(t)\}$ for all technologies$j \in J$, all nodes $n \in N$ and all segments $k \in K$ during all time intervals $t \in T$. The decision variables are defined as follows: $p_n^g(t)$ is the generation from thermal units, $r_{jn}^c(t)$ and $r_{jn}^d(t)$correspond to the charging and discharging rates of each storage technology, $s_{jn}(t)$ represents the storage level, k_{jn} represents the installed storage capacity, $\delta_n(t)$ corresponds to the voltage angle at a node, $\Delta_{nm}(t)$ represents the difference in voltage angles between two buses and time t for a particular approximation segment, and $\Delta'_{nm}(t)$ represents the square of this difference.

The objective function of the model calculates the total system costs:

$$\min_{\Omega} \sum_{t\in T}\{\sum_{n\in G} F_n^g\left(p_n^g(t), t\right) + \sum_{n\in N, j\in J} F_{jn}^d\left(r_{jn}^d(t), t\right)\} \quad (1)$$

This objective is comprised of the production cost function, $F_n^g\left(p_n^g(t), t\right) := C_n^{g1}(t)p_n^g(t) + C_n^{g2}(t)\left(p_n^g(t)\right)^2$ and the discharging costs $F_{jn}^d\left(r_{jn}^d(t), t\right) := C_{jn}^{d1}(t)r_{jn}^d(t) + C_{jn}^{d2}(t)\left(r_{jn}^d(t)\right)^2$ which together represent the fixed and variable costs associated with network storage. $C_n^{g1}(t)$ and C_n^{g2} are the linear and quadratic production cost coefficients respectively. Similarly, $C_{jn}^{d1}(t)$ and $C_{jn}^{d2}(t)$ represent the linear and quadratic discharging cost coefficients. For thermal generation units, convex quadratic cost functions are commonly used in unit commitment formulations [116]. While this study does not take unit commitment into consideration, the solution of such a formulation results in a model that is straightforward using conic optimization algorithms. For this reason, it was adopted here. Cost functions associated with charging and discharged stored power have been included by other authors in previous studies [100]–[117]. These allow the model to take into account optimal system deployment as well as allocation and investment.

Before the constraints are explained, some useful parameters will be defined:

η_j^c	Charging efficiency of technologies

η_j^d	Discharging efficiency of technologies
Δt	Duration of time step
R_j^c	Maximum charging capacity
R_j^d	Maximum discharging capacity
P_n^{min}	Minimum thermal power output
P_n^{max}	Maximum thermal power output
$+RR_n;\ -RR_n$	Upper and lower ramp rate limits
$W_{n(t)}$	Total wind generation
TC_{nm}^{max}	Maximum line transmission capacity
Gt_{nm}	Circuit Conductance

Let us discuss the constraints used in formulating this optimization problem. The storage level in each technology will be defined for $\forall j, n, t \geq 2$ such that

$$s_{jn}(t) = s_{jn}(t-1) + \left(\eta_j^c r_{jn}^c(t) - r_{jn}^d(t)/\eta_j^d\right)\Delta t \quad (2)$$

This states that the energy storage level of each technology at each node during every time step past the second one, must be equal to the storage in the previous period plus the difference of the energy charged and discharged between the previous period and the current time step. Additionally, the problem variables were bounded as follows:

$$0 \leq r_{jn}^c(t) \leq R_j^c \qquad \forall j, n, t \qquad (3)$$

$$0 \leq r_{jn}^d(t) \leq R_j^d \qquad \forall j, n, t \qquad (4)$$

$$0 \leq s_{jn}(t) \leq k_{jn} \qquad \forall j, n, t \qquad (5)$$

$$s_{jn}(t=1) = s_{jn}(t=T) \qquad \forall j, n \qquad (6)$$

$$P_n^{min} \leq p_n^g(t) \leq P_n^{max} \qquad \forall j, n \qquad (7)$$

$$-RR_n \leq p_n^g(t) - p_n^g(t-1) \leq +RR_n \qquad \forall j, n \qquad (8)$$

$$k_{jn} = 0\ \forall j, n \in GR_{jn} \qquad \forall j, n \qquad (9)$$

$$\sum_{n \in N} k_{jn} \leq SC_j^{max} \qquad \forall j \qquad (10)$$

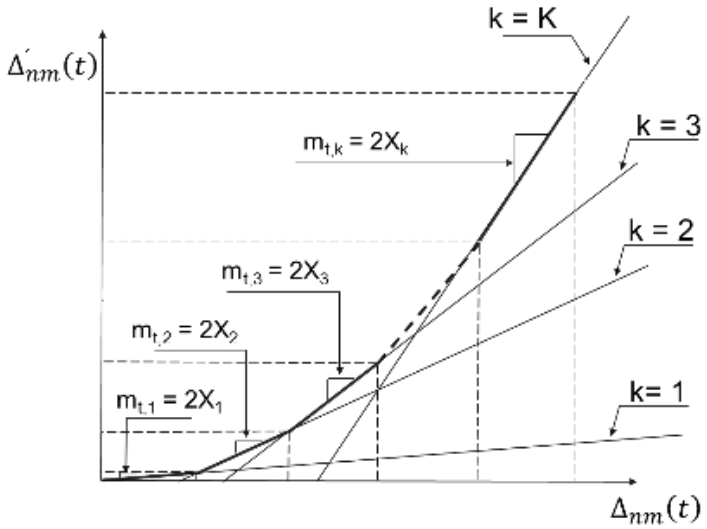

Fig. 1 Piecewise Linear Approximation of Ohmic Losses

$$\Delta_{nm}(t) = \delta_n(t) - \delta_m(t) \qquad \forall m \in \Theta_n, t \qquad (11)$$

Bounds (3) and (4) define the upper and lower limits for charging and discharging respectively. Constraint (5) states that the storage level for a technology cannot exceed the amount of installed capacity of technology *j* at node *n* during time *t.* Constraint (6) states the ending energy storage level of a technology must be the same as the starting value. Bound (7) defines the minimum and maximum thermal generation limits. (8) defines the upper and lower ramping limitations of thermal generators. Let GR_{jn} be defined as the set of nodes where geographical, zoning or social issues prevent the installation of a particular technology at that node. For example, a pumped hydro storage facility cannot work in an area without abundant water [98]. Consequently, (9) states that no capacity can be installed for a technology at a node that falls within that set. Bound (10) states that the total installed capacity over all nodes for technology *j* cannot exceed SC_j^{max}, which denotes the total available storage capacity of a given technology. Lastly (11) defines the voltage angle difference for the set Θ_n, of buses *m* connected to bus *n*.

The energy at each node *n* during each time period *t* can be defined as an equality between the inflows and outflows of power. The inflows of power include wind generation, thermal energy production and discharged power at each node—these are $W_{n(t)}$, $p_n^g(t)$ and r_{jn}^d respectively. This model assumes that all generated wind was consumed, and therefore no wind curtailment was observed. Therefore, wind could be treated as input data. The outflows of power include the demand at each node, the power transmitted between nodes, the energy charged by all technologies at all nodes during each period, and the linearized ohmic losses—the demand and charged energy are defined as $D_n(t)$ and $r_{jn}^c(t)$ respectively. The energy transmitted between nodes is defined as $B_{nm}\big(\delta_n(t) - \delta_m(t)\big)$. Transmission losses are given by the exact active power dissipated, $2Gt_{nm}\big(1 - \cos\big(\Delta_{nm}(t)\big)\big)$ and will be linearized in Section 2.5.1.2.

The energy balance described above is given by the following for all buses and time intervals:

$$W_{n(t)} + p_n^g(t) + \sum_{j\in J} r_{jn}^d(t) = D_n(t) + \sum_{m\in\Theta_n} B_{nm}\big(\delta_n(t) - \delta_m(t)\big) + \sum_{j\in J} r_{jn}^c(t) + 2Gt_{nm}\big(1-\cos\big(\Delta_{nm}(t)\big)\big) \quad (12)$$

Transmission limits needed to be put in place to account for network congestion. (13) limits the power flow between two nodes to the line limit as TC_{nm}^{max}. The set Θ_n defined previously will be used here to ensure that only lines that exist are bounded. The constraint is for $\forall\ m \in\ \Theta_n$ and given by

$$-TC_{nm}^{max} \le B_{nm}\big(\delta_n(t) - \delta_m(t)\big) \le TC_{nm}^{max} \quad (13)$$

The corresponding voltage angles are bounded for $\forall\ n, t$ by

$$-\pi \le \delta_n(t) \le \pi \quad (14)$$

Finally, *n* = 1 is defined as the slack bus for all time steps *t* by

$$\delta_{n=1}(t) = 0 \quad (15)$$

The model given by (1) to (15) represents an optimization problem that is to be solved in this study. However, this model is non-convex and non-linear and will be adjusted in the following section.

2.5.1.2 Explanation of Transmission Loss Formulation

The key attribute of this study is the consideration of losses throughout the system. To maintain the optimization model's tractability, a linearized piecewise ohmic loss approximation is used. Doing this requires starting with cosine and quadratic estimations of transmission losses. First, a cosine curve was used to represent the exact active power dissipated in a circuit. This provides the most accurate approximation of losses. While the function itself is convex, the problem remains non-convex and non-linear preventing a globally optimal solution from being found. To address this we first use a Taylor Series expansion of the cosine function to obtain a quadratic approximation of transmission losses.

The resulting losses can be estimated to the first two elements of the expansion and are given by $Gt_{nm}\big(\Delta_{nm}(t)\big)^2$ since the subsequent terms yield negligible values [115]. This is a relatively standard method of simplifying the optimization problem. However, it results in the same problem as before—the model remains non-convex and non-

linear. To correct for this, the quadratic approximation can be estimated using a linearized piecewise function [115]. Figure 1 shows the linear piecewise approximation relative to the original cosine representation.

In Section 2.5.1.1 the set *K* was introduced. Three new parameters will be introduced using this set in order to perform the linear approximation:

Y_k	Quadratic function values
X_k	Original x-axis values used
I_k	y-intercept values for each segment

These parameters allow us to calculate the equations of each segment used to approximate the quadratic function with linear curves at specific points via (16). Using them we find that the values of $\Delta'_{nm}(t)$ are approximately equal to the square of the voltage angle differences used in the general quadratic approximation. Transmission losses on a line can then be represented as $0.5\left(Gt_{nm}\Delta'_{nm}(t)\right)$. Note that product is halved as to prevent counting both the positive and negative sides of the approximated curve.

$$\Delta'_{nm}(t) \geq \left(2X_k\Delta_{nm}(t)\right) + I_k \qquad \forall k, m \in \Theta_n, t \qquad (16)$$

With this approximation, the optimization problem becomes both linear and convex. It can therefore be solved to obtain a globally optimal solution. Generally, it is possible that the optimal solution could choose a fictitious amount of system losses (e.g. a point above the approximation curve). This is most likely to occur in a unit commitment problem, where the model would find it more economically favourable to artificially increase transmission losses to prevent a thermal generator from incurring relatively large shut-down costs. But it is not physically possible to make a transmission line more resistive than its material composition allows for. To correct this, binary variables can be used to restrict power loss values to the piecewise function, thereby creating a MIP, and consequently an increasingly complex problem. Because this study did not deal with unit-commitment, this was unnecessary.

Lastly, we must adjust (12) to represent our linearized approximation of losses in the system energy balance. The new equation for this is displayed in (17). The new optimization problem we solve, includes all the same constraints as before, but replaces (12) with (17) and incorporates additional constraint (16). Note that for cases in Section 2.5.2 where we did not consider losses, this term was excluded from the energy balance and the subsequent parameters and variables had no effect on the model.

$$W_{n(t)} + p_n^g(t) + \sum_{j\in J} r_{jn}^d(t) = D_n(t) + \sum_{m\in\Theta_n} B_{nm}\left(\delta_n(t) - \delta_m(t)\right) + \sum_{j\in J} r_{jn}^c(t) + \sum_{m\in\Theta_n} 0.5\left(Gt_{nm}\Delta'_{nm}(t)\right) \quad (17)$$

2.5.1.3 Storage Investment Model

The model can now be extended to consider the investment costs of new storage capacity. In Section 2.5.1.1, the available capacity was assumed fixed for each technology, therefore implicitly accounting for an investment decision. The new objective function will include the cost function of storage investment, $F_j^i(k_{jn}) = k_{jn}^i C_j^i / DD_j$ where C_j^i corresponds to the per MW cost of a new technology and DD_j corresponds to the average discharge duration of each technology. The objective function is now given by (18) and subject to constraints (2) – (17).

$$\min_{\Omega} \sum_{t\in T}\left\{\sum_{n\in G} F_n^g\left(p_n^g(t), t\right) + \sum_{n\in N, j\in J} F_{jn}^d\left(r_{jn}^d(t), t\right)\right\} + \sum_{n\in N, j\in J} F_j^i\left(k_{jn}\right) \quad (18)$$

The model defined by (2) – (18) portrays a convex optimization problem with linear constraints, and a quadratic objective function. In our model, k_{jn} are treated as continuous values. This concludes the mathematical formulation of the storage allocation and storage investment problems with and without losses. In the following section, we carry out several case studies to better understand the effects of congestion, losses and renewable penetration when planning and designing storage for a given network.

2.5.1.4 Additional Storage Metrics

To best comprehend model output and draw conclusions on allocation and investment strategies, three additional metrics were calculated using the aforementioned parameters. These metrics are defined as follows:

$$OM_{jn} = 1 - \frac{max_t\{s_{jn}(t)\}}{k_{jn}} \qquad \forall j,n \quad (19)$$

$$CM_{jn} = \frac{\sum_{t\in T}[r^c_{jn}(t)\cdot \Delta t]}{k_{jn}} \qquad \forall j,n \ if \ k_{jn} > 0 \quad (20)$$

$$OSL_j = \frac{\sum_{n,t} s_{jn}(t)}{\sum_{n,t} s\_BaseCase_{jn}(t)} \qquad \forall j \quad (21)$$

The Overall Capacity Metric (OM) in (19) compares the maximum storage level in MWh attained over the time horizon to the actual amount of capacity of that technology installed at each node. The Cycling Metric (CM) in (20) keeps track of how many full charging cycles a technology goes through over the total time horizon at each node. Lastly, the Overall Storage Level Metric (OSL) in (21) provides an idea of how much energy each technology stores throughout a day for each scenario in comparison to the base case of an unconstrained network.

2.5.2 Case Studies

In this section we present case studies to validate the previously presented methodology and formulation. Section 2.5.2.1 describes the data used for these studies. Sections 3.2 to 3.5 contain different scenarios for the allocation and investment models with the consideration of ohmic losses described earlier. In Section 2.5.2.2 we compare the storage allocation model assuming an unconstrained network. Section 2.5.2.3. studies the same system for two different scenarios of network congestion. Sections 2.5.2.4 and 2.5.2.5 expand on the allocation model to consider installation and operating costs for storage. Section 2.5.2.4 looks at the effects of varying degrees of wind generation on investment decisions. Section 2.5.2.5 builds on this to consider the effects of transmission losses and congestion. Lastly, section 2.5.2.6 contains an analysis and review of the results from these.

2.5.2.1 Input Data

The numerical examples in this section are based on the 14-bus IEEE benchmark system [118]. Transmission constraints are adopted into this model via TC^{max}_{nm}. Unless otherwise stated the transmission capacity between any two nodes is 400 MW. Note that all data inputs (excluding those relevant to the losses formulation) are adopted from [115]. This includes information regarding the charge/discharge rates [119] and

total storage capacity and charge/discharge efficiencies [120]. Relevant information regarding the available storage portfolio is in Table 1.

Table 1 Storage Technology Parameters

Storage Technology	Dis/Charge Efficiency η^c, η^d [*p.u.*]	Investment Cost, C_j^i[$/MW/d]	Discharge Duration, DD_j [hr]
PSH	0.87	250	12
CAES	0.78	24	24
LI-ION	0.94	800	4
FES	0.96	550	0.0833

Four different storage technologies were considered: pumped-storage hydro (PSH), compressed air energy storage (CAES), lithium ion batteries (LI-ION), and flywheel energy storage (FES). Additional data regarding the physical attributes of FES was obtained from [121] which studied large scale deployment of Flywheel technology. Studies were run over a 24-hr time horizon with time steps Δ*t* = 5-min throughout the day allowing for both long and short time scale observations. Demand data for the network represents a typical day in Southern California during July of 2010 [118]. The data provided by [118] was provided in 10-min intervals and interpolated to 5-min time steps to be used in this case study. Both conventional thermal and wind generation occur at buses 1, 2, 3, 6 and 8. Wind is treated as a parameter. As such, the model is set up to force all wind generated power to be accepted. Similar to what may happen when feed-in tariffs to require the use of renewably generated power. The information is adopted from the 2006 NREL Western Wind Resources Dataset [122]. Wind data was available in 10-min intervals. A set of interpolated 5-min intervals was used to run these cases.

In Sections 3.4 and 3.5, the wind generation was scaled up and down by fixed multipliers to represent different generation scenarios. The operational cost of charging is determined by the locational marginal pricing (LMP) of power at a given bus. Thermal generation energy is priced as follows: Operational costs for the cheapest thermal plants located at buses *n* = {1, 2} are $C_n^{g1}(t)$ = 20 [$/MW] and $C_1^{g2}(t)$ = 0.043, $C_2^{g2}(t)$ = 0.25 [$/MW^2]. Buses *n* = {3, 6, 8} had higher costs associated with thermal production. The linear cost coefficients associated with these buses, *n*, were $C_n^{g1}(t)$ = 40 [$/MW] and $C_n^{g2}(t)$ = 0.1 [$/MW^2]. The lower bound for all generators across all nodes was $P^{\min}$ = 0. The upper bounds for each thermal unit were as follows: $P_1^{\min}$ = 332.4, $P_2^{\min}$ =140, $P_3^{\min}$ = $P_6^{\min}$ = $P_8^{\min}$ = 100. All thermal generation units were assumed to have ramp rates of *RR* = 2

MW per 5-min time step in both directions .The model is developed in GAMS 25.1.1 and solved using the commercial solver GUROBI 8.0. The solver defaults settings were used for all the experiments, which were run on an Intel-i7 CPU @3.4-GHz computer with 16GB of RAM memory and four cores.

2.5.2.2 Storage Allocation in an Unconstrained Network

Here we analyse the allocation of storage in an unconstrained network with losses. We assume in this scenario that the maximum amount of capacity for each storage technology will always be allocated throughout the network. Excluding losses, we find that the locational marginal pricing (LMP) at every node is the same. No technology is favoured, and the capacity of each technology is distributed evenly system wide. However, no CAES storage was chosen at all. The absence of this technology is likely the result of its low round-trip efficiency. The introduction of losses into the model led to changes in the spatial distribution of storage capacity and the temporal usage of each technology. FES and PSH technologies exhibited the greatest changes. We can observe the changes in nodes 3 and 9 to best understand this.

Table 2: Storage Allocation, Additional Storage Metrics

Case Study	Tech	CM		OM		OSL
		n3	n9	n3	n9	
Congestion = NO Losses = NO	PSH	0.0025	0.0025	0.9999	0.9999	1.00
	CAES	0.0031	0.0031	1.0000	1.0000	0.00
	LION	1.7335	1.7335	0.9286	0.9286	1.00
	FES	5.3050	5.3050	0.9286	0.9286	1.00
Congestion = NO Losses = YES	PSH	0.0037	0.0011	0.9998	0.9999	1.24
	CAES	0.0000	0.0000	1.0000	1.0000	0.00
	LION	3.1188	1.0445	0.8863	0.9799	1.00
	FES	18.0912	10.6613	0.7088	0.8669	1.00
Congestion = YES Losses = NO	PSH	0.1265	0.0000	0.9918	1.0000	15.53
	CAES	0.0000	0.0000	1.0000	1.0000	0.00
	LION	1.1742	2.1102	0.0937	1.0000	1.07
	FES	6.6397	0.0000	0.2446	1.0000	1.11
Congestion = YES Losses = YES	PSH	0.0898	0.0000	0.9923	1.0000	15.80
	CAES	0.0000	0.0000	1.0000	1.0000	0.00
	LION	1.0396	0.0000	0.1081	1.0000	1.07
	FES	6.1778	0.0000	0.2582	1.0000	1.09

As expected the CM (See Table 2) indicates that FES goes through the most full cycles of any technology in the portfolio. This is likely attributed to its short ramp time which allows it to fully charge and discharge within a single timestep. When losses are introduced, the number of cycles more than triples at node 3 and doubles at node 9 even though the overall capacity remains unchanged. FES is the “fastest” technology allowing it to stabilize short term fluctuations in load caused by wind generation. This

characteristic becomes increasingly advantageous when there is less flexibility in power transmission to ease load volatility. PSH is a slow-moving technology but its large allowable capacity permits it to employ a day/night arbitrage pattern of operation. The OSL (See Table 2) illustrates this trend with an increase of 24% in PSH storage usage midday, allowing a system operator to dissipate stored energy at the evening peaks, Looking at Fig. 2 we see this pattern of storage deployment illustrated by the step down in network-wide PSH storage level starting around time-step 175. The storage level remained at a plateau midday when demand was lower in order to be discharged when it was needed most.

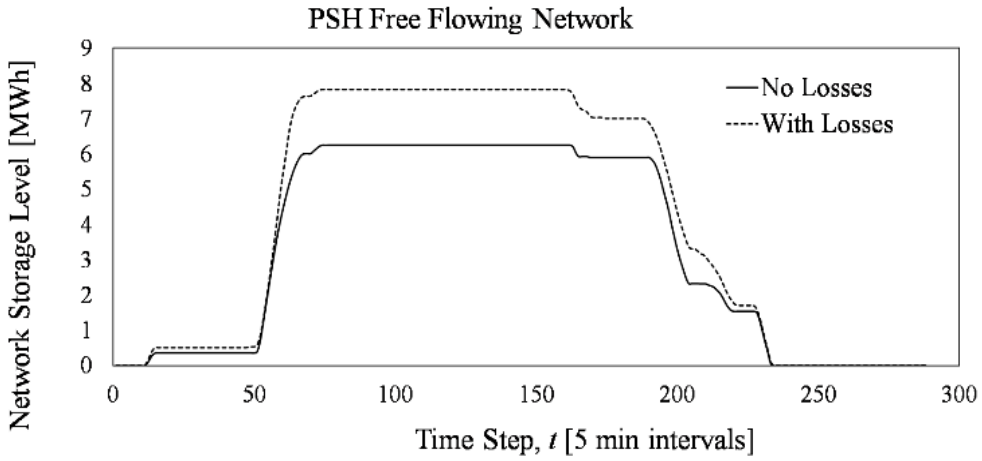

Fig. 2 System-Wide PSH Storage level in a free-flowing network with and without losses over all timesteps

2.5.2.3 Storage Allocation in a Constrained Network

In this section we explore how network congestion impacts storage allocation. Originally values representing a very congested network were used to simulate the case of "full" congestion. Congestion was introduced into the network as follows: $TC_{12}^{MAX} = 80MW, TC_{15}^{MAX} = 40MW, TC_{23}^{MAX} = TC_{42}^{MAX} = 30MW$. The remaining lines had a capacity of 400 MW [98].

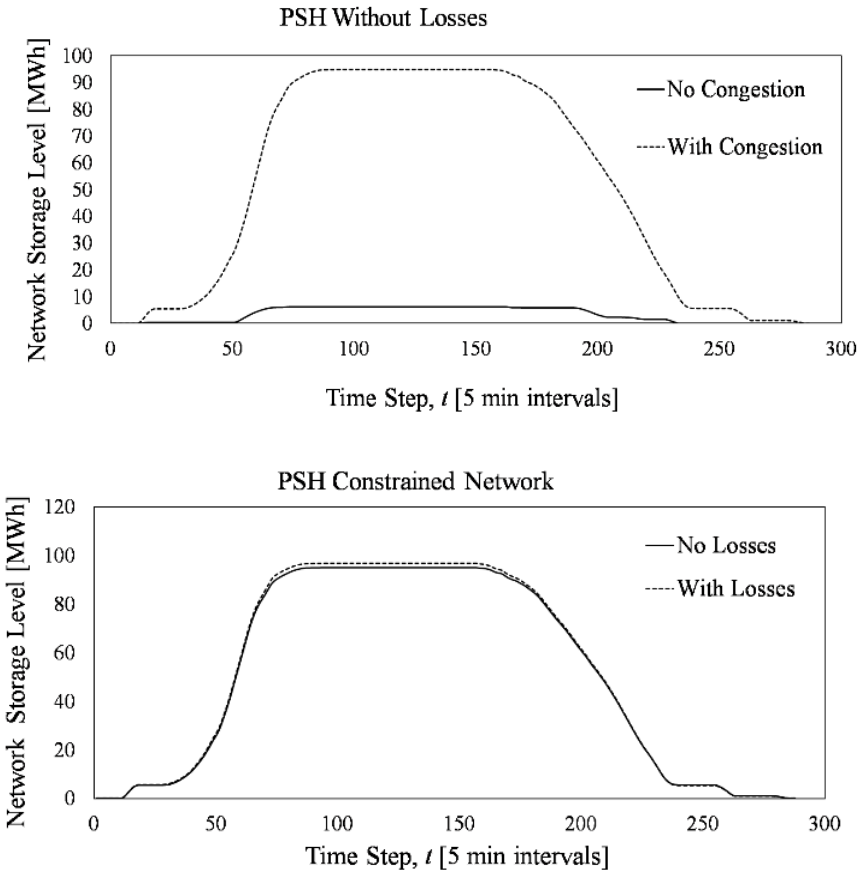

Fig. 3 (Top) System-Wide PSH Storage in a congested network, with and without losses over all timesteps
Fig. 4. (Bottom) System-wide PSH storage with and without congestion, ignoring transmission losses.

Storage in an uncongested network exhibited significant changes in location and usage when losses were introduced, however this was not the case for the constrained case. In this scenario, a system operator is limited as to where they can route power to meet demand. This makes the system unable to deal with rapidly changing power flows such as those discharging from flywheels. The CM and OM metrics at bus 3 for FES in Table 2 indicate this. The CM did not change significantly, and the OM dropped to 24%, indicating that FES storage was not used at full capacity in the constrained network. Considering losses did not change these values significantly. For PSH storage network congestion increased the OSL fifteen-fold system-wide from the base case. Again, considering losses yielded no significant changes.

In Figures 3 and 4, we see that losses take a backseat as the driver of capacity allocation in congested networks, creating no significant shifts in storage operations. This is best illustrated in Fig. 3 by looking at how the storage level curve with losses has negligible differences to the based case curve. However, when congestion was introduced on its own, we observe a drastic impact on PSH storage as shown by the

dramatic increase in system wide storage level in Fig. 4. Thus, while it may be important to consider transmission losses in a free-flowing network, in a congested they will not significantly impact how a storage system should be integrated.

2.5.2.4 Storage Investment for Varying Wind Generation

While the previous cases worked on the premise that all the available storage capacity is allocated and free of charge, the next two cases will include the cost of installation as well. In every one of the four scenarios investigated for allocation, FES was the only storage technology worth investing in. This is because of its flexibility in deployment, and ability to stabilize load. However, no significant changes in capacity investment were observed when losses, congestion, or both forms of blockage were introduced. We can conclude that network inhibitors did not increase the marginal value of storage capacity, making the investment costs too high to bare for large-scale expansion at the base level of renewable penetration. To investigate the value-add that storage can provide as a load stabilizing technology, the net demand profile was shifted by introducing different degrees of wind generation. Since the erratic generation pattern of wind was likely pushing all investment into FES, we wanted to understand what would happen with different magnitudes of wind generation. The NREL Western Wind Sources Data Set [122] was applied to the model at 25%, 50%, 100%, 200%, 250% and 300% of the base values used in Sections 3.2 and 3.3. The Standard Value of wind production will be used to refer to the case of 100% of production provided in the NREL Western Wind Data Set.

Table 3 Total invested capacity for each technology in kWh, for all scenarios of congestion, transmission losses and wind generation

Case Study	Tech	Wind production					
		x 0.25	x 0.50	x 1.0	x 2.0	x 2.5	x 3.0
Congestion = NO Losses = NO	PSH	0	0	0	0	9	206
	CAES	0	0	0	0	103	535
	LION	0	0	0	0	0	55
	FES	200	200	211	237	298	0
Congestion = NO Losses = YES	PSH	0	0	0	0	19	211
	CAES	0	1	0	0	123	538
	LION	0	0	0	0	0	57
	FES	204	204	217	257	312	0
Congestion = YES Losses = NO	PSH	0	0	0	0	49	398
	CAES	1	1	0	0	209	965
	LION	0	0	0	0	14	116
	FES	188	266	212	363	309	16
Congestion = YES Losses = YES	PSH	0	0	0	0	53	373
	CAES	0	1	0	0	204	818
	LION	0	0	0	0	13	117
	FES	184	262	221	361	326	17

For the case of an unconstrainted network at or below standard wind production, FES was the only storage technology invested in. In fact, when wind generation was reduced to the lower boundary of 25% of standard production, the total invested capacity of FES only dropped by 5% as indicated by the capacity investment values in Table 3. This implies that the need for FES capacity may primarily be to provide general load balance as opposed to just dealing with fluctuations from volume of wind generation. Despite this, when wind production is increased in the network, a significant change in investment strategy is observed. At a 2.5-fold increase, investment in FES capacity increase by 41% and with an additional 103 MWh of CAES being sited as shown in the second to last column of Table 3. This is the first instance where the model chose to invest in CAES across all scenarios. Recall that in the allocation cases, the low efficiency [98] of this technology seemed to make it an unfavourable choice. Similarly, at low levels of wind generation, CAES was not advantageous to install.

However, when wind production rose (and thus overall energy produced in the network increased) there grew a need for large-scale energy reservoirs. Table 3 indicates this pattern in the first case, right-most column, by the high volume of capacity investment (darkest green cells). The cost of installing new technologies is a function of the discharge duration as well as a capacity cost. Technologies with longer discharge durations have a lower cost per MWh. Looking back to Table 1, we see that this likely caused the model to favour CAES despite its inefficiency. In the Standard Wind case, a significantly more expensive technology like FES is favourable because of its ability to smooth out the energy balance seen in (17). In the high production scenarios, the sheer increase in volume of energy seems to be the most significant driver of investment decisions. The model chooses to find a way to use all the power in the network anyway

it can as a priority. It should be noted that in the 300% case, no energy was produced from thermal generation.

2.5.2.5 Storage Investment for Varying Wind Generation in a Constrained Network.

Congestion was introduced identically to the allocation case, as follows: $TC_{12}^{MAX} = 80MW, TC_{15}^{MAX} = 40MW, TC_{23}^{MAX} = TC_{42}^{MAX} = 30MW$. As was the case in the allocation model, congestion had a more significant impact on the investment strategy than did losses. In the free-flowing case, most of the system wide storage capacity was sited at the bus with the greatest load—bus 3. When wind generation increases over twice the standard rate, FES is replaced with CAES. The introduction of losses alone only led to a slight increase in system storage capacity while maintaining the same technology selection shown in Figure 6. This held true even for the highest wind generation scenarios. When congestion was introduced into the network, system-wide storage capacity nearly doubled. Most of this change can be attributed to an 80% increase in CAES capacity investment.

Much like the free-flowing case, the largest share of storage capacity, specifically CAES, was located at bus 3. Looking at Table 3, we observe that as wind generation increased from 250% to 300%, this pattern was exemplified. It manifested itself in a nearly 5-fold increase in CAES, 5.5 times increase in PSH and a doubling of LION at bus 3. These results are reflected in the two right-most columns of Table 3. This was significantly higher than the increases observed when introducing losses alone. The model seemed to generally follow this pattern as wind generation in the system increased.

Adding both transmission constraints and losses into the model dampened these effects slightly. While there were significant changes in storage capacity investment from observing losses alone in the model, the network appears to be too constrained to invest in quite as much storage. Inhibiting power flow makes it less economic to have storage located only at demand and generation hubs. Since losses must be incurred when moving throughout the network, it makes less sense both logistically and economically to rely on stored power. For this reason, a decrease in overall storage capacity of 10% is observed.

2.5.2.6 Case Study Analysis

To better understand the results of the case studies this section will explore the implications of the observations made earlier. For the various allocation scenarios, we find that round-trip efficiency governs the way the storage capacity is sited, and

therefore the technology with the lowest efficiency, CAES was never chosen. When investigating the effects of losses and congestion, we find that congestion is a more forceful driver in capacity allocation than are losses. Both network inhibitors push capacity siting towards nodes with high demand and high wind generation, with congestion doing so to a much greater degree. Introducing losses to a congested network results in no change in capacity siting or in technology deployment. It is therefore imperative for a system operator to consider network congestion above losses as an unforeseen cost when planning grid-scale storage integration. As for transmission losses alone, ignoring them may lead to some initial saving but long term will require network upgrades.

The second set of cases focused on storage capacity investment. When running the same scenarios as the allocation model, we find that the model output did not vary significantly with the introduction of congestion or losses. The model always favours investment in FES storage since the marginal value of storage capacity is tied to its load stabilizing capabilities. To study different degrees of load variability, the cases were rerun with varying levels of renewable penetration.

When scaling wind production down no substantial changes to the FES investment strategy are observed, affirming that this technology's primary use is for system load-balance needed irrespective of non-dispatchable generation. However, when production is increased, the investment strategy changes greatly, buying mostly into CAES capacity. Since the model does not allow for any spillage, all wind power generated must be consumed to meet demand, lost via transmission or stored. We find that losses do not significantly change the investment strategy at any level of renewable penetration. On the other hand, congestion leads to nearly double system-wide storage capacity for the highest wind production case. This is in line with the observations made when looking at the allocation model—congestion plays a more important factor in planning large-scale energy storage integration than do losses.

Looking at the objective function output for these cases we can reaffirm this observation. Note that the demand in every case was held constant. The base case objective function value (equivalently system operating cost) was $841,890.71. For the allocation model, introducing losses, only causes a 2.4% increase in operating cost, while congestion results in a 13.5% increase. When adding losses to the constrained network, we only see an additional increase of 2% to the objective function value.

Table 4 Summary of p.u. change to objective value for investment case studies with varying wind production

Case Study	Wind Production					
	x 0.25	x 0.50	x 1.0	x 2.0	x 2.5	x 3.0
Congestion = NO Losses = NO	1.645	1.419	1.000	0.290	0.031	0.000
Congestion = NO Losses = YES	1.681	1.451	1.024	0.301	0.037	0.000
Congestion = YES Losses = NO	1.854	1.598	1.129	0.307	0.035	0.000
Congestion = YES Losses = YES	1.880	1.622	1.149	0.320	0.041	0.000

The objective function in the base case for the investment model was $836,343.04. A summary of the per-unit change in system operating costs for the set of investment studies can be seen in Table 4. We see that with standard wind generation, losses again only add 2.4% to the objective function value while congestion increases costs by a factor of 12.9%. As was seen in the allocation model, the addition of losses to a congested system only increases the overall operating cost by 2%. Moving horizontally across the table we observe that operational cost has an inverse relationship to the amount of wind generation available. Since demand is held constant in all cases, as free wind generation decreases, thermal generation must be deployed to compensate. This cost increase becomes larger in a constrained network.

2.5.3 **Conclusions**

In this paper the effects of network congestion, transmission losses and the varying degrees of intermittent wind generation on energy storage allocation and investment were explored. We consider a DC OPF model that considers storage allocation and adjusts it using a linearized approximation for ohmic losses. The model included dispatchable thermal generation and intermittent wind generation as the primary sources of energy in the grid. Thermal output is treated as a decision variable while wind generation is adopted from a data set as a parameter [122].

To better interpret model outputs from the allocation cases, we formulate three additional metrics allowing for greater insight into how the storage capacity is distributed throughout the network, used over the set time-horizon, and affected by the introduction of transmission inhibitors. Two sets of case studies were run—one for investigating storage allocation and the other for understanding storage investment strategies. In both cases it was found that losses had a relatively small effect on storage siting and investment decisions, while congestion significantly impacted the model output. Congestion drove higher storage capacity siting with more of it located close to

demand centres. When both forms of network constraints were introduced simultaneously, losses did not drastically change the results. In addition, both sets of case studies showed that faster ramping technologies such as flywheels were favoured for increased renewable penetration for their load stabilizing capabilities. However, after a certain threshold of renewable capacity was reached the investment model favoured larger scale to better manage excess energy supply and avoid spillage.

In future research we consider addressing how energy storage can be used to deal with grid stability for more unpredictable scenarios. Excess congestion, and damage to power lines have the potential to create outages. Stochastic optimization can be applied to understand how energy storage can be used as reserves for blackouts or to prevent isolated nodes from going dark if transmission options are limited.

2.6 Net Present Value as a tool for assessing investment

Net present value (NPV) is a widely used concept to calculate the value of assets or whole companies not only in an electric framework but also in most of industrial sectors. It has been largely used in economic analysis long ago. Although previous work already had already made use of the underlying idea of discounting, NPV was formalized at the beginning of 20th century by Irving Fisher [123]. The idea of present value consists in using a discount factor to represent how the value of money changes along time when evaluating incomes, cost or profits that occur in different years along the time. Although a modified value of this discount rate could be used to take into account risk consideration, a risk free discount rate will be considered herein leaving risk consideration beyond the intended scope of this work. It is also possible, and conceptually easy although unnecessarily complicated, to include the effect on inflation adapting the value of the discount rate. For the sake of simplicity, we will not consider the effect of inflation either.

The other characteristic of NPV is the idea of net value. It refers to the consideration of the results of the investment taking into account incomes, investment costs, operation costs and corporate taxes, and summing it up over an infinite time horizon, including a residual value for the furthest years. There are some alternatives to NPV that are used to evaluate electric assets, such as payback period, internal rate of return (IRR), real options, (which attempt to include the flexibility in the time of the investment, assumed away in NPV) or cost-benefit analysis, (which may include issues other than cash, i. e. environmental or quality issues). Anyway, the use of NPV, with some simplifications such as disregarding corporate taxes and financial costs, is widely extended in the electricity sector.

A common technique used to evaluate profitability of a project, is evaluating its NPV using as discount rate the company WACC (weighted average capital cost). If NPV is

positive the project or the firm is profitable, if it is zero, it breaks even and if it is negative, it is not profitable. The value of WACC depends on the company debt structure and integrates the expected profitability for the shareholders and the interest rate paid for the company debt. In this context, breaking even means, being able to pay the debt interest and giving the shareholders an acceptable level of profitability [124].

NPV is commonly used when evaluating electric assets in long-term studies, to ensure that the aggregation of the values along the years is suitable. NPV by itself does not provide a method to estimate incomes and cost along the years, and thus it requires the use of exogenous data or estimation models. An approach that is very common in the electric studies, is using a mathematical programming to maximize discounted profit (approximated as income minus overall costs). In this approach, the objective function can be considered as an approximation of NPV, but frequently, taxes and amortization are not considered, and residual value is often disregarded or estimated in a rough way. An alternative approach, is using NPC (net present cost, considering overall costs) as objective function and minimize it. As will be discussed later, under some hypothesis this is equivalent to make the NPV equal to zero, and thus computing the point where the company breaks even.

The work by Campos et. al [125] studies the links between the value of NPV and other profitability measures, and the solutions that are obtained when discounted cost minimization is used to stablish capacity expansion. The present work intends to shed light on the proper use of a detailed representation of NPV and NPC in the framework of electric systems generation expansion planning taking into account residual value as part of the investment model.

2.6.1 Literature Review

Some of the studies of generation capacity expansion planning use the so-called static approach. They study a single year in the future and determine the optimal mix for this time, not taking care of the path of investment that has led to this situation along the years. This method requires to assign part of the overall investment cost to the analyzed year. Some classical works in the field of expansion planning use this static approach for a single year. In Ramos et al [126] NPC is minimized using this approach. Discounted benefit, that can be considered as a simplification of NPV is used by Ventosa in [127] and by Murphy and Smeers in [128]. More recent works use a static approach. For example a cost minimization model including the network [129], a MILP cost minimization model for carbon dioxide emission analysis [130], two models including network and market representation [131], [132] and a cost minimization model including operating reserves [133]. Pozo et. al [134] uses a three level static approach to simultaneously analyze generation and transmission expansion. GENCO profits are maximized using an

annualized investment cost. A different three level approach is also used in [135] to analyze minimum cost expansion, taking account reliability issues.

Being useful in some situations or for simplified studies, this single year static approach may be misleading, i. e. in the current context of rapid development of renewables technologies as their investment cost are rapidly changing. Results of a static analysis may be very ambiguous regarding the year in which investments should be done, as this may have a huge value in the annualized cost.Other works deal with a several-year horizon and use an annualized investment cost for each year. Some examples are the works by Gorenstin [136], Wogrin [137], Vespucci [138], Nogales [139] and Dominguez [140]. All these works as well as the previously mentioned [125], do not consider a residual value to represent the years beyond the study horizon. A residual value is considered in [141] for generation assets, that in this case is the value of resale of the assets at the end of the study year (savage value). This value may be useful for the study of the value of a single plant, nevertheless for a whole company it is not very adequate, because on the one hand the resale value of a whole company is volatile and complex to compute, and on the other hand it is more realistic to consider that the company is going to be running for a long period of time, beyond the end of the studied horizon. The residual value is represented by replicating indefinitely the last year of the study in [142].

Residual value, may be disregarded in some circumstances (long study horizon and high discount rate values) but in general it should be included as part of the NPV or NPC. This approximation may make sense if only the investment decisions for the initial years of the horizon are to be considered. However, the value of NPV or NPC will not be correct. For example, it the study horizon is 15 years and discount rate is 5%, residual value accounts approximately for 50% of the total NPV or NPC.

An additional advantage of considering residual value is that we can use a more realistic criteria (known as free cash flow in the economic literature), and include the overall investment cost, the year when each plant is built. By doing so, we do not need to consider this annualized cost exogenously as is common practice in the literature. This is a major advantage of the method presented herein. This way there is no need for arbitrarily fixing a method for annualization. Besides we can take into account closures and replacement by including new plants and its building cost, the year they enter the system.All of the above works, as is common use, consider that investment cost, is distributed among the years and then years are separately computed.

This paper makes a contribution by extending the previous works, allowing for the deterministic consideration of the NPC of a whole company with a discount rate, under the infinite life hypothesis, taking into account at the same time finite life span of assets by properly including residual value and considering overall investment costs. The

presented model is compared with the annualized alternative, analyzing when minimizing net present cost is equivalent to considering NPV=0, what makes the company break even.

The rest of the paper is structured as follows: section 2.6.2 presents the definition of net present value, section 2.3.3 describes the annualized and overall models, section 2.3.5 compare its performance in a study case and in section 2.6.5 some conclusions are drawn.

2.6.2 Net Present Value Formulation

2.6.2.1 Annual profit

Annual profit for a generation company is defined as follows:

$$\pi_y = I_y - C_y - T_y \qquad (1)$$

In this expression π_y is the profit in year y, I_y is the income in day ahead market, C_y is cost, including investment and operation cost and T_y is the corporate income tax. Other taxes such as generation taxes that do not depend on the company profits, should be taken into account as costs. The consideration of corporate taxes is beyond the scope of this paper and thus they will be disregarded.

2.6.2.2 Net present value (NPV)

It can be defined for a project or for a company as follows.

$$NPV = \sum_{y=1}^{Y} \frac{1}{r^{y-1}} . \pi_y + RV \qquad \textbf{(2)}$$

Here $r = 1 + d$, being *d* the discount rate.

NPV as is defined here may be used in two ways. In the first one *d* is set to the company or project WACC, and then VAN is computed and profitability stablished as a consequence of its sign. The second one involves searching in an iterative way, the value of *d* that leads to a zero value for NPV, that is the Internal Return Rate (IIR). The models presented in this paper may be useful for both approaches.

2.6.3 Models Formulation

We will consider a perfect competition market with elastic demand. No capacity payments will be considered. For the sake of simplicity, but without losing generality, no spinning reserve or other technical constraints are considered for operation nor coverage index for demand.

2.6.3.1 Cost for a single year Y

Cost for a single year can be obtained by solving a basic linear programming problem.

$$min_{x_{jY},q_{jYl},h_{Yl},D_{lY}} \sum_{j}(\beta_{jY}x_{jY}) + \sum_{jl}\delta_{jY}t_l q_{jYl} - \sum_{l}\frac{1}{2a_{lY}}(D'_{Yl} - D_{Yl})^2 \quad \textbf{(3)}$$

s.t.

$$0 \le q_{jYl} \quad : \quad \rho_{jYl} \qquad \forall\, j,l \quad \textbf{(4)}$$

$$q_{jYl} \le k_j x_{jY} \quad : \quad \mu_{jYl} \quad \forall\, j,l \quad \textbf{(5)}$$

$$\sum_{j}(q_{jYl}) + h_{Yl} = D_{Yl} \quad : \quad p_{Yl} \qquad \forall\, l \quad \textbf{(6)}$$

$$\sum_{l}(t_l h_{Yl}) = E_Y \quad : \quad \sigma_Y \quad \textbf{(7)}$$

Subscript *l* stands for load level and *j* for technology (thermal or renewable), x_{jY} is the total capacity of each technology during the year and is a decision variable of the model that will be considered as continuous. The rest of decision variables are the production of each technology at each load level, q_{jYl} (thermal or renewable), h_{Yl} (hydro), and demand at each load level, D_{Yl}.The objective function in this model represents yearly cost for a single year *Y*, including a term of demand utility to represent demand elasticity. Operation cost is δ_{jY} and load level durations is t_l.

By writing the problem KKT conditions it can be easily proved that

$$D_{Yl} = D'_{Yl} - a_{Yl}p_{Yl}\,, \quad \textbf{(8)}$$

in this expression, $D'_{Yl}$and a_{Yl} are parameters that define linear demand.

In (3) β_{jY} is the so-called annualized investment cost for each technology computed for year *Y*, and should be chosen for all the years (including *Y*) so that along the plant life span *ls* (taking into account the discount rate) it sums up the overall investment cost.

$$B_{jY} = \sum_{i=1}^{i=ls(j)} \frac{\beta_{j(Y+i-1)}}{(1+d)^{i-1}} \quad \textbf{(9)}$$

There is an infinite set of values that satisfy this expression. If in addition to this condition it is imposed that the annualized cost, for an asset built on year *Y*, must be the same for all years along its life-span (this is the so called French method, but there are other alternatives as it will be shown later) then it can be computed as:

$$\beta_{jY} = \frac{B_{jY} d}{(1+d)} \cdot \frac{1}{1-(1+d)^{-ls(j)}} \quad \textbf{(10)}$$

It will be considered in all the models presented herein, as is commonly done in capacity expansion models, that both investment and operation cost are charged at the beginning of the year. This may lead to expressions slightly different from the standard ones that can be found in economy books. The model constraints include lower limit for production (4), upper limit for production, including utilization factor k_j (5), generation-demand balance (6), and hydro production energy balance (7) being E_Y total hidro available energy. Dual variables are written after the colon.

2.6.3.2 Cost annualized non-monotonic model (for several years)

The previous model can be easily extended to several year just by adding them discounted. Now *y* is the subscript for year. Nevertheless, it is immediate that each year could be solved separately. In this model years are represented separately, and hence the value of the investment *x*, may decrease along the time (accepting early closure of plants).

$$min_{x_{jy}, q_{jyl}, D_{yl}, h_{yl}}$$

$$\sum_{y=1}^{y=Y} \left[\frac{1}{r^{y-1}} \left(\sum_{j} (\beta_{jy} x_{jy}) + \sum_{lj} \delta_{jy} t_l q_{jyl} \right) - \sum_{yl} \frac{1}{2a_{yl}} \left(D'_{yl} - D_{yl} \right)^2 \right] \quad \textbf{(11)}$$

s.t.

$$0 \le q_{jyl} \quad : \quad \rho_{jyl} \qquad \forall\, j,y,l \tag{12}$$

$$q_{jyl} \le k_j x_{jy} \quad : \quad \mu_{jyl} \qquad \forall\, j,y,l \tag{13}$$

$$\sum_j (q_{jyl}) + h_{yl} = D_{yl} \quad : \quad p_{yl} \qquad \forall\, y,l \tag{14}$$

$$\sum_l (t_l h_{yl}) = E_y \quad : \quad \sigma_y \qquad \forall\, y \tag{15}$$

2.6.3.3 Cost annualized monotonic model (for several years)

The cost annualized monotonic model can be converted into a monotonic one by adding this new constraint:

$$x_{j,y+1} \ge x_{jy} \quad : \quad \varepsilon_{jy} \qquad \forall\, j,y \tag{16}$$

Now, reducing the overall quantity of a technology is not accepted, considering that this is a decision difficult to make. This model makes sense if the demand is increasing along the years.

2.6.3.4 Overall cost model

In this model, the investment cost is considered as a whole and it is not annualized. Demand is again represented as elastic:

$$D_{ly} = D'_{ly} - a_{ly} p_{ly} \tag{17}$$

The yearly cost expression for this model is:

$$C_y = \sum_j \beta'_j x'_j \gamma_{jy} + \sum_j B^*_{jy} dx_{jy} + \sum_{jl} \delta_j t_l q_{jyl} \tag{18}$$

The first term is used to represent stranded investment costs of pre-existent generation assets x'_j. Only these assets' investment cost is annualized with a known value for each technology, β'_j. γ_{jy} is 1 if the end of the plant life span has not yet been reached and hence y<=ls'(j), and is 0 otherwise. ls' is the remaining life span for preexisting groups.

We will assume that ls'(j)<Y. For the sake of clarity, this term will be neglected in the remaining of the paper. The second and third term represent investment cost of newly built plants and production cost respectively. The variable $dx_{jy}$is the investment done in year y (incremental value, not total value as used in the previous model). B^*_{jy} is the corrected overall investment cost, and will be explained in detail below.
For residual value RV_Y, we will replicate year *Y*, but investment cost is now annualized, otherwise it makes no sense to accept that each year is equal to the next one, and unrealistic results will be obtained. So, the cost we will replicate will be $\hat{C}_Y$, a modified cost for year *Y*. *g* is the yearly growth rate and must satisfy g<d. The expression is the result of the infinite geometric series sum from year *Y+1*, discounted to year *Y*.

$$\hat{C}_Y = \sum_j \beta_{jY} x_{jY} + \sum_{jl} \delta_{jY} t_l q_{jYl} \quad \textbf{(19)}$$

$$RV_Y = \left(\frac{1+g}{d-g}\right)\hat{C}_Y \quad \textbf{(20)}$$

With the previous definitions, we can already compute Net Present Cost (NPC) discounted for year 1, for this overall model:

$$NPC = \sum_{y=1}^{y=Y} \left[\frac{1}{r^{y-1}} C_y\right] + \frac{1}{r^{Y-1}} RV_Y \quad \textbf{(21)}$$

There is a key point in the previous formulation. If some investment is made and its life span finishes after year *Y*, we could be adding twice its investment cost for the last year. It would be included in the value of the overall investment cost B_{jy} (sometimes called overnight investment cost), and it also partially in the residual value. So, a corrected overall yearly cost B^*_{jy} is defined. It is equal to B_{jy} if *y+ls(j)-1> Y* and otherwise it is:

$$B^*_{jy} = B_{jy} - \sum_{yy=Y+1}^{yy=y+ls(j)-1} \frac{\beta_{jY}}{r^{yy-y}} \quad (22)$$

In this expression $\beta_{j,yy}$ is computed using (10) for year *Y*. The objective function for this model includes NPC and the term to represent elastic demand. Constraints include lower limit for production *(24)*, upper limit for production *(25)*, including utilization factor k_j, generation-demand balance *(26)*, and hydro production energy balance being E_Y total hydro available energy *(27)* as in the previous model. Additionally, early retirements for

plants are forbidden *(28)*. Constraint *(29)* represents the relationship between total cumulated capacity *x* and incremental yearly investment *dx*, taking into account plants life span. Dual variables are at the right of each constraint.

$$min_{\,x_{jy},dx_{jy},q_{jyl},D_{yl}} \quad NPC - \sum_{y=1}^{y=Y} \frac{1}{2a_{yl}} \left(D'_{yl} - D_{yl}\right)^2 \tag{23}$$

s.t.

$$0 \le q_{jyl} \quad : \quad \rho_{jyl} \qquad \forall\, j,y,l \tag{24}$$

$$q_{jyl} \le k_j x_{jy} \quad : \quad \mu_{jyl} \qquad \forall\, j,y,l \tag{25}$$

$$\sum_j \left(q_{jyl}\right) + \; h_{yl} \; = D_{yl} \qquad : \; p_{yl} \qquad \forall\, y,l \tag{26}$$

$$\sum_l \left(t_l h_{yl}\right) = E_y \qquad : \quad \sigma_y \qquad \forall\, y \tag{27}$$

$$dx_{jy} \ge 0 \quad : \quad \varepsilon_{jy} \qquad \forall\, j,y \tag{28}$$

$$x_{jy} = x'_j \gamma_{jy} + \sum_{yy=\max(1,y-ls(j)+1)}^{yy=\min(y,Y)} dx_{j,yy} \qquad : \; \lambda_{jy} \tag{29}$$

$$\forall y \mid 1 \le y \le \left[Y + max_{j<J}\, ls(j) - 1\right]$$

$$\forall j \mid 1 \le j \le J - 1$$

Variable dx (incremental yearly investment) is defined from year 1 to year *Y*, that is the last one that is represented in detail. However, *x* is defined from year 1 to year *Y+ls(j)-1*. These variables are not defined for the last technology, *j=J* because it corresponds to non-served energy, and thus there is no associated investment cost.The main advantages of this model in comparison to the annualized one is that using overall investment costs and the free cash flow criterion, no annualization of investment cost is required, obtaining thus a decision not affected by the arbitrary decision of how cost is distributed among the years.

2.6.3.5 Optimality criteria analysis

In the appendix it is shown that when corporate tax is disregarded, as it has been considered for all the models presented herein, by minimizing NPC and under certain assumptions we are in fact computing the solution that produces NPV = 0. This is true

for the annualized model if the monotonicity constraint (16) is not active, and for the overall model when the following assumptions are considered:

- the monotonicity constraint (28) is not active,
- the system starts from scratch, in other words, overall investment is zero for all technologies in year 0 (green field planning),
- and the solution for investment for the last year is the same than the one that is obtained for this year if it is solved separately using the annualized model using the French method for computing the annualized investment cost.

2.6.4 Case study and Results

2.6.4.1 Base case

The case base represents a 30-year horizon, for a system with four available technologies: imported coal (CIMP), combined cycle gas turbine (CCGT), gas turbine (TGAS) and on-shore wind power (WIND). No hydro power is considered for this case. *TABLE XV* shows investment and production costs for these generation technologies. There are no previously existing plants in the system, those that are required to supply the demand in the first year are built from scratch.

TABLE XV. DATA FOR BASE CASE

		CIMP	CCGT	TGAS	WIND
Investment cost (yearly)	*€/MW/year*	125240	50858	35600	90000
Production cost	*€/MWh*	34	52	75	0
Life span	*years*	30	25	25	25
Utilization factor	*p.u.*	1	1	1	0.25

Demand is inelastic (although the model would allow a elastic one) and is divided into twenty blocks each year with uneven durations to represent a realistic load-duration curve. Demand level for year 1 ranges from 19 to 41 GW. Demand increases yearly with different rates for each year and each load block. Yearly demand increase rates vary between 1 and 1.8%, for the last year of the horizon they are close to 1%. Discount rate is set to 7%. Growth rate for years beyond the studied horizon is 1% and non-supply energy cost was set to 2000 €/MWh.

2.6.4.2 Results

2.6.4.2.1 Comparison between annualized and overall model

The base case was solved both with the annualized model (without and with the condition of monotonicity (16) for investment) and for the overall model. Fig 1 shows how investment in wind power is greater for the annualized one (same results are obtained without and with monotonicity) for the first years, slowly approaching to the same value, that is reached around year 15. Fig 2, Fig 3 and Fig 4 show the investment for the rest of technologies (thermal) for the three alternatives. There are small differences in intermediate years in the value of investments when the monotonicity constraint is included in the annualized model. On the other hand, investment values for year one are different for annualized and overall model, but they slowly converge to a similar value at the end of the time horizon.

Cost recovery along the plants life span was checked for the investments done in the first year for the four technologies, finding that it is achieved for the annualized cost without monotonicity (as expected) but, surprisingly, also for the case with monotonicity. In the overall model, all technologies recover investment cost, except for CCGT that recovers everything except a small quantity below 0.2% of investment overall cost.
In order to compare how investment cost is recovered in each situation, an equivalent yearly investment cost for each technology has been defined, being yearly income cost per MW minus yearly operation cost per MW.

$$\beta eq_{jy} = \sum_{l} \left[t_l q_{jy} \left(\frac{p_{yl}}{t_l} r^{y-1} - \delta_{jy} \right) \right] * \frac{1}{x_{jy}} \qquad (30)$$

In Fig 5 this parameter is shown for the annualized model with monotonicity. Differences with the annualized investment cost when is evenly distributed are not large, and this explains why cost is recovered despite of monotonicity.

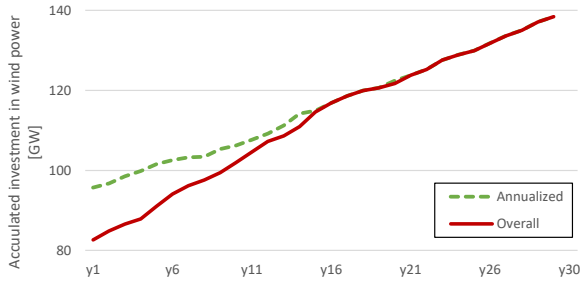

Fig 1. Accumulated investment for each year in wind power. Base case. (Annualized model with and without monotonicity have the same value).

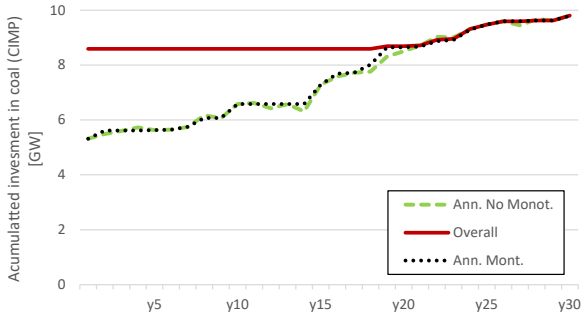

Fig 2. Accumulated investment for each year in coal. Base case.

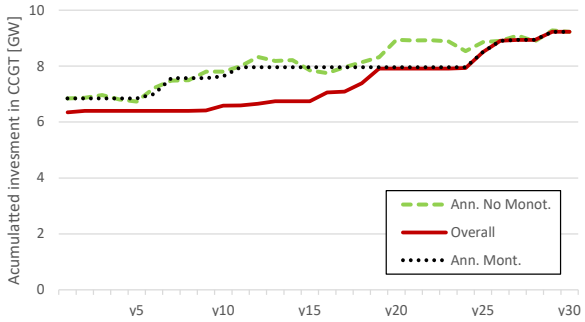

Fig 3. Accumulated investment for each year in CCGT. Base case.

The same parameter for the overall model is shown in Fig 6. It is interesting to see how on the one hand this value for the first year is over the annualized investment cost when it is evenly distributed. On the other hand, it is at the same value or below for the last years of the horizon. This means that in order to minimize the overall system cost, optimal investments do not correspond to annualized optimal investments unless this modified value is used for yearly investment cost, instead of the usual uniform annualized value (French method).

2.6.4.2.2 Effect of decreasing investment costs for wind power

The objective of this alternative case is to check how the investment and its cost recovery depend on the evolution of investment cost. All the data are the same as in the base case, including investment cost for all the technologies except for wind power, which is represented considering a decrease of 20% of cost every ten years. Fig 7, Fig 8, Fig 9 and Fig 10 show the new values for investment. For thermal technologies, in the annualized cost model with monotonicity, investment is made only in the first year (1.9, 7.3 and 6.3 GW for coal, CCGT and gas turbine respectively). Obviously, wind power investment increases for the last years with respect to the base case, decreasing for the other technologies, that besides, in the last years, are constant for the overall model and have small variations for the rest of technologies when the annualized model is used, except for gas turbines that share the demand supply with wind power for years 25 to 30. CCGT and gas turbine plants that are built in the first year are closed in year 25, and in year 26 there is an additional demand that is covered also with gas turbines. This effect is not seen by the annualized model. Besides, both annualized model overestimate investment with respect to the overall model that includes investment cost in a more adequate way.

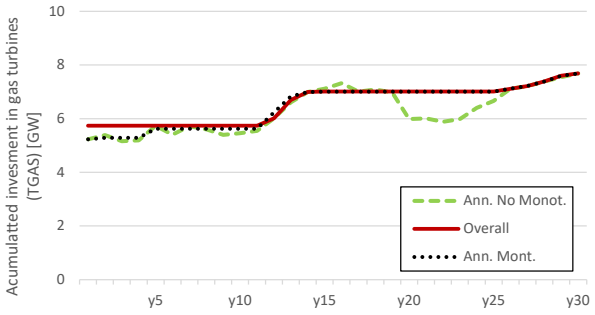

Fig 4. Accumulated investment for each year in gas turbines (TGAS). Base case.

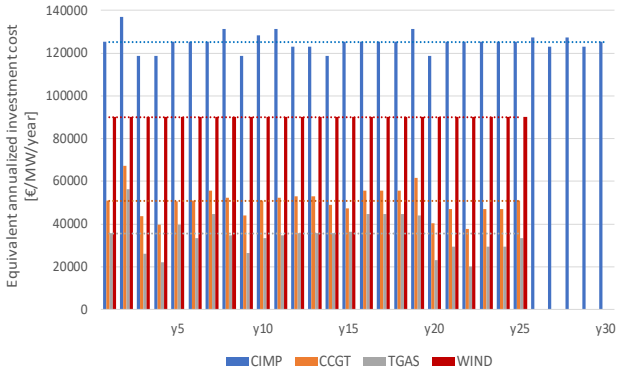

Fig 5. Equivalent annualized investment cost for each technology for annualized case with monotonicity. Base case. Horizontal dotted lines represent the yearly uniform cost for the annualized case.

In this case, the total investment for year 30 is very different in the annualized and overall models for coal and CCGT. Moreover, cost recovery for the investments made in the first year, is again achieved for the annualized cost without and (surprisingly again) with monotonicity. In the overall model, all technologies recover investment cost, (wind even obtains a profit around 1% of investment cost) except for coal that only recovers 65% of investment cost.Cost recovery distribution is analyzed in Fig 11. Now the equivalent yearly investment cost, is very significant in the first years for all thermal technologies. The increase of wind power capacity for the last year makes prices decrease and thus recovery must be done during the first years. The discrepancies are related to the large difference between the investment decided for the annualized case without monotony (0 GW) and the overall model (4 GW).

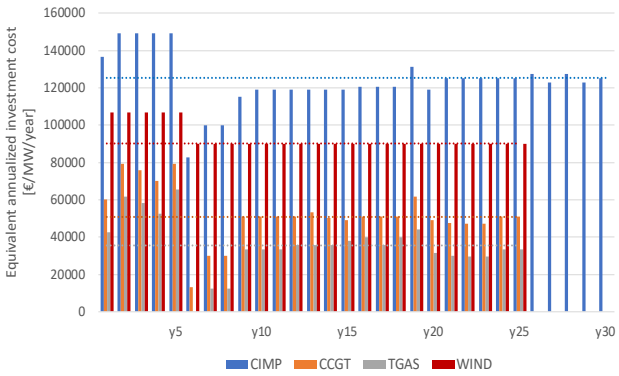

Fig 6. Equivalent annualized investment cost for each technology for overall case. Base case. Horizontal dotted lines represent the yearly uniform cost for the annualized case.

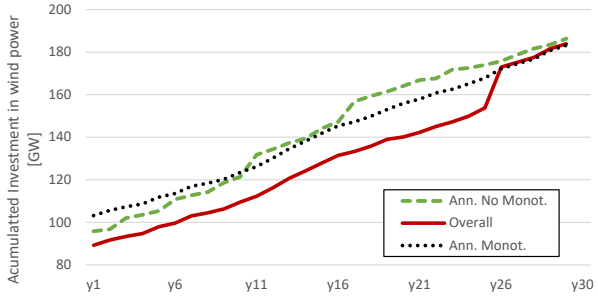

Fig 7. Accumulated investment for each year in wind power. Case with decreasing cost for wind power.

2.6.5 Conclusions

Two different models to compute generation capacity expansion planning by minimizing net present cost have been presented. The former uses an annualized investment cost for each year, while the later uses overall investment cost and includes a residual value.

In some situations, these models obtain the decisions for capacity expansion that lead to a net present value of zero, being interesting to determine the profitability threshold where a generation company breaks even. The conditions that lead to cost recovery in both models have been analyzed. The use of the overall model allows to explore the best path for cost recovery along the years, while annualizing the investment cost means making this decisions exogenously. It also uses a more realistic representation of plants closures.

A basic case example including both thermal and renewable technologies has been used to compare both models. For the case with investment cost uniform along time, cost recovery has been obtained for both models. Nevertheless, when decreasing investment cost has been considered for wind power, cost recovery has only been achieved for all technologies for the annualized model. In the case of the overall model, coal only got a partial cost recovery. The results suggest that uniform annualization overestimates optimal investment and may not be the most adequate option in a decreasing investment-cost context.

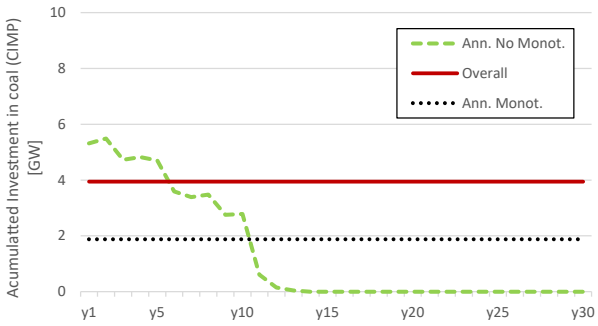

Fig 8. Accumulated investment for each year in coal (CIMP). Case with decreasing cost for wind power.

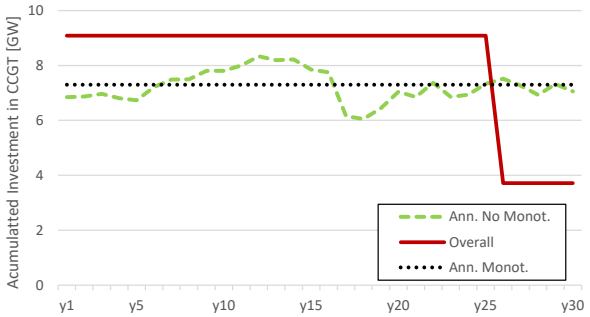

Fig 9. Accumulated investment for each year in coal in CCGT. Case with decreasing cost for wind power.

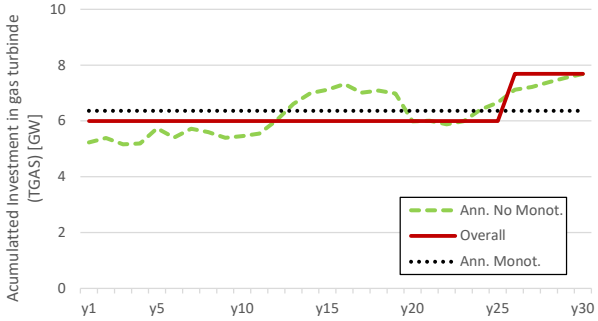

Fig 10. Accumulated investment for each year in coal in gas turbines (TGAS). Case with decreasing cost for wind power.

An adequate representation of net present value, provides useful additional information for analyzing generation investments and cost recovery, especially in situations with decreasing long-term investment cost, as is the case of most of renewable technologies. Further research should deal with the inclusion of corporate tax in the computation of net present value, which is out of the scope of this work. Other improvements may include the analysis of the effect of the value of WACC on demand when it is elastic and the consideration of uncertainty in renewable production availability. The models presented herein could also be extended to analyze transmission or storage expansion.

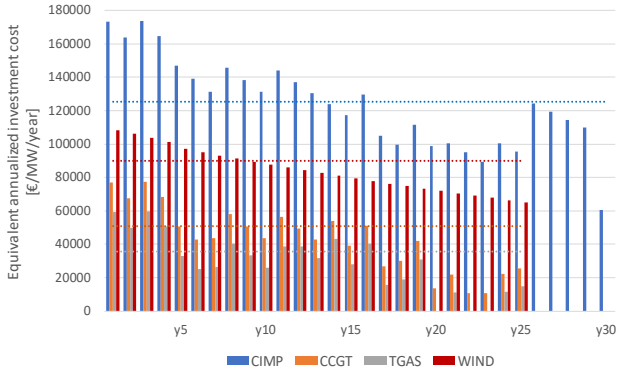

Fig 11. Equivalent annualized investment cost for each technology for overall case. Case with decreasing cost for wind power. Horizontal dotted lines represent the yearly uniform cost for the annualized case.

3. Integration of short- and long-term uncertainties in long-term models

Transmission Expansion Planning (TEP) and Generation Expansion Planning (GEP) are becoming more and more complex with the uncertainty introduced by the growing presence of renewable energy resources and other technological advances, along with constant uncertainties such as fuel prices and load demand.

The goal of TEP is to provide safe and cost-effective electricity services to society. It intends to optimize power systems operation by minimizing costs, and therefore, maximizing efficiency. This optimization can be limited through different restrictions, such as environmental or government mandated [143]. With all previous considerations, TEP defines when, where and how many new lines should be installed in the network to

ensure a sufficient level of energy supply to customers, taking into account a number of uncertainties, while minimizing investment, operation, and interruption costs [2]. TEP uses forecasting, candidate identification, optimization/cost-benefit analysis, reliability assessment, and security assessment [144]. TEP uses forecasting, candidate identification, optimization/cost-benefit analysis, reliability assessment, and security assessment [145]. TEP attempts to satisfy demand while at the minimum cost operationally.

GEP relates to the investment on energy production as it attempts to expand the current power system by determining the size, place, technology, and time of new plants. GEP must satisfy reliability criteria and meet the increasing future demand in order to be successful [144]. It aims to minimize costs, both operational and investment-wise, to create a power system with the most efficient technologies considering the near future. GEP aids with investment decisions as it attempts to reduce costs of expansion.

The penetration of renewable energy sources has been continuously increasing in modern day power systems and are likely to continue to do so. Renewables have a major impact on the investment and expansion decisions that are made. While leading to CO2 reductions, renewable energy (RE) sources are often intermittent, such as wind, and therefore represent a challenge for power systems. Their power output is uncertain and strongly affects short-term operation of the system. Long-term models that disregard short-term uncertainties due to the lack of proper representation of short-term behavior, might be more prone to commit planning mistakes. STEXEM is planning to introduce this short-term behavior into strategic expansion models. By doing so, we will be able to provide further insights about the game-theoretic consequences of greater RE penetration coupled with smart-grid technologies such as energy storage. Such interactions are increasingly important and can have unexpected results that are only beginning to be explored in the literature. However, the literature generally does not address investment in wind and energy storage, which is why our approach would be novel in terms of providing policy insights.

Uncertainty clouds the planning and modeling of GEP and TEP programs. Uncertainty is a state in which it is not possible to describe this exact moment, nor the future outcome. This uncertainty within expansion planning can be in the forms of demand growth, weather occurrences, and changes in fuel prices, along with many others. Uncertainty can be broken down into two types: aleatory and epistemic. Aleatory uncertainty has a “natural variability” in relation to a certain process [143]. For example, humans are naturally unpredictable in their behavior and choices. It is very difficult to manage or account for this uncertainty, if not impossible, in the same way that one cannot predict when and where an earthquake will occur in the future. Epistemic uncertainty results from imperfect knowledge, such as failure rates or a competitive market. Investment modeling can remove this uncertainty, whereas aleatory uncertainty can only be described by probabilities [146]. The impact of these uncertainties is known as risk, which can be quantified through cost-benefit analysis. Risk has the potential to create

consequences for expansion planning, which are usually negative. Uncertainty and risk make it more complex to optimize system planning for expansion.

GEP and TEP consider many similar uncertainties when attempting to optimize systems. For example, both rely on the prices of energy, reserves and regulation, which are uncertain. Also, fuel prices and availability affect both markets, as well as energy demand. Many regulations also affect GEP and TEP when optimizing investment decisions [147]. Common uncertainties allow for the co-optimization of energy systems in modeling.

Some uncertainties more specific to GEP include price volatility, demand evolution, reliability of generation units, investment and operation costs. Similarly, there is uncertainty with fuel prices, investment and maintenance costs and electricity prices. These influence generation planning in the way that it relates to investment on energy production, where investors must be aware of what will happen to prices, demand, and costs in the short- and long-term future [148]. Planners must also take into account these uncertainties in order to maximize the investment that they could potentially receive from these investors, as well as maximize the profits.

Uncertainty in TEP influences how to optimize power systems in the way that transmission planning accounts for “whether, where, when, and what types of transmission facilities to build in terms of minimizing costs and maximizing net economic benefits” [149]. Uncertainty can negatively affect making these decisions, as it becomes more challenging to optimize when dealing with multiple unknown or unknowable factors. This uncertainty comes in various forms, such as price, power system modeling, input data, and load. Some common uncertainties are:

- load uncertainty
- availability of supplies, such as generators and system facilities
- installation and closure of transmission facilities
- market rules and government policy, such as carbon tax [149]
- generation expansion and closure [145], [150]

Most importantly, however, uncertainty can be broken down by time. The timing affects the severity of uncertainty as well as the modeling structure. Short, medium, and long-term uncertainties can also affect decisions in regard to the scope. Short-term uncertainties, between hours and months, consist of hourly demand, equipment availability, wind production, and spot fuel prices, among others. Long-term uncertainty could be new technologies or smart grids, for example. These are much harder to account for, and decisions create a much larger impact while providing little detail. Somewhere between months and decades are the medium-term uncertainties, such as demand growth, generation expansion, supply contracts, or the evolution of current technology. These are taken into account through modeling approaches that produce optimized investment decisions.

STEXEM plans to introduce TEP and GEP short-term uncertainties into optimization systems in order to improve the investment decision process by taking into account both long- and short-term uncertainties. The programming tools utilized take uncertainties from both TEP and GEP, as well as overlapping uncertainties.

3.1 General Overview

TEP and GEP can be grouped together when creating optimization models, known as co-optimization. They both use large-scale highly constrained mixed-integer nonlinear programming, and are multi-objective optimization problems. Optimization programs for GEP and TEP can be used to account for uncertainties and to find the optimal investment and operation solutions. The main methodologies for treating uncertainty in GEPTEP problems are stochastic programming, adaptive programming, and robust optimization. The structure of uncertainty can be useful when comparing modeling approaches. It can be broken down as known, unknown, and unknowable uncertainties [146]. Known uncertainties, such as yearly demand growth, can be modeled through stochastic programming. These are random uncertainties that mostly come from historical data, which means the uncertainty can be assigned a probability. Unknown uncertainties are difficult to assign probabilities, and thus are modeled by sets bounding outcome. These can also be modeled through fuzzy sets or robust optimization, which are less structured models. Unknowable uncertainties are long-term and usually cannot even be identified in advance. These can be optimized with robust or flexibility.

There are multiple programs which can optimize decisions for TEP and GEP under uncertainty. Stochastic programming limits the number of scenarios and uses probability-defined uncertainties in order to create parameters. It attempts to minimize overall cost while maximizing profits [151]. Chance-constrained approaches are useful in solving TEP, as it has a predefined level as it solves using probabilities. Stochastic optimization systems use two decision stages: the here-and-now decisions and wait-and-see decisions. Here-and-now decisions are commitments made before resolving long-run uncertainties. Wait-and-see decisions are made after the scenario has occurred, also known as recourse decisions [149].

Adaptive programming is very similar to stochastic, where it minimizes cost and maximizes economic benefits. However, the “here and now” decisions of stochastic are transformed into core design investments, while “wait and see” decisions become scenario specific investments [152]. Also, in adaptation the scenario specific capacity investments are not saved over time. Adaptation also utilizes a number of the same uncertainties as stochastic programming.

Robust optimization can be used for co-optimized expansion planning, as it takes different sources of uncertainty and objective functions into account. Robust optimization attempts to minimize the worst-case cost and regret. Uncertainty sets must be utilized in order to “characterize possible realizations of the uncertain

parameter" [151]. It provides conservative decisions because it minimizes operational costs and considers the worst-case scenario given the uncertainty [151]. Robust optimization does not need probabilities, rather probabilistic sets, and its goal is to minimize the maximum risk overall.

3.2 Stochastic Programming

Stochastic programming allows for decisions to be made easily in regard to the best investment and the optimal investment time. Stochastic programming allows the decision maker to consider and compare multiple possibilities. The two-stage process has proved to be very successful with transmission expansion. The three types of mathematical modeling to solve these programs are recourse, deterministic, and probability-constrained. The first issue is the decision time framework, where "here and now" must be separated from "wait and see" decisions. Stochastic programming solves a limited number of scenarios that follow a certain distribution by using probabilities [151]. It attempts to find the best investment decision given that many different futures are possible, while taking into account several uncertainties, including that future energy standards are unknown [153]. It utilizes scenario trees with probability distributions to account for uncertainty.

The uncertain parameters taken into account in stochastic programming are either limited by the number of scenarios or assumed to follow a certain distribution. The objective is either to maximize expected profit without regard to risk, or to maximize profit while limiting the risk. A scenario tree can help to describe each variable with its assigned probability [147]. When many scenarios and uncertainties are present, a decomposition method can help to break down the problem within mixed integer programming. Bender's Decomposition model separates the problem into the investment and operation problems, naming them the master and slave, respectively. This method is most useful when the number of variables linking the two stages of the stochastic program is small, or when the master problem and subproblem are fundamentally different [154]. The early version of the prototype in this project does not require decomposition as it only takes a few variables into account, however for future implementation of the Spanish or European case a decomposition could be necessary.

In Table 16, general short-term and long-term uncertainties are given regarding stochastic programming. The main uncertainties taken into account are the short-term uncertainties, such as wind power generation and weather conditions. This is because a probability can be assigned to these uncertainties, usually based on past historical data. However, long-term uncertainties are also taken into account, as they cannot be ignored when attempting to find the optimal solution to expansion planning. Technological advancements, including the introduction of renewable energy options, are long-term uncertainties that must be faced. Renewables are bound to enter the transmission and

generation expansion plans in the future. Also, load demand is short-term, while load growth in long-term. This is because demand focuses on the near future of power storage, while load growth is the positive or negative expansion of power required by a facility further into the future. These are the main uncertainties taken into account within stochastic programming as it chooses the optimal investment decision.

Table 16: Short-term and long-term uncertainties of stochastic programming.

Short-Term Uncertainties within SP	Long-Term Uncertainties within SP
Wind power generation [153]	Natural Disasters [147]
Fuel prices [147]	Technological advancements, renewables [147]
Weather conditions [155]	Regulatory issues/policy changes [147][153]
Load demand [155]	Load growth [148]
	Economic growth [155]

3.3 Adaptive Programming

Adaptive programming can be described as a form of stochastic programming. This means that it is very similar to stochastic programming, as they are often combined, but it has its own variations. Adaptive and stochastic programming both are recourse-based mathematical programs that aim to solve co-optimized scenarios while considering a number of uncertainties. However, stochastic programming solves a set of core investments starting at t=1, but it does not define later time periods until later stages are realized [152]. In adaptation, a single plan is created for all time periods, and the plan is re-evaluated in the future and updated. Also, stochastic “here and now” decisions are adaptive investments into the core design, and “wait and see” stochastic decisions become scenario specific investments in adaptation. Scenario specific investments have no memory through time, as “wait and see” decisions are evaluated at each time step within stochastic programming. In adaptation, core investments are defined for all time periods at once. Unlike stochastic programming, adaptation also has a capacity update equation for both the core and scenarios [152]. Adaptation is similar to stochastic programming, but it faces a number of variations in formulation and decision making.

In Table 17, it becomes very clear that adaptation is very similar to stochastic programming. Many of the uncertainties considered in stochastic programming are also considered in adaptation. However, the formulation varies slightly, as mentioned above. Wind and solar energy uncertainty appears in all of the types of programming, as it is unavoidable considering the growth of renewable energies as a power source around the globe. Short-term weather conditions must be considered because renewables will not function as well, if at all, if there is no wind one week or it is a particularly cloudy

month. Taking many factors and uncertainties into account allows the program to select a much safer and better decision regarding TEP and GEP plans.

Table 17: Difference in uncertainties by time relating to adaptive programming.

Short-Term Uncertainties within AP	Long-Term Uncertainties within AP
Wind/Solar power [145]	Introduction of renewable energies [147]
Load demand [155]	Technological advancements [147]
Fuel price [148]	Policy changes [153]
Market changes [148]	Economic growth [155]

3.4 Robust Optimization

Robust Optimization has fundamental differences from Adaptive and Stochastic programming. It utilizes a probability distribution within a confidence set to assess uncertainties. It fits best in the case that enough data is not available for the uncertainties to solve in a way such as stochastic programming. Robust Optimization works by using the past historical data available regarding uncertain conditions. It models through sets, where the data and scenario are bounded within certain limits. This optimization method considers the worst-case scenario to achieve a cost-effective solution. It has been applied to wind, price, power generation, and load uncertainty [156]. Robust Optimization finds the best possible choice to avoid the worst scenario and risks.

Robust Optimization addresses some of the issues that arise from stochastic programming. For example, it uses probability distribution sets with an infinite number of scenarios. This is in contrast to stochastic programming, which uses probability distribution functions to analyze a number of uncertainties. Robust Optimization can assess numerous scenarios more easily than stochastic, which requires specific data, as well as decomposition methods sometimes, to break down the large number of uncertainties.

In Table 18, the main uncertainties for Robust Optimization are proposed. Many are similar to Table 16 and Table 17, as they consider the same problem usually regarding transmission and generation expansion planning. However, the case studies sometimes favor some uncertainties over others when creating a new program. Human demand and investment behavior tend to appear more in robust optimization. Human demand and investment uncertainty refer to the unpredictable nature of consumers. The term 'environmental factors' also appears many times, which refers to wind generation power, available thermal energy, or solar power. This reflects on the fact that weather is unpredictable and can affect the power generation if renewable energy systems are

introduced. Many of the other uncertainties have been mentioned in regard to stochastic or adaptive programming.

Table 18: Difference in uncertainties by time relating to robust optimization.

Short-Term Uncertainties within RO	**Long-Term Uncertainties within RO**
Wind/solar generation [156]	Technological advancements [157]
Load demand [156][157]	Natural Disasters [157]
Human demand variations [157]	Policy changes [157]
Investment behavior [146]	Load growth [157]

3.5 Conclusions

The overview of generation and transmission expansion planning has been discussed, as well as their differences and meanings. Co-optimization of these two is starting to be introduced when creating programs to make optimized decisions for future investments. These expansion plans face uncertainty regarding the future, because not everything can be known for certain. There are uncertainties specific to GEP, TEP, and also uncertainties that cover co-optimization. Adding these factors to the programming formulations accounts for many of the risks and works to reduce it when choosing the best decision. Stochastic programming, adaptive programming, and robust optimization all aim to choose the optimal solution for the given scenario within expansion planning. These programs vary from one another slightly and sometimes produce different solutions regarding the same case. STEXEM has created its own programs to consider long-term and short-term uncertainties to solve cases regarding the co-optimization of generation and transmission expansion planning.

4. References

[1] L. Reichenberg, A. S. Siddiqui, and S. Wogrin, "Policy implications of downscaling the time dimension in power system planning models to represent variability in renewable output," *Energy*, vol. 159, pp. 870–877, Sep. 2018, doi: 10.1016/j.energy.2018.06.160.

[2] D. A. Tejada-Arango, M. Domeshek, S. Wogrin, and E. Centeno, "Enhanced Representative Days and System States Modeling for Energy Storage Investment Analysis," *IEEE Trans. Power Syst.*, pp. 1–1, 2018, doi: 10.1109/TPWRS.2018.2819578.

[3] EUROPEAN COMMISSION, "Communication from the Commission to the European Parliament, the Council, the European Economic and Social Committee and the Committee of the Regions, Energy Roadmap 2050," EUROPEAN COMMISSION, Brussels, COM(2011) 885 final, Dec. 2011. Accessed: Jul. 19, 2018. [Online]. Available: https://eur-lex.europa.eu/LexUriServ/LexUriServ.do?uri=COM:2011:0885:FIN:EN:PDF.

[4] "NREL: Energy Analysis - Regional Energy Deployment System (ReEDS) Model," 2016. http://www.nrel.gov/analysis/reeds/ (accessed Apr. 12, 2016).

[5] B. A. Frew, S. Becker, M. J. Dvorak, G. B. Andresen, and M. Z. Jacobson, "Flexibility mechanisms and pathways to a highly renewable US electricity future," *Energy*, vol. 101, pp. 65–78, Apr. 2016, doi: 10.1016/j.energy.2016.01.079.

[6] B. A. Frew and M. Z. Jacobson, "Temporal and spatial tradeoffs in power system modeling with assumptions about storage: An application of the POWER model," *Energy*, vol. 117, pp. 198–213, Dec. 2016, doi: 10.1016/j.energy.2016.10.074.

[7] P. Nahmmacher, E. Schmid, L. Hirth, and B. Knopf, "Carpe diem: A novel approach to select representative days for long-term power system modeling," *Energy*, vol. 112, pp. 430–442, Oct. 2016, doi: 10.1016/j.energy.2016.06.081.

[8] U.S. Energy Information Administration, "Levelized Cost and Levelized Avoided Cost of New Generation Resources in the Annual Energy Outlook 2018," EIA, Mar. 2018.

[9] K. Poncelet, E. Delarue, D. Six, J. Duerinck, and W. D'haeseleer, "Impact of the level of temporal and operational detail in energy-system planning models," *Appl. Energy*, vol. 162, pp. 631–643, Jan. 2016, doi: 10.1016/j.apenergy.2015.10.100.

[10] A. E. MacDonald, C. T. M. Clack, A. Alexander, A. Dunbar, J. Wilczak, and Y. Xie, "Future cost-competitive electricity systems and their impact on US CO_2

emissions," *Nat. Clim. Change*, vol. 6, no. 5, pp. 526–531, May 2016, doi: 10.1038/nclimate2921.

[11] S. Pfenninger, A. Hawkes, and J. Keirstead, "Energy systems modeling for twenty-first century energy challenges," *Renew. Sustain. Energy Rev.*, vol. 33, pp. 74–86, May 2014, doi: 10.1016/j.rser.2014.02.003.

[12] S. Wogrin, P. Duenas, A. Delgadillo, and J. Reneses, "A New Approach to Model Load Levels in Electric Power Systems With High Renewable Penetration," *IEEE Trans. Power Syst.*, vol. 29, no. 5, pp. 2210–2218, Sep. 2014, doi: 10.1109/TPWRS.2014.2300697.

[13] M. Lehtveer, N. Mattsson, and F. Hedenus, "Using resource based slicing to capture the intermittency of variable renewables in energy system models," *Energy Strategy Rev.*, vol. 18, pp. 73–84, Dec. 2017, doi: 10.1016/j.esr.2017.09.008.

[14] S. Wogrin, D. Galbally, and J. Reneses, "Optimizing Storage Operations in Medium- and Long-Term Power System Models," *IEEE Trans. Power Syst.*, vol. PP, no. 99, pp. 1–10, 2015, doi: 10.1109/TPWRS.2015.2471099.

[15] J. H. Merrick, "On representation of temporal variability in electricity capacity planning models," *Energy Econ.*, vol. 59, pp. 261–274, Sep. 2016, doi: 10.1016/j.eneco.2016.08.001.

[16] H. Lund, P. A. Østergaard, D. Connolly, and B. V. Mathiesen, "Smart energy and smart energy systems," *Energy*, vol. 137, pp. 556–565, Oct. 2017, doi: 10.1016/j.energy.2017.05.123.

[17] V. Virasjoki, A. S. Siddiqui, B. Zakeri, and A. Salo, "Market Power with Combined Heat and Power Production in the Nordic Energy System," *IEEE Trans. Power Syst.*, pp. 1–1, 2018, doi: 10.1109/TPWRS.2018.2811959.

[18] B. Zhao, A. J. Conejo, and R. Sioshansi, "Coordinated Expansion Planning of Natural Gas and Electric Power Systems," *IEEE Trans. Power Syst.*, vol. 33, no. 3, pp. 3064–3075, May 2018, doi: 10.1109/TPWRS.2017.2759198.

[19] A. J. Conejo, L. B. Morales, S. J. Kazempour, and A. S. Siddiqui, *Investment in Electricity Generation and Transmission: Decision Making under Uncertainty*. Springer International Publishing, 2016.

[20] K. Eurek *et al.*, "Regional Energy Deployment System (ReEDS) Model Documentation: Version 2016," NREL (National Renewable Energy Laboratory (NREL), Golden, CO (United States)), 2016. Accessed: Jul. 31, 2017. [Online]. Available: http://www.nrel.gov/docs/fy17osti/67067.pdf.

[21] M. Odenberger, T. Unger, and F. Johnsson, "Pathways for the North European electricity supply," *Energy Policy*, vol. 37, no. 5, pp. 1660–1677, May 2009, doi: 10.1016/j.enpol.2008.12.029.

[22] L. Reichenberg, A. Wojciechowski, F. Hedenus, and F. Johnsson, "Geographic aggregation of wind power—an optimization methodology for avoiding low outputs," *Wind Energy*, vol. 20, no. 1, pp. 19–32, doi: 10.1002/we.1987.

[23] Fraunhofer ISE, "Levelized Cost of Electricity Renewable Energy Technologies," Nov. 2013.

[24] M. Haller, S. Ludig, and N. Bauer, "Decarbonization scenarios for the EU and MENA power system: Considering spatial distribution and short term dynamics of renewable generation," *Energy Policy*, vol. 47, pp. 282–290, Aug. 2012, doi: 10.1016/j.enpol.2012.04.069.

[25] D. A. Tejada-Arango, S. Wogrin, and E. Centeno, "Representation of Storage Operations in Network-Constrained Optimization Models for Medium- and Long-Term Operation," *IEEE Trans. Power Syst.*, vol. 33, no. 1, pp. 386–396, Jan. 2018, doi: 10.1109/TPWRS.2017.2691359.

[26] International Renewable Energy Agency (IRENA), "Planning for the renewable future: Long-term modelling and tools to expand variable renewable power in emerging economies." Jan. 2017, Accessed: Dec. 20, 2017. [Online]. Available: /publications/2017/Jan/Planning-for-the-renewable-future-Longterm-modelling-and-tools-to-expand-variable-renewable-power-in.

[27] R. Loulou and M. Labriet, "ETSAP-TIAM: the TIMES integrated assessment model Part I: Model structure," *Comput. Manag. Sci.*, vol. 5, no. 1–2, pp. 7–40, Feb. 2008, doi: 10.1007/s10287-007-0046-z.

[28] "Resource Planning Model | Energy Analysis | NREL," 2016. https://www.nrel.gov/analysis/models-rpm.html (accessed Jan. 30, 2018).

[29] G. Strbac *et al.*, "Opportunities for Energy Storage: Assessing Whole-System Economic Benefits of Energy Storage in Future Electricity Systems," *IEEE Power Energy Mag.*, vol. 15, no. 5, pp. 32–41, Sep. 2017, doi: 10.1109/MPE.2017.2708858.

[30] J. Haas *et al.*, "Challenges and trends of energy storage expansion planning for flexibility provision in low-carbon power systems – a review," *Renew. Sustain. Energy Rev.*, vol. 80, pp. 603–619, Dec. 2017, doi: 10.1016/j.rser.2017.05.201.

[31] R. Kannan, "The development and application of a temporal MARKAL energy system model using flexible time slicing," *Appl. Energy*, vol. 88, no. 6, pp. 2261–2272, Jun. 2011, doi: 10.1016/j.apenergy.2010.12.066.

[32] R. Kannan and H. Turton, "A Long-Term Electricity Dispatch Model with the TIMES Framework," *Environ. Model. Assess.*, vol. 18, no. 3, pp. 325–343, Jun. 2013, doi: 10.1007/s10666-012-9346-y.

[33] Elaine Hale, Brady Stoll, and Trieu Mai, "Capturing the Impact of Storage and Other Flexible Technologies on Electric System Planning," National Renewable Energy Laboratory (NREL), Technical Report NREL/TP-6A20-65726, May 2016. Accessed: Dec. 08, 2017. [Online]. Available: https://energy.gov/eere/analysis/downloads/capturing-impact-storage-and-other-flexible-technologies-electric-system.

[34] S. Fazlollahi, S. L. Bungener, P. Mandel, G. Becker, and F. Maréchal, "Multi-objectives, multi-period optimization of district energy systems: I. Selection of typical operating periods," *Comput. Chem. Eng.*, vol. 65, pp. 54–66, Jun. 2014, doi: 10.1016/j.compchemeng.2014.03.005.

[35] K. Poncelet, H. Höschle, E. Delarue, A. Virag, and W. D'haeseleer, "Selecting Representative Days for Capturing the Implications of Integrating Intermittent Renewables in Generation Expansion Planning Problems," *IEEE Trans. Power Syst.*, vol. 32, no. 3, pp. 1936–1948, May 2017, doi: 10.1109/TPWRS.2016.2596803.

[36] F. J. D. Sisternes, M. D. Webster, O. J. D. Sisternes, and M. D. Webster, "Optimal Selection of Sample Weeks for Approximating the Net Load in Generation Planning Problems," 2013, Accessed: Jan. 31, 2017. [Online]. Available: http://citeseerx.ist.psu.edu/viewdoc/citations;jsessionid=12C1211D1F204694768957FA69AB418F?doi=10.1.1.362.8358.

[37] E. Shayesteh, B. F. Hobbs, L. Söder, and M. Amelin, "ATC-Based System Reduction for Planning Power Systems With Correlated Wind and Loads," *IEEE Trans. Power Syst.*, vol. 30, no. 1, pp. 429–438, Jan. 2015, doi: 10.1109/TPWRS.2014.2326615.

[38] E. Shayesteh, B. F. Hobbs, and M. Amelin, "Scenario reduction, network aggregation, and DC linearisation: which simplifications matter most in operations and planning optimisation?," *Transm. Distrib. IET Gener.*, vol. 10, no. 11, pp. 2748–2755, 2016, doi: 10.1049/iet-gtd.2015.1404.

[39] W. J. Cole, C. Marcy, V. K. Krishnan, and R. Margolis, "Utility-scale lithium-ion storage cost projections for use in capacity expansion models," in *2016 North American Power Symposium (NAPS)*, Sep. 2016, pp. 1–6, doi: 10.1109/NAPS.2016.7747866.

[40] G. Morales-Espana, J. M. Latorre, and A. Ramos, "Tight and Compact MILP Formulation for the Thermal Unit Commitment Problem," *IEEE Trans. Power Syst.*, vol. 28, no. 4, pp. 4897–4908, Nov. 2013, doi: 10.1109/TPWRS.2013.2251373.

[41] ENTSO-E, "Ten Year Network Development Plan 2016," 2016. http://tyndp.entsoe.eu/ (accessed Aug. 03, 2017).

[42] I. Staffell and S. Pfenninger, "Using bias-corrected reanalysis to simulate current and future wind power output," *Energy*, vol. 114, pp. 1224–1239, Nov. 2016, doi: 10.1016/j.energy.2016.08.068.

[43] S. Pfenninger and I. Staffell, "Long-term patterns of European PV output using 30 years of validated hourly reanalysis and satellite data," *Energy*, vol. 114, pp. 1251–1265, Nov. 2016, doi: 10.1016/j.energy.2016.08.060.

[44] European Association for Storage of Energy (EASE) and European Energy Research Alliance (EERA), "European Energy Storage Technology Development Roadmap Towards 2030," EASE/EERA, Technical Report, Mar. 2013. Accessed: Aug. 23, 2017. [Online]. Available: http://ease-storage.eu/easeeera-energy-storage-technology-development-roadmap-towards-2030/.

[45] X. Zhang and A. J. Conejo, "Robust Transmission Expansion Planning Representing Long- and Short-term Uncertainty," *IEEE Trans. Power Syst.*, vol. PP, no. 99, pp. 1–1, 2017, doi: 10.1109/TPWRS.2017.2717944.

[46] M. Huber, D. Dimkova, and T. Hamacher, "Integration of wind and solar power in Europe: Assessment of flexibility requirements," *Energy*, vol. 69, pp. 236–246, May 2014, doi: 10.1016/j.energy.2014.02.109.

[47] J. Ma, V. Silva, R. Belhomme, D. S. Kirschen, and L. F. Ochoa, "Evaluating and Planning Flexibility in Sustainable Power Systems," *IEEE Trans. Sustain. Energy*, vol. 4, no. 1, pp. 200–209, Jan. 2013, doi: 10.1109/TSTE.2012.2212471.

[48] J. I. Pérez-Díaz and J. Jiménez, "Contribution of a pumped-storage hydropower plant to reduce the scheduling costs of an isolated power system with high wind power penetration," *Energy*, vol. 109, pp. 92–104, Aug. 2016, doi: 10.1016/j.energy.2016.04.014.

[49] S. Wogrin and D. F. Gayme, "Optimizing Storage Siting, Sizing, and Technology Portfolios in Transmission-Constrained Networks," *IEEE Trans. Power Syst.*, vol. 30, no. 6, pp. 3304–3313, Nov. 2015, doi: 10.1109/TPWRS.2014.2379931.

[50] R. Moreno, R. Ferreira, L. Barroso, H. Rudnick, and E. Pereira, "Facilitating the Integration of Renewables in Latin America: The Role of Hydropower Generation and Other Energy Storage Technologies," *IEEE Power Energy Mag.*, vol. 15, no. 5, pp. 68–80, Sep. 2017, doi: 10.1109/MPE.2017.2708862.

[51] V. R. Sherkat, R. Campo, K. Moslehi, and E. O. Lo, "Stochastic Long-Term Hydrothermal Optimization for a Multireservoir System," *IEEE Trans. Power Appar.*

Syst., vol. PAS-104, no. 8, pp. 2040–2050, Aug. 1985, doi: 10.1109/TPAS.1985.318779.

[52] H. Zhang, J. Zhou, N. Fang, R. Zhang, and Y. Zhang, "Daily hydrothermal scheduling with economic emission using simulated annealing technique based multi-objective cultural differential evolution approach," *Energy*, vol. 50, pp. 24–37, Feb. 2013, doi: 10.1016/j.energy.2012.12.001.

[53] V. L. de Matos and E. C. Finardi, "A computational study of a stochastic optimization model for long term hydrothermal scheduling," *Int. J. Electr. Power Energy Syst.*, vol. 43, no. 1, pp. 1443–1452, Dec. 2012, doi: 10.1016/j.ijepes.2012.06.021.

[54] A. R. de Queiroz, "Stochastic hydro-thermal scheduling optimization: An overview," *Renew. Sustain. Energy Rev.*, vol. 62, pp. 382–395, Sep. 2016, doi: 10.1016/j.rser.2016.04.065.

[55] M. E. P. Maceira, V. Duarte, D. Penna, L. Moraes, and A. Melo, "Ten years of application of stochastic dual dynamic programming in official and agent studies in brazil-description of the newave program," *16th PSCC Glasg. Scotl.*, pp. 14–18, 2008.

[56] S. Cerisola, J. M. Latorre, and A. Ramos, "Stochastic dual dynamic programming applied to nonconvex hydrothermal models," *Eur. J. Oper. Res.*, vol. 218, no. 3, pp. 687–697, May 2012, doi: 10.1016/j.ejor.2011.11.040.

[57] J. H. Zheng, J. J. Chen, Q. H. Wu, and Z. X. Jing, "Reliability constrained unit commitment with combined hydro and thermal generation embedded using self-learning group search optimizer," *Energy*, vol. 81, pp. 245–254, Mar. 2015, doi: 10.1016/j.energy.2014.12.036.

[58] N. E. Koltsaklis and M. C. Georgiadis, "A multi-period, multi-regional generation expansion planning model incorporating unit commitment constraints," *Appl. Energy*, vol. 158, pp. 310–331, Nov. 2015, doi: 10.1016/j.apenergy.2015.08.054.

[59] L. Kotzur, P. Markewitz, M. Robinius, and D. Stolten, "Time series aggregation for energy system design: Modeling seasonal storage," *Appl. Energy*, vol. 213, pp. 123–135, Mar. 2018, doi: 10.1016/j.apenergy.2018.01.023.

[60] S. Pineda and J. M. Morales, "Chronological time-period clustering for optimal capacity expansion planning with storage," *IEEE Trans. Power Syst.*, pp. 1–1, 2018, doi: 10.1109/TPWRS.2018.2842093.

[61] D. A. Tejada-Arango, M. Domeshek, S. Wogrin, and E. Centeno, "Enhanced Representative Days and System States Modeling for Energy Storage Investment Analysis," *IEEE Trans. Power Syst.*, vol. 33, no. 6, pp. 6534–6544, Nov. 2018, doi: 10.1109/TPWRS.2018.2819578.

[62] J. M. Latorre, S. Cerisola, and A. Ramos, "Clustering algorithms for scenario tree generation: Application to natural hydro inflows," *Eur. J. Oper. Res.*, vol. 181, no. 3, pp. 1339–1353, Sep. 2007, doi: 10.1016/j.ejor.2005.11.045.

[63] W. L. de Oliveira, C. Sagastizábal, D. D. J. Penna, M. E. P. Maceira, and J. M. Damázio, "Optimal scenario tree reduction for stochastic streamflows in power generation planning problems," *Optim. Methods Softw.*, vol. 25, no. 6, pp. 917–936, Dec. 2010, doi: 10.1080/10556780903420135.

[64] A. Shapiro, "Analysis of stochastic dual dynamic programming method," *Eur. J. Oper. Res.*, vol. 209, no. 1, pp. 63–72, Feb. 2011, doi: 10.1016/j.ejor.2010.08.007.

[65] J. Reneses, J. Barquín, J. García-González, and E. Centeno, "Water value in electricity markets," *Int. Trans. Electr. Energy Syst.*, vol. 26, no. 3, pp. 655–670, 2016, doi: 10.1002/etep.2106.

[66] S.-E. Razavi, A. Esmaeel Nezhad, H. Mavalizadeh, F. Raeisi, and A. Ahmadi, "Robust hydrothermal unit commitment: A mixed-integer linear framework," *Energy*, vol. 165, pp. 593–602, Dec. 2018, doi: 10.1016/j.energy.2018.09.199.

[67] PSR – Energy Consulting and Analytics, "SDDP – Stochastic hydrothermal dispatch with network restrictions," *Software | PSR – Energy Consulting and Analytics*, 2018. https://www.psr-inc.com/softwares-en/ (accessed May 09, 2018).

[68] M. V. F. Pereira and L. M. V. G. Pinto, "A Decomposition Approach to the Economic Dispatch of Hydrothermal Systems," *IEEE Trans. Power Appar. Syst.*, vol. PAS-101, no. 10, pp. 3851–3860, Oct. 1982, doi: 10.1109/TPAS.1982.317035.

[69] G. F. Bregadioli, E. C. Baptista, L. Nepomuceno, A. R. Balbo, and E. M. Soler, "Medium-term coordination in a network-constrained multi-period auction model for day-ahead markets of hydrothermal systems," *Int. J. Electr. Power Energy Syst.*, vol. 82, pp. 474–483, Nov. 2016, doi: 10.1016/j.ijepes.2016.03.032.

[70] M. Maceiral *et al.*, "Twenty Years of Application of Stochastic Dual Dynamic Programming in Official and Agent Studies in Brazil-Main Features and Improvements on the NEWAVE Model," in *2018 Power Systems Computation Conference (PSCC)*, 2018, pp. 1–7.

[71] B. G. Gorenstin, N. M. Campodonico, J. P. da Costa, and M. V. F. Pereira, "Stochastic optimization of a hydro-thermal system including network constraints," *IEEE Trans. Power Syst.*, vol. 7, no. 2, pp. 791–797, May 1992, doi: 10.1109/59.141787.

[72] M. Alvarez, S. K. Rönnberg, J. Bermúdez, J. Zhong, and M. H. J. Bollen, "Reservoir-type hydropower equivalent model based on a future cost piecewise

approximation," *Electr. Power Syst. Res.*, vol. 155, pp. 184–195, Feb. 2018, doi: 10.1016/j.epsr.2017.09.028.

[73] B. F. Hobbs, "Optimization methods for electric utility resource planning," *Eur. J. Oper. Res.*, vol. 83, no. 1, pp. 1–20, May 1995, doi: 10.1016/0377-2217(94)00190-N.

[74] V. Oree, S. Z. Sayed Hassen, and P. J. Fleming, "Generation expansion planning optimisation with renewable energy integration: A review," *Renew. Sustain. Energy Rev.*, vol. 69, pp. 790–803, Mar. 2017, doi: 10.1016/j.rser.2016.11.120.

[75] H. Saboori and R. Hemmati, "Considering Carbon Capture and Storage in Electricity Generation Expansion Planning," *IEEE Trans. Sustain. Energy*, vol. 7, no. 4, pp. 1371–1378, Oct. 2016, doi: 10.1109/TSTE.2016.2547911.

[76] N. E. Koltsaklis and A. S. Dagoumas, "State-of-the-art generation expansion planning: A review," *Appl. Energy*, vol. 230, pp. 563–589, Nov. 2018, doi: 10.1016/j.apenergy.2018.08.087.

[77] B. Hua, R. Baldick, and J. Wang, "Representing Operational Flexibility in Generation Expansion Planning Through Convex Relaxation of Unit Commitment," *IEEE Trans. Power Syst.*, vol. 33, no. 2, pp. 2272–2281, Mar. 2018, doi: 10.1109/TPWRS.2017.2735026.

[78] B. S. Palmintier and M. D. Webster, "Impact of Operational Flexibility on Electricity Generation Planning With Renewable and Carbon Targets," *IEEE Trans. Sustain. Energy*, vol. 7, no. 2, pp. 672–684, Apr. 2016, doi: 10.1109/TSTE.2015.2498640.

[79] B. F. Hobbs and S. S. Oren, "Three Waves of U.S. Reforms: Following the Path of Wholesale Electricity Market Restructuring," *IEEE Power Energy Mag.*, vol. 17, no. 1, pp. 73–81, Jan. 2019, doi: 10.1109/MPE.2018.2873952.

[80] G. Morales-España, L. Ramírez-Elizondo, and B. F. Hobbs, "Hidden power system inflexibilities imposed by traditional unit commitment formulations," *Appl. Energy*, vol. 191, pp. 223–238, Apr. 2017, doi: 10.1016/j.apenergy.2017.01.089.

[81] W. Lise, J. Sijm, and B. F. Hobbs, "The Impact of the EU ETS on Prices, Profits and Emissions in the Power Sector: Simulation Results with the COMPETES EU20 Model," *Environ. Resour. Econ.*, vol. 47, no. 1, pp. 23–44, Apr. 2010, doi: 10.1007/s10640-010-9362-9.

[82] G. Morales-Espana, A. Ramos, and J. Garcia-Gonzalez, "An MIP Formulation for Joint Market-Clearing of Energy and Reserves Based on Ramp Scheduling," *Power Syst. IEEE Trans. On*, vol. 29, no. 1, pp. 476–488, Jan. 2014, doi: 10.1109/TPWRS.2013.2259601.

[83] G. Morales-España, R. Baldick, J. García-González, and A. Ramos, "Power-Capacity and Ramp-Capability Reserves for Wind Integration in Power-Based UC," *IEEE Trans. Sustain. Energy*, vol. 7, no. 2, pp. 614–624, Apr. 2016, doi: 10.1109/TSTE.2015.2498399.

[84] Xiaohong Guan, Feng Gao, and A. J. Svoboda, "Energy delivery capacity and generation scheduling in the deregulated electric power market," *IEEE Trans. Power Syst.*, vol. 15, no. 4, pp. 1275–1280, Nov. 2000, doi: 10.1109/59.898101.

[85] Y. Yang, J. Wang, X. Guan, and Q. Zhai, "Subhourly unit commitment with feasible energy delivery constraints," *Appl. Energy*, vol. 96, pp. 245–252, Aug. 2012, doi: 10.1016/j.apenergy.2011.11.008.

[86] G. Morales-España, C. Gentile, and A. Ramos, "Tight MIP formulations of the power-based unit commitment problem," *Spectr.*, vol. 37, no. 4, pp. 929–950, Oct. 2015, doi: 10.1007/s00291-015-0400-4.

[87] J. Meus, K. Poncelet, and E. Delarue, "Applicability of a Clustered Unit Commitment Model in Power System Modeling," *IEEE Trans. Power Syst.*, vol. 33, no. 2, pp. 2195–2204, Mar. 2018, doi: 10.1109/TPWRS.2017.2736441.

[88] G. Morales-Espana and D. A. Tejada-Arango, "Modelling the Hidden Flexibility of Clustered Unit Commitment," *IEEE Trans. Power Syst.*, pp. 1–1, 2019, doi: 10.1109/TPWRS.2019.2908051.

[89] C. Gentile, G. Morales-España, and A. Ramos, "A tight MIP formulation of the unit commitment problem with start-up and shut-down constraints," *EURO J. Comput. Optim.*, pp. 1–25, Apr. 2016, doi: 10.1007/s13675-016-0066-y.

[90] G. Morales-Espana, J. M. Latorre, and A. Ramos, "Tight and Compact MILP Formulation of Start-Up and Shut-Down Ramping in Unit Commitment," *Power Syst. IEEE Trans. On*, vol. 28, no. 2, pp. 1288–1296, May 2013, doi: 10.1109/TPWRS.2012.2222938.

[91] I. Momber, G. Morales-España, A. Ramos, and T. Gómez, "PEV Storage in Multi-Bus Scheduling Problems," *IEEE Trans. Smart Grid*, vol. 5, no. 2, pp. 1079–1087, Mar. 2014, doi: 10.1109/TSG.2013.2290594.

[92] R. Philipsen, G. Morales-España, M. de Weerdt, and L. de Vries, "Trading power instead of energy in day-ahead electricity markets," *Appl. Energy*, vol. 233–234, pp. 802–815, Jan. 2019, doi: 10.1016/j.apenergy.2018.09.205.

[93] D. A. Tejada-Arango, "Case Studies for Power-based Capacity Expansion Planning: datejada/PB-CEP," Dec. 21, 2018. https://github.com/datejada/PB-CEP (accessed Dec. 21, 2018).

[94] G. Morales-España, "Unit Commitment: Computational Performance, System Representation and Wind Uncertainty Management," Doctoral thesis, Universidad Pontificia Comillas, KTH Royal Institute of Technology, and Delft University of Technology, 2014.

[95] ENTSO-E, "Ten Year Network Development Plan 2018," 2018. https://tyndp.entsoe.eu/ (accessed Dec. 21, 2018).

[96] H.-S. Park and C.-H. Jun, "A simple and fast algorithm for K-medoids clustering," *Expert Syst. Appl.*, vol. 36, no. 2, Part 2, pp. 3336–3341, Mar. 2009, doi: 10.1016/j.eswa.2008.01.039.

[97] M. Sun, F. Teng, X. Zhang, G. Strbac, and D. Pudjianto, "Data-Driven Representative Day Selection for Investment Decisions: A Cost-Oriented Approach," *IEEE Trans. Power Syst.*, pp. 1–1, 2019, doi: 10.1109/TPWRS.2019.2892619.

[98] S. Wogrin and D. F. Gayme, "Optimizing Storage Siting, Sizing, and Technology Portfolios in Transmission-Constrained Networks," *IEEE Trans. Power Syst.*, vol. 30, no. 6, pp. 3304–3313, Nov. 2015, doi: 10.1109/TPWRS.2014.2379931.

[99] T. Yau, L. N. Walker, H. L. Graham, A. Gupta, and R. Raithel, "Effects of Battery Storage Devices on Power System Dispatch," *IEEE Trans. Power Appar. Syst.*, vol. PAS-100, no. 1, pp. 375–383, Jan. 1981, doi: 10.1109/TPAS.1981.316866.

[100] D. Gayme and U. Topcu, "Optimal power flow with large-scale storage integration," *IEEE Trans. Power Syst.*, vol. 28, no. 2, pp. 709–717, May 2013, doi: 10.1109/TPWRS.2012.2212286.

[101] Y. M. Atwa and E. F. El-Saadany, "Optimal Allocation of ESS in Distribution Systems With a High Penetration of Wind Energy," *IEEE Trans. Power Syst.*, vol. 25, no. 4, pp. 1815–1822, Nov. 2010, doi: 10.1109/TPWRS.2010.2045663.

[102] S. Bose, D. F. Gayme, U. Topcu, and K. M. Chandy, "Optimal placement of energy storage in the grid," in *2012 IEEE 51st IEEE Conference on Decision and Control (CDC)*, Dec. 2012, pp. 5605–5612, doi: 10.1109/CDC.2012.6426113.

[103] A. Castillo and D. F. Gayme, "Profit maximizing storage allocation in power grids," in *52nd IEEE Conference on Decision and Control*, Dec. 2013, pp. 429–435, doi: 10.1109/CDC.2013.6759919.

[104] A. Gopalakrishnan, A. U. Raghunathan, D. Nikovski, and L. T. Biegler, "Global optimization of multi-period optimal power flow," in *2013 American Control Conference*, Jun. 2013, pp. 1157–1164, doi: 10.1109/ACC.2013.6579992.

[105] Z. Hu and W. T. Jewell, "Optimal power flow analysis of energy storage for congestion relief, emissions reduction, and cost savings," in *2011 IEEE/PES Power*

Systems Conference and Exposition, Mar. 2011, pp. 1–8, doi: 10.1109/PSCE.2011.5772576.

[106] D. Van Hertem, J. Verboomen, K. Purchala, R. Belmans, and W. L. Kling, "Usefulness of DC power flow for active power flow analysis with flow controlling devices," in *The 8th IEE International Conference on AC and DC Power Transmission*, Mar. 2006, pp. 58–62, doi: 10.1049/cp:20060013.

[107] E. Sjödin, D. F. Gayme, and U. Topcu, "Risk-mitigated optimal power flow for wind powered grids," in *2012 American Control Conference (ACC)*, Jun. 2012, pp. 4431–4437, doi: 10.1109/ACC.2012.6315377.

[108] C. Thrampoulidis, S. Bose, and B. Hassibi, "On the distribution of energy storage in electricity grids," in *52nd IEEE Conference on Decision and Control*, Dec. 2013, pp. 7590–7596, doi: 10.1109/CDC.2013.6761094.

[109] K. Dvijotham, M. Chertkov, and S. Backhaus, "Storage Sizing and Placement through Operational and Uncertainty-Aware Simulations," in *2014 47th Hawaii International Conference on System Sciences*, Jan. 2014, pp. 2408–2416, doi: 10.1109/HICSS.2014.302.

[110] M. Ghofrani, A. Arabali, M. Etezadi-Amoli, and M. S. Fadali, "A Framework for Optimal Placement of Energy Storage Units Within a Power System With High Wind Penetration," *IEEE Trans. Sustain. Energy*, vol. 4, no. 2, pp. 434–442, Apr. 2013, doi: 10.1109/TSTE.2012.2227343.

[111] S. Lumbreras and A. Ramos, "The new challenges to transmission expansion planning. Survey of recent practice and literature review," *Electr. Power Syst. Res.*, vol. 134, pp. 19–29, May 2016, doi: 10.1016/j.epsr.2015.10.013.

[112] W. Jewell and Zhouxing Hu, "The role of energy storage in transmission and distribution efficiency," in *PES T D 2012*, May 2012, pp. 1–4, doi: 10.1109/TDC.2012.6281537.

[113] M. F. Romlie, M. Rashed, C. Klumpner, and G. M. Asher, "An analysis of efficiency improvement with the installation of energy storage in power systems," in *7th IET International Conference on Power Electronics, Machines and Drives (PEMD 2014)*, Apr. 2014, pp. 1–6, doi: 10.1049/cp.2014.0514.

[114] F. Zhang, Z. Hu, and Y. Song, "Mixed-integer linear model for transmission expansion planning with line losses and energy storage systems," *Transm. Distrib. IET Gener.*, vol. 7, no. 8, pp. 919–928, Aug. 2013, doi: 10.1049/iet-gtd.2012.0666.

[115] Pedro Sanchez-Martinez, Andrés Ramos, "Modeling Transmission Ohmic Losses," *Inst. Investig. Tecnológica*, p. 8.

[116] M. F. Anjos and A. J. Conejo, "Unit Commitment in Electric Energy Systems," *Found. Trends® Electr. Energy Syst.*, vol. 1, no. 4, pp. 220–310, Dec. 2017, doi: 10.1561/3100000014.

[117] D. Pozo, J. Contreras, and E. E. Sauma, "Unit Commitment With Ideal and Generic Energy Storage Units," *IEEE Trans. Power Syst.*, vol. 29, no. 6, pp. 2974–2984, Nov. 2014, doi: 10.1109/TPWRS.2014.2313513.

[118] "Power Sysem Test Case." https://labs.ece.uw.edu/pstca/pf14/pg_tca14bus.htm (accessed May 09, 2020).

[119] "Electrical Energy Storage," International Electrotechnical Commission, White Paper. [Online]. Available: https://www.iec.ch/whitepaper/pdf/iecWP-energystorage-LR-en.pdf.

[120] "Prospects for Large-Scale Energy Storage in Decarbonised Power Grids – Analysis," *IEA*. https://www.iea.org/reports/prospects-for-large-scale-energy-storage-in-decarbonised-power-grids (accessed May 09, 2020).

[121] "Flywheel Energy Storage Systems," Beacon Power. [Online]. Available: https://beaconpower.com/wp-content/themes/beaconpower/inc/beacon_power_brochure_032514.pdf.

[122] "Western Wind Data Set | Grid Modernization | NREL." https://www.nrel.gov/grid/western-wind-data.html (accessed May 10, 2020).

[123] I. Fisher, *The Rate of Interest*. Garland Pub., 1982.

[124] M. Z. Frank and T. Shen, "Investment and the weighted average cost of capital," *J. Financ. Econ.*, vol. 119, no. 2, pp. 300–315, Feb. 2016, doi: 10.1016/j.jfineco.2015.09.001.

[125] F. A. Campos, J. Villar, and C. Cervilla, "Profitability measures and cost minimization in electricity generation investments," in *2015 12th International Conference on the European Energy Market (EEM)*, May 2015, pp. 1–5, doi: 10.1109/EEM.2015.7216602.

[126] A. Ramos, I. J. Perez-Arriaga, and J. Bogas, "A nonlinear programming approach to optimal static generation expansion planning," *IEEE Trans. Power Syst.*, vol. 4, no. 3, pp. 1140–1146, Aug. 1989, doi: 10.1109/59.32610.

[127] M. Ventosa, R. Denis, and C. Redondo, "Expansion planning in electricity markets. Two different approaches," in *Proceedings of the 14th Power Systems Computation Conference (PSCC), Seville*, 2002, vol. 26, Accessed: Aug. 30, 2017. [Online]. Available: http://www.pscc-central.org/uploads/tx_ethpublications/s43p04.pdf.

[128] F. H. Murphy and Y. Smeers, "Generation Capacity Expansion in Imperfectly Competitive Restructured Electricity Markets," *Oper. Res.*, vol. 53, no. 4, pp. 646–661, Aug. 2005, doi: 10.1287/opre.1050.0211.

[129] V. Hinojosa, "Static generation capacity expansion planning using linear transmission distribution factors," in *2016 IEEE PES Transmission Distribution Conference and Exposition-Latin America (PES T D-LA)*, Sep. 2016, pp. 1–6, doi: 10.1109/TDC-LA.2016.7805678.

[130] H. Park and R. Baldick, "Stochastic Generation Capacity Expansion Planning Reducing Greenhouse Gas Emissions," *IEEE Trans. Power Syst.*, vol. 30, no. 2, pp. 1026–1034, Mar. 2015, doi: 10.1109/TPWRS.2014.2386872.

[131] J. Wang, M. Shahidehpour, Z. Li, and A. Botterud, "Strategic Generation Capacity Expansion Planning With Incomplete Information," *IEEE Trans. Power Syst.*, vol. 24, no. 2, pp. 1002–1010, May 2009, doi: 10.1109/TPWRS.2009.2017435.

[132] S. J. Kazempour, A. J. Conejo, and C. Ruiz, "Strategic Generation Investment Using a Complementarity Approach," *IEEE Trans. Power Syst.*, vol. 26, no. 2, pp. 940–948, May 2011, doi: 10.1109/TPWRS.2010.2069573.

[133] A. van Stiphout, K. D. Vos, and G. Deconinck, "The Impact of Operating Reserves on Investment Planning of Renewable Power Systems," *IEEE Trans. Power Syst.*, vol. 32, no. 1, pp. 378–388, Jan. 2017, doi: 10.1109/TPWRS.2016.2565058.

[134] D. Pozo, E. E. Sauma, and J. Contreras, "A Three-Level Static MILP Model for Generation and Transmission Expansion Planning," *IEEE Trans. Power Syst.*, vol. 28, no. 1, pp. 202–210, Feb. 2013, doi: 10.1109/TPWRS.2012.2204073.

[135] S. Dehghan, N. Amjady, and A. J. Conejo, "Reliability-Constrained Robust Power System Expansion Planning," *IEEE Trans. Power Syst.*, vol. 31, no. 3, pp. 2383–2392, May 2016, doi: 10.1109/TPWRS.2015.2464274.

[136] B. G. Gorenstin, N. M. Campodonico, J. P. Costa, and M. V. F. Pereira, "Power system expansion planning under uncertainty," *IEEE Trans. Power Syst.*, vol. 8, no. 1, pp. 129–136, Feb. 1993, doi: 10.1109/59.221258.

[137] S. Wogrin, J. Barquín, and E. Centeno, "Capacity Expansion Equilibria in Liberalized Electricity Markets: An EPEC Approach," *IEEE Trans. Power Syst.*, vol. 28, no. 2, pp. 1531–1539, May 2013, doi: 10.1109/TPWRS.2012.2217510.

[138] M. T. Vespucci, M. Bertocchi, S. Zigrino, and L. F. Escudero, "Stochastic optimization models for power generation capacity expansion with risk management," in *2013 10th International Conference on the European Energy Market (EEM)*, May 2013, pp. 1–8, doi: 10.1109/EEM.2013.6607352.

[139] A. Nogales, S. Wogrin, and E. Centeno, "Impact of technical operational details on generation expansion in oligopolistic power markets," *Transm. Distrib. IET Gener.*, vol. 10, no. 9, pp. 2118–2126, 2016, doi: 10.1049/iet-gtd.2015.1148.

[140] R. Domı´nguez, A. J. Conejo, and M. Carrión, "Investing in Generation Capacity: A Multi-Stage Linear-Decision-Rule Approach," *IEEE Trans. Power Syst.*, vol. 31, no. 6, pp. 4784–4794, Nov. 2016, doi: 10.1109/TPWRS.2016.2522505.

[141] W. Shengyu, C. Lu, Y. Xiaoqing, and Y. Bo, "Long-term generation expansion planning under uncertainties and fluctuations of multi-type renewables," in *2015 IEEE 5th International Conference on Power Engineering, Energy and Electrical Drives (POWERENG)*, May 2015, pp. 612–616, doi: 10.1109/PowerEng.2015.7266387.

[142] E. Gil, I. Aravena, and R. Cárdenas, "Generation Capacity Expansion Planning under hydro uncertainty using Stochastic Mixed Integer Programming and scenario reduction," in *2015 IEEE Power Energy Society General Meeting*, Jul. 2015, pp. 1–1, doi: 10.1109/PESGM.2015.7285838.

[143] Niharika, S. Verma, and V. Mukherjee, "Transmission expansion planning: A review," in *2016 International Conference on Energy Efficient Technologies for Sustainability (ICEETS)*, Apr. 2016, pp. 350–355, doi: 10.1109/ICEETS.2016.7583779.

[144] X. Zhang and A. J. Conejo, "Coordinated Investment in Transmission and Storage Systems Representing Long- and Short-term Uncertainty," *IEEE Trans. Power Syst.*, pp. 1–1, 2018, doi: 10.1109/TPWRS.2018.2842045.

[145] J. H. Zhao, Z. Y. Dong, P. Lindsay, and K. P. Wong, "Flexible transmission expansion planning with uncertainties in an electricity market," *IEEE Trans. Power Syst.*, vol. 24, no. 1, pp. 479–488, 2009, doi: 10.1109/TPWRS.2008.2008681.

[146] C. Velasquez, D. Watts, H. Rudnick, and C. Bustos, "A Framework for Transmission Expansion Planning: A Complex Problem Clouded by Uncertainty," *IEEE Power Energy Mag.*, vol. 14, no. 4, pp. 20–29, 2016, doi: 10.1109/MPE.2016.2547278.

[147] L.-A. Barroso and A. J. Conejo, "Decision making under uncertainty in electricity markets," *Power Eng. Soc. Gen. Meet. 2006 IEEE*, p. 3 pp., 2006.

[148] R. Hemmati, R.-A. Hooshmand, and A. Khodabakhshian, "Comprehensive review of generation and transmission expansion planning," *IET Gener. Transm. Distrib.*, vol. 7, no. 9, pp. 955–964, 2013, doi: 10.1049/iet-gtd.2013.0031.

[149] B. F. Hobbs *et al.*, "Adaptive Transmission Planning: Implementing a New Paradigm for Managing Economic Risks in Grid Expansion," *IEEE Power Energy Mag.*, vol. 14, no. 4, pp. 30–40, Jul. 2016, doi: 10.1109/MPE.2016.2547280.

[150] M. O. Buygi, H. M. Shanechi, G. Balzer, M. Shahidehpour, and N. Pariz, "Network planning in unbundled power systems," *IEEE Trans. Power Syst.*, vol. 21, no. 3, pp. 1379–1387, Aug. 2006, doi: 10.1109/TPWRS.2006.873016.

[151] A. Bagheri, J. Wang, and C. Zhao, "Data-Driven Stochastic Transmission Expansion Planning," *IEEE Trans. Power Syst.*, vol. 32, no. 5, pp. 3461–3470, Sep. 2017, doi: 10.1109/TPWRS.2016.2635098.

[152] P. Maloney, O. Olatujoye, A. J. Ardakani, D. Mejïa-Giraldo, and J. McCalley, "A comparison of stochastic and adaptation programming methods for long term generation and transmission co-optimization under uncertainty," in *2016 North American Power Symposium (NAPS)*, Sep. 2016, pp. 1–6, doi: 10.1109/NAPS.2016.7747906.

[153] P. Maloney and J. McCalley, "Long term planning model value of stochastic solution and expected value of perfect information calculations with uncertain wind parameters," *2017 North Am. Power Symp. NAPS 2017*, no. 5, 2017, doi: 10.1109/NAPS.2017.8107370.

[154] S. Huang and V. Dinavahi, "Security constrained transmission expansion planning by accelerated benders decomposition," in *2016 North American Power Symposium (NAPS)*, Sep. 2016, pp. 1–6, doi: 10.1109/NAPS.2016.7747984.

[155] V. Krishnan *et al.*, *Co-optimization of electricity transmission and generation resources for planning and policy analysis: review of concepts and modeling approaches*, vol. 7, no. 2. Springer Berlin Heidelberg, 2016.

[156] S. Dehghan, N. Amjady, and S. Member, "Robust Transmission and Energy Storage Expansion Planning in Wind Farm-Integrated Power Systems Considering ... Robust Transmission and Energy Storage Expansion Planning in Wind Farm-Integrated Power Systems Considering Transmission Switching," *IEEE Trans. Sustain. Energy*, vol. 7, no. December, pp. 1–10, 2015, doi: 10.1109/TSTE.2015.2497336.

[157] R. A. Jabr, "Robust transmission network expansion planning with uncertain renewable generation and loads," *IEEE Trans. Power Syst.*, vol. 28, no. 4, pp. 4558–4567, 2013, doi: 10.1109/TPWRS.2013.2267058.

5. Annex

This annex describes the above references in detail, citing the overall topics and main points for each document individually.

5.1 Transmission expansion planning: a review

Title	Author	Subject	Main Points
Transmission expansion planning: a review	Niharika, Verma, Mukherjee	TEP: --Approaches --Planning models --Solution methods --Optimization tools	TEP can be broken down into static and dynamic planning. Dynamic takes into account size, placement, and time consideration. TEP can be modeled based on different criteria, like transportation, DC power flow, AC power flow, hybrid, or disjunctive models. Mathematical optimization methods determines an optimum expansion plan. The plan should be technically, financially, and environmentally verified. Heuristic methods optimize step-by-step, sometimes also using sensitivity analysis. Some programming languages to help solve include Fortran, C, C++, Python, Java, MATLAB, GAMS, LINGO, AMPLY, or AIMMS.

5.2 Robust Transmission Expansion Planning Representing Long- and Short-Term Uncertainty

Title	Author	Subject	Main Points
Robust Transmission Expansion Planning Representing Long- and Short-Term Uncertainty	Zhang, Conejo	Difference b/w short and long-term uncertainties Problem formulation and model Benders' Decomposition	Short term TEP uncertainties include daily variation of demand and power production. Long-term uncertainties include actual peak demand and available generation capacity in 10-20 years from now. Short term uncertainties are represented by scenarios, while long-term are represented by robust sets. An example of Benders' Decomposition is also given and explained thoroughly. A 118 bus case study is given complete with tables and charts as well.

5.3 Flexible Transmission Expansion Planning With Uncertainties in an Electricity Market

Title	Author	Subject	Main Points
Flexible Transmission Expansion Planning With Uncertainties in an Electricity Market	Zhao, Dong, Lindsay, Wong	Uncertainties in deregulated market Stakeholders desires TEP solving method and formulation 14-bus system test	Some uncertainties listed are load forecast, availability of system facilities, installation/closure of facilities, fuel availability and cost, energy at risk, market rules, government policies, and expected unserved energy cost. TEP is modeled through a mixed integer nonlinear programming method. Another method and formulation is proposed, and has been tested against a 14-bus system. Market deregulation fundamentally changes TEP and creates more uncertainties. The new method created uses adaptation costs and scenarios to generate more flexible decisions. This proposal uses a multiobjective optimization method to also optimize conflicting planning objectives.

5.4 A Framework for Transmission Expansion Planning

Title	Author	Subject	Main Points
A Framework for Transmission Expansion Planning	Velasquez, Watts, Rudnick, Bustos	Uncertainties --Aleatory vs Epistemic --Uncertainty vs Risk --KuU uncertainties --Short, medium, long-term --Sources Optimization approaches	Aleatory is a a natural variability inherent to a particular process, such as hourly wind speed, human behavioral variability, and earthquake incidents,which cannot always be represented by a probability. Epistemic uncertainty is produced by imperfect knowledge, such as the model to describe competition in electricity markets, generation expansion, and failure rates for new facilities. Known uncertainties can be represented by a probability, which can be modeled through stochastic programming. Unknown uncertainties use bounded sets, such as with robust optimization. Unknowable uncertainties are events that can't be identified in advance. There is much more important information within this paper as well.

5.5 Decision Making under Uncertainty in Electricity Markets

Title	Author	Subject	Main Points
Decision Making under Uncertainty in Electricity Markets	Barroso, Conejo	Stochastic programming for uncertainties Main sources of uncertainty	Main sources of uncertainty are: prices of energy, reserves and regulation, fuel prices, fuel availability, energy demand, and regulatory issues. For decision making under uncertainty, the issues to address are the decision time framework, maximizing expected profit, and maximizing expected profit limiting the volatility (minimize risk). Stochastic programming has recently been using decomposition methods to overcome the "curse of dimensionality", when the number of scenarios becomes too large and the problem becomes so complex that it must be broken down to solve faster.

5.6 Comprehensive Review of generation and transmission expansion planning

Title	Author	Subject	Main Points
Comprehensive Review of generation and transmission expansion planning	Hemmati, Hooshmand, Khodabakhsian	Differences between GEP and TEP TEP and GEP formulation overview Resources for different, specific optimization models adv/disadv of mathematical and heuristic models Uncertainties in TEP, GEP	GEP relates to the investment on energy production. GEP determines size, place, technology and the time of installing new plants to satisfy forecasted load. GEP-specific uncertainties include price volatility, demand evolution, reliability of generation units, investment and operation costs. TEP defines when, where, and how many new lines should be installed to provide and adequate level of energy to customers. TEP takes into account load growth, forecasted demand, and more while minimizing investment, operation, and interruption costs. Uncertainties in 6.1-6.2 could be useful in charts for paper.

5.7 Adaptive Transmission Planning

Title	Author	Subject	Main Points
Adaptive Transmission Planning	Hobbs, Xu, Ho, Donohoo, Kasina, Ouyang, Park, Eto, Satyal	Intro to uncertainty in future Intro to TEP and considerations Short vs Long term uncertainties Existing optimization methods Stochastic programming	The future is highly unpredictable with the technological advancements we are seeing now. Investments need to take into account many short term uncertainties and be able to consider many possible conditions. For the long term, the investment must be robust, considering the policy, technological, and economic changes that can occur. Adaptability is also very important in regards to long term uncertainties. Stochastic programming demonstrates the difference between here and now decisions and wait and see decisions. Chance nodes describe possible scenarios, while decision nodes represent the proposed solutions. The example of JHSMINE is also given and explained in detail.

5.8 Network Planning in Unbundled Power Systems

Title	Author	Subject	Main Points
Network Planning in Unbundled Power Systems	Buygi, Shanechi, Balzer, Shahidehpour, Pariz	Random vs nonrandom uncertainties Model overview Fuzzy Index, risk assessment	Random uncertainties are deviations from parameters that are repeatable and have a known probability distribution. Non-random uncertainties are evolution of parameters that are non-repeatable, and their statistics cannot be found from past historical data. Modelling random uncertainties considers reliability, flexibility, transmission expansion cost, and environmental impacts. Fuzzy numbers are introduced, as well as intervals and appropriateness indexes. This is in regards to risk assessment and minimax regret.

5.9 Data-Driven Stochastic Transmission Expansion Planning

Title	Author	Subject	Main Points
Data-Driven Stochastic Transmission Expansion Planning	Bagheri, Wang, Zhao	Stochastic programming with decomposition methods (Bender's, column-and-constraint generation methods) Robust optimization	The objective of stochastic programming is to minimize the total expected cost or to maximize the expected profit or social welfare corresponding to the generated scenarios or assumed distribution. Robust optimization attempts to minimize the worst-case cost and the worst-case regret. An in-depth novel decomposition method is proposed using a stochastic program using historical data. The proposed method is tested with a 6- and 18-bus system considering a 20 year horizon.

5.10 A Comparison of Stochastic and Adaptation Programming Methods for Long Term Generation and Transmission Co-optimization under Uncertainty

Title	Author	Subject	Main Points
A Comparison of Stochastic and Adaptation Programming Methods for Long Term Generation and Transmission Co-optimization under Uncertainty	Patrick Maloney, Oluwaseyi Olatujoye, Ali Jahanbani Ardakani, Diego Mej´ıa-Giraldo, James McCalley	Adaptation and stochastic programming methods Differences in formulation and structure Case study	Stochastic programming models have similarly structured first and later stage decisions. Adaptation selects the minimum maximum adaptation cost. It is also possible to integrate adaptation costs into stochastic programming. Stochastic is usually represented by scenario trees regarding capacity investments, while adaptation depicts core investments. The objective functions of both are structurally similar. Adaptation solves a set of core investments through all time. Stochastic programming tells the planner the optimal set of investments at a particular stage. Stochastic here and now decisions become investments in the core design, and wait and see decisions are the adaptive scenario specific investments.

5.11 Long Term Planning Model Value of Stochastic Solution and Expected Value of Perfect Information Calculations with Uncertain Wind Parameters

Title	Author	Subject	Main Points
Long Term Planning Model Value of Stochastic Solution and Expected Value of Perfect Information Calculations with Uncertain Wind Parameters	Patrick Maloney, James McCalley	Wind uncertainty Stochastic programming for wind uncertainty Solving for expected value Case study	The most frequently used uncertainty regarding wind is the variability of wind power output. Wind generation parameters that are uncertain include, build costs, variable operations and maintenance (VOM) costs, fixed operations and maintenance (FOM) costs, capacity factor, capacity credit, variability, construction lead times, and renewable portfolio policies. Load growth is a parameter more traditionally studied in uncertainty analysis and more directly affects most investment and operational decisions. This paper is mostly a case study and giving formulas to solve stochastic programming with data. There is not much overview of the topic, but the formulas seem useful for programming.

5.12 Security Constrained Transmission Expansion Planning by Accelerated Benders Decomposition

Title	Author	Subject	Main Points
Security Constrained Transmission Expansion Planning by Accelerated Benders Decomposition	Huang, Dinavahi	Stochastic programming Benders cuts/decomposition	Valid inequality, multicut strategy, and optimal precondition variations to the classic benders decomposition are introduced and explained. Three case studies are provided with varying numbers of bus systems. This paper almost completely focuses on Benders decomposition, which is not valuable if we do not use this method in our research. However, it was mentioned in one of the paragraphs regarding the decomposition method in stochastic programming.

5.13 Co-optimization of electricity transmission and generation resources for planning and policy analysis: review of concepts and modeling approaches

Title	Author	Subject	Main Points
Co-optimization of electricity transmission and generation resources for planning and policy analysis: review of concepts and modeling approaches	Krishnan, Ho, Hobbs, Liu, McCalley, Shahidehpour, Zheng	Background and history of co-optimization and its importance Modeling approaches for co-optimization Chart of existing models AC/DC power flow models Short and long term uncertainties	Co-optimized solutions create less expensive solutions than decoupled optimization solns. Many modeling choices are also described, including inter-temporal constraints, time steps, storage technologies and demand response, geographical coverage, salvage value, equilibrium, and extended simulation. It also mentions that it is best to have a long simulation time in a model. It also gives pros and cons of time step choices, but this may or may not be valuable. Long run uncertainties given are economic growth, technological advancements, and regulatory developments for stochastic programming. There is a lot more said in 4.4.1 regarding stochastic programming and uncertainties.

5.14 Robust Transmission and Energy Storage Expansion Planning in Wind Farm-Integrated Power Systems Considering Transmission Switching

Title	Author	Subject	Main Points
Robust Transmission and Energy Storage Expansion Planning in Wind Farm-Integrated Power Systems Considering Transmission Switching	Dehghan, Amjady	Stochastic model of TEP Uncertainty Handling Stochastic/Deterministic and Robust formulations Test systems	This paper creates robust and deterministic models for co-optimization. It introduces uncertainty such as wind power and load demand. The robust model minimizes regret and maximizes output. It also uses a decomposition algorithm to solve. It proves that increasing the budget of uncertainty creates more conservative expansion plans in the end. Additionally, the bus-system test showed that topology optimization is effective at reducing total costs of expansion and operations. The formulations proposed in this paper could prove to be beneficial in creating new programs of co-optimization as well.

5.15 Robust Transmission Network Expansion Planning with Uncertain Renewable Generation and Loads

Title	Author	Subject	Main Points
Robust Transmission Network Expansion Planning with Uncertain Renewable Generation and Loads	Jabr	Robust optimization Benders Decomposition TNEP without uncertainty TNEP with load and renewable generation uncertainty	Robust optimization minimizes the maximum regret possible of the choices and risks. TNEP with uncertainty takes into account renewable power generation and load demand, represented by uncertainty sets. Benders decomposition creates a master problem and slave problems to break down complex algorithms to solve faster. The BD type algorithm gives a plan that works for all realizations of the uncertainty, but it could fall out of the bounds of the uncertainty set. An uncertainty budget is also helpful with this modeling method and parameters.

Santa Cruz de Marcenado, 26
28015 Madrid
Tel +34 91 542 28 00
Fax + 34 91 542 31 76
secretaria.tecnica@iit.comillas.edu
www.iit.comillas.edu